

See discussions, stats, and author profiles for this publication at: <https://www.researchgate.net/publication/272183308>

A tectonic model reconciling evidence for the collisions between India, Eurasia and intra-oceanic arcs of the...

Article *in* Gondwana Research · January 2015

DOI: 10.1016/j.gr.2015.01.001

CITATIONS

38

READS

1,146

5 authors, including:



Sabin Zahirovic

University of Sydney

39 PUBLICATIONS 974 CITATIONS

[SEE PROFILE](#)



Dietmar Müller

University of Sydney

384 PUBLICATIONS 12,988 CITATIONS

[SEE PROFILE](#)



Joanne M Whittaker

University of Tasmania

75 PUBLICATIONS 1,128 CITATIONS

[SEE PROFILE](#)



Yatheesh Vadakkeyakath

National Institute of Oceanography

30 PUBLICATIONS 280 CITATIONS

[SEE PROFILE](#)

Some of the authors of this publication are also working on these related projects:



Project Congested Subduction [View project](#)



Project The geodynamics of past sea level changes [View project](#)



GR Focus Review

A tectonic model reconciling evidence for the collisions between India, Eurasia and intra-oceanic arcs of the central-eastern Tethys

A.D. Gibbons ^{a,*¹}, S. Zahirovic ^a, R.D. Müller ^a, J.M. Whittaker ^b, V. Yatheesh ^c^a School of Geosciences, University of Sydney, NSW 2006, Australia^b Institute for Marine and Antarctic Studies, 20 Castray Esplanade, Hobart, Tasmania, Australia^c CSIR-National Institute of Oceanography, Dona Paula, Goa 403 004, India

ARTICLE INFO

Article history:

Received 3 October 2014

Received in revised form 17 January 2015

Accepted 20 January 2015

Available online 7 February 2015

Handling Editor: M. Santosh

Keywords:

Gondwana
Eurasian margin
Tethys Ocean
Greater India
India-Eurasia collision
Indian Ocean

ABSTRACT

Despite several decades of investigations, inferences on the timing and nature of collisions along the Mesozoic-Cenozoic Eurasian margin remain controversial. We assimilate geological and geophysical evidence into a plate tectonic model for the India-Eurasia collision that includes continuously-closing topological plate polygons, constructed from a time-dependent network of evolving plate boundaries, with synthetic plates constructed for now-subducted ocean floor, including back-arc basins that formed on the southern Eurasian margin. Our model is regionally-constrained and self-consistent, incorporating geophysical data from abyssal plains offshore West Australia and East Antarctica, including Jurassic age data from offshore Northwest Australia, limiting much of northern Greater India to a ~1000 km-long indenter, originally reaching to the Wallaby-Zenith Fracture Zone. Southern Eurasia and Southeast Asia are riddled with dismembered oceanic arcs indicating long-lived Tethyan intra-oceanic subduction. This intra-oceanic subduction system was well-established from Cretaceous time in the India-Eurasia convergence zone in the NeoTethys, which was consumed during Greater India's northward trajectory towards Eurasia from the Early Cretaceous. Fragments of obducted oceanic crust within the Yarlung-Tsangpo Suture Zone, between India and Eurasia, predominantly date to the Late Jurassic or mid Cretaceous (Barremian-Aptian). The various ophiolites along strike and a hiatus in subduction-related magmatism during the Tithonian-Aptian suggest that there was at least one generation of intra-oceanic arc formation, whose plate boundary configuration remains uncertain. Paleomagnetic and magmatic studies suggest that the intra-oceanic arc was at equatorial latitudes during the Early Cretaceous before subduction resumed further north beneath the Eurasian margin (Lhasa terrane), with another hiatus in subduction-related magmatism along southern Lhasa during ~80–65 Ma, possibly as the back-arc spreading centre approached the active Andean-style margin. In our model, Greater India collided with the Tethyan intra-oceanic arc in Paleocene-Eocene time, finally closing the Tethyan seaway from Mid-Late Eocene time, which is consistent with the age of the youngest marine deposits found between India and Eurasia. Geological evidence from the collision zone indicates an age of initial arc-continent collision by ~52 Ma, followed by the “soft” (initial) continent-continent collision between India and Eurasia by ~44 ± 2 Ma. This timing is supported by marine geophysical data, where the spreading centres in the Indian Ocean record a drastic decline in seafloor spreading rates and changes in spreading directions first at ~52 Ma, followed by another reorganisation at ~43 Ma. The abandonment of spreading in the Wharton Basin and the onset of extrusion tectonics in Asia by ~36 Ma are likely indicators of “hard” (complete) continent collision, and highlight the multi-stage collisional history of this margin. Our continuously evolving network of mid-ocean ridge and subduction zone geometries, and divergence/convergence vectors through time, provide a basis for future refinements to assimilate new data and/or test alternative tectonic scenarios.

© 2015 International Association for Gondwana Research. Published by Elsevier B.V. All rights reserved.

Contents

1. Introduction	452
2. Eurasian and Southeast Asian geology	455

^{*} Corresponding author.E-mail address: angi@statoil.com (A.D. Gibbons).¹ Now at Statoil ASA, Martin Linges vei 33, Fornebu 1330, Norway.

2.1.	Karakoram terrane	457
2.2.	Kohistan–Karakoram–Shyok Suture Zone	457
2.3.	Kohistan–Ladakh Arc	459
2.4.	Indus Suture Zone	460
2.5.	Trans-Himalayan batholith(s) and igneous bodies	461
2.6.	The Himalaya	461
2.7.	Yarlung–Tsangpo Suture Zone	462
2.8.	Lhasa terrane (South Tibet)	464
2.9.	Bangong–Nujiang Suture Zone	465
2.10.	Qiangtang terrane (North Tibet)	465
2.11.	West Burma (Myanmar)	465
2.12.	Southeast Asia	465
3.	Methodology, data and kinematic constraints	466
3.1.	Argoland and Greater India	470
3.2.	The Eurasian margin	473
3.3.	Intra-oceanic arc(s)	473
4.	Tectonic model and discussion	475
4.1.	Argoland	479
4.2.	Implications of the 100 Ma global plate reorganisation on Tethyan evolution	480
4.3.	Greater India and its collision(s)	480
4.4.	Implications of India–Eurasia convergence for mantle structure	482
5.	Conclusions	484
	Acknowledgements	485
	Appendix A. Supplementary data	485
	References	485

1. Introduction

The Himalayas and Tibetan Plateau of Southern Eurasia represent the most studied orogenic belt on earth. Much of the continental material that accreted to Southern Eurasia rifted from the northern margin of East Gondwana, composed of Greater India, Australia, Antarctica, Madagascar, and other micro-continental fragments, such as Argoland, the Seychelles and Sri Lanka. The ensuing drift and dispersal of East Gondwana, initiating from the Late Jurassic, created the Indian Ocean (Fig. 1), and its evolution resulted in successive closure of the preceding Tethyan ocean basins (e.g. Audley-Charles et al., 1988; Veevers et al., 1991; Metcalfe, 2006; Seton et al., 2012). Yet, the exact timing of collisions along the Mesozoic–Cenozoic Eurasian margin, stretching from the Mediterranean to Southeast Asia, as well as the terranes involved, remains controversial. This is despite decades of mapping and data collection from this complex and long-lived convergence zone that is an archetypal Wilson cycle of ocean basin opening and closure.

The accretion of India to Eurasia culminated in the consumption of the Tethyan oceanic basin, raising the Tibetan Plateau (e.g. Hetzel et al., 2011; Rohrmann et al., 2012), forming the vast Alpine–Himalayan orogenic belt that has shaped the southern Eurasian margin following India's indentation into Tibet (Molnar and Tapponier, 1975), eventually leading to extrusion tectonics in SE Asia (Replumaz et al., 2004). Such a drastic change in topography has also fundamentally influenced regional and global climate, for instance in bolstering the South Asian monsoon by the blocking of a subtropical jet stream, or to cooling and the formation of ice sheets in both hemispheres, and increased chemical weathering causing reduction in atmospheric CO₂ concentration (Raymo and Ruddiman, 1992; Molnar et al., 2010). Changes in oceanic circulation contributing to Eocene/Oligocene events have also been discussed, particularly the end of circumterrestrial low-latitude circulation, which existed from Pangea breakup (Ricou et al., 1986). However, the nature and chronology of this terminal collision remain debated. The terminal continent–continent collision window is typically constrained to a range between ~65 and 55 Ma (e.g. Garzanti et al., 1987; Rowley, 1998; Wan et al., 2002; Garzanti, 2008), while other studies have proposed a “soft” initial collision between Greater India and a Tethyan intra-oceanic arc that preceded the final “hard” continent–continent collision at ~34 Ma (e.g. Sharma, 1987;

Soler-Gijón and López-Martínez, 1998; Aitchison et al., 2000, 2002b, 2007; Davis et al., 2002).

Although geological observations indicate a number of major changes in the convergence characteristics between ~65 and 35 Ma, identifying one or more discrete collisions becomes problematic due to the uncertainties in the locations and geometries of the pre-collision margins and the diachronous nature of the collisions along the active southern Eurasian margin. Uncertainty around the timings and geometry of accretionary episodes along the Eurasian margin is compounded by competing alternative models proposed for the breakup of East Gondwana, which are built from syntheses of geophysical and geological data but often without regional kinematic constraints. As a result, the proposed extent of Greater India varies by up to several thousand kilometres, which is hard to constrain since its leading edge is now underthrust and crumpled in the suture zone (e.g. Replumaz and Tapponier, 2003; Ali and Aitchison, 2005; van Hinsbergen et al., 2011a). Controversy also surrounds the extent, location and ultimate fate of Argoland, a continental terrane that rifted from East Gondwana in the Late Jurassic, leaving the Argo Abyssal Plain offshore NW Australia (e.g. Fullerton et al., 1989; Heine and Müller, 2005; Gibbons et al., 2012). The size and geometry of Greater India and Argoland can be better constrained using geological and geophysical data from the eastern Indian Ocean (Fig. 1), where relatively undeformed oceanic crust, punctuated by fracture zones, volcanic edifices and submerged plateaus, was recently incorporated into a regional, self-consistent plate kinematic model (Gibbons et al., 2012, 2013).

Plate kinematic models based on marine geophysical data from the Indian Ocean alone cannot be used to infer the timing and geometry of collisions along the Eurasian margin. Unravelling the chronology of these events requires knowledge of whether, or when and where, backarc basins in the Tethyan Ocean opened and were destroyed, as well as the nature of the colliding terranes, for instance distinguishing between continent–continent and arc–continent collisions. Previous studies have used seismic tomography models of the mantle to infer the location of Tethyan oceanic slabs and compared them to regional plate kinematic models. An early study interpreted positive P-wave seismic velocity anomalies in the upper mantle as delaminated sub-continental lithosphere, still attached to India, while deeper (>1000 km) anomalies beneath the Indian sub-continent were identified as sunken Tethyan

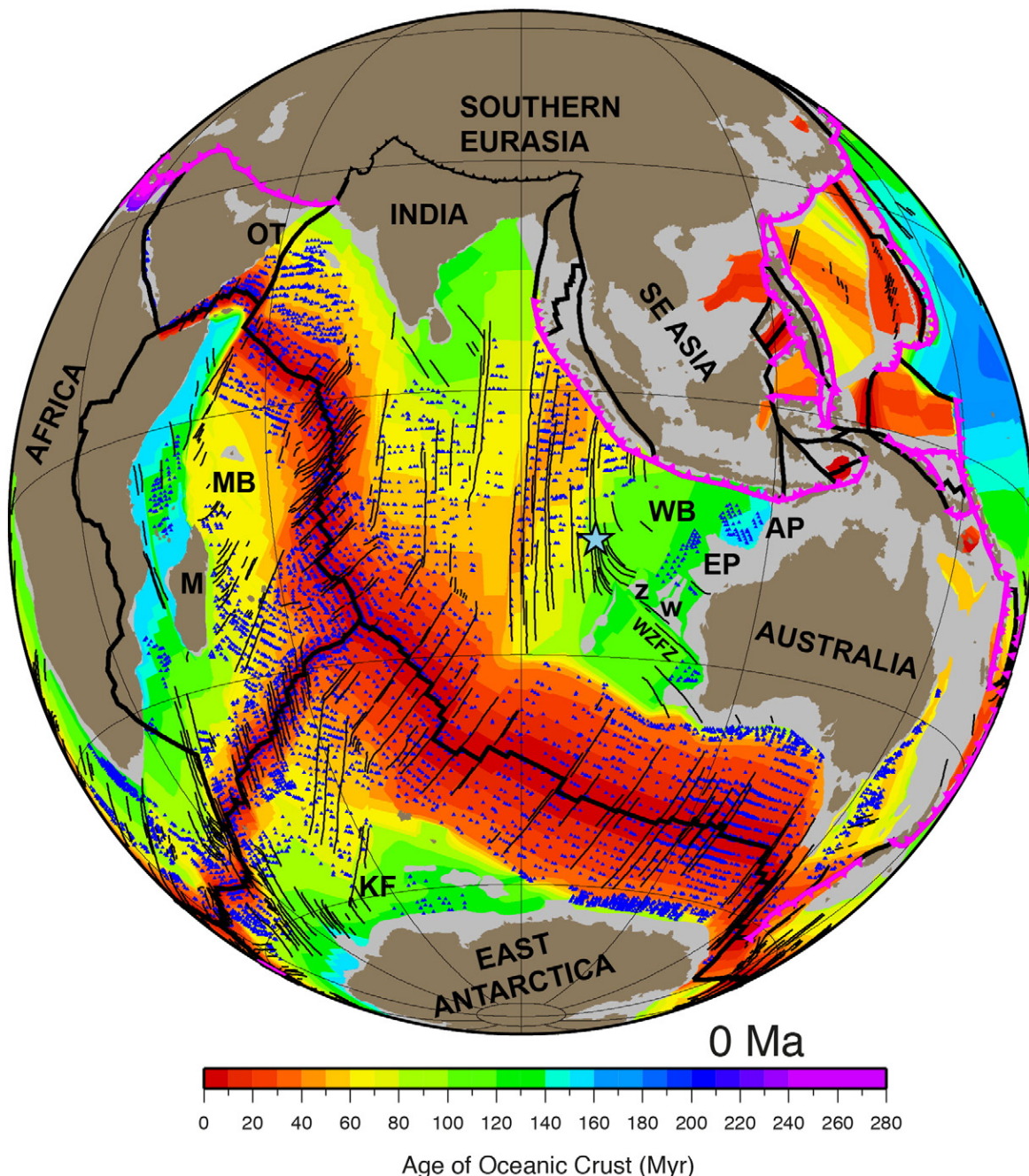


Fig. 1. Map featuring the present-day age grid of the Indian Ocean, including the main tectonic boundaries (thick black lines) based on Bird (2003), and geophysical data used to constrain the relative motion between the continental components of East Gondwana. These include magnetic anomaly picks (blue triangles), subduction zones (teethed pink lines), thrust faults (teethed black lines), and fracture zones (thin black lines, digitised from Matthews et al., 2011) offshore western Australia and East Antarctica, created by the motion between Argoland, Greater India, Australia and Antarctica. AP is Argo Abyssal Plain (labelled to the left), EP is Exmouth Plateau, KF is Kerguelen Fracture Zone, M is Madagascar, MB is Mascarene Basin, OT is Owen Transform (thick black line, labelled to the left), WB is Wharton Basin, the Wallaby-Zenith Fracture Zone (WZFZ) runs from SW Australia along the southern margins of the Wallaby (W) and Zenith (Z) plateaus. The blue star off western Australia (west of Wharton Basin) indicates the location of the Jurassic gabbro sample dredged during the CHRISP research cruise (Gibbons et al., 2012), providing a kinematic constraint on the extent of Greater India, as described in the text.

oceanic basin remnants, while more southerly deep-mantle anomalies were interpreted as remnants of intra-oceanic subduction that potentially occurred coevally with Andean-type subduction along the Eurasian margin in the Late Cretaceous (Van der Voo et al., 1999). More recent tectonic reconstructions, also derived from seismic tomographic methods, support the presence of a large backarc basin extending southwards, approximately to the equator between India and Eurasia (Hafkenscheid et al., 2006), while recent

geodynamic modelling also supports Tethyan intra-oceanic subduction (Zahirovic et al., 2012).

The aim of this paper is to review and synthesise the collisional history along the southern Eurasian margin, including the timing and nature of magmatism, suturing, crustal deformation, and onset of extrusion tectonics, and incorporate this information into a self-consistent global plate model with continuously-closing topological plate polygons and plate velocities through time. We incorporate recent

Table 1

Summary of geological events for each terrane.

Terranes/suture zones	Event	Age of event	Reference
Karakoram terrane	Three stages of batholith emplacement and a Paleogene tectonometamorphic event	Mid Cretaceous (110–95 Ma), Paleogene (up to 43 Ma), Upper Miocene	Debon et al. (1987)
	Continental arc rocks emplaced	~130–104 Ma	Heuberger et al. (2007)
	Calc-alkaline granites and granodiorites emplaced	~120–96 Ma	Searle et al. (1990a), Fraser et al. (2001), Thanh et al. (2010)
	Metamorphic rocks (sillimanite and kyanite-grade), cross cut by leucogranite dykes, and then plutons	63–4 Ma ~50–52 and 35 Ma ~36–34 Ma	Searle et al. (1999), Searle (2011)
	Karakoram Fault gneisses intruded by leucogranites	~23 Ma	Fraser et al. (2001), Searle (2011) Rex et al. (1988) Lacassin et al. (2004), Leloup et al. (2011)
Karakoram–Kohistan–Shyok Suture Zone	Age of Shyok Volcanics, north of Ladakh, if correlated west	Albian–Santonian or ~124 Ma	Coulon et al. (1986)
	Age of Shyok mélange diorite	145–130 Ma	Dunlap and Wysoczanski (2002)
	MORB-like basalts exhumed and thrust onto Karakoram margin near Ladakh	104 Ma (i.e., initiation of northward subduction beneath Karakoram)	Reynolds et al. (1983)
	Intrusions in Albian–Aptian limestones of Shyok mélange	~111–62 Ma	Thanh et al. (2012)
	Shyok mélange Tirit granite (similar age and composition to Ladakh Batholith)	~68 Ma (Andean-type characteristics)	Pudsey (1986)
	Post-collisional granites (isotopic links to ancient Asian crust)	47 and 41 Ma (intruding north Kohistan)	Rao and Rai (2009), Weinberg et al. (2000)
	Dacite and granodiorite intrusions in North Ladakh	Middle Eocene	Khan et al. (2009)
Kohistan–Ladakh Arc	Bulk of the KLA formed,	~134–95 Ma	Brookfield and Reynolds (1981)
	Sub-crustal mantle accretion,	~117 Ma	Petterson (2010)
	Thickening and metamorphism, intense (collisional) deformation	~95 Ma	
	Kohistan intruded by Matum Das tonalite, (backarc) dyke swarm, trondhjemite pluton	~90 Ma	Schaltegger et al. (2003)
	Dykes intrude Kohistan Kohistan Batholith, cross-cut by granodiorites, then granites	~154 Ma (proto-arc?) ~134 Ma ~102 Ma ~75 Ma ~54 Ma ~40 Ma	Khan et al. (2007)
	Kohistan Arc I-type granitoids (mantle-derived)	~75–42 ± 4.5 Ma (from amphibole fractionation)	Petterson and Windley (1985)
	Kohistan Batholith intruded by aplite–pegmatite sheets	34 ± 14 Ma (end of oceanic subduction)	Petterson and Windley (1992)
	Kohistan Batholith intruded by Chilas complex, following intra-arc rifting and extension	~85 Ma	Petterson (1985) (unpublished Ph.D. Thesis)
	Kamila Amphibolite Belt, tilted, exhumed and deformed	~107–81 Ma (then cooled in the early Campanian)	Jagoutz et al. (2009)
	Jijil Complex metamorphosed to granulite facies	~118 and 83 ± 12 Ma	Petterson and Windley (1985)
	KLA slab retreat	~105–91 Ma	Khan et al. (1996), Burg et al. (1998), Schaltegger et al. (2002), Dhuime et al. (2009)
	Dras/Ladakh Arc granodiorite	105–99 Ma	Yamamoto et al. (2005)
	Ladakh Arc experienced two granitic intrusion events, then its last major magmatic pulse, and rapid cooling	~103 Ma ~58 Ma and ~47 Ma ~50 Ma 49–44 Ma	Treloar et al. (1989). Yamamoto and Nakamura (2000), Dhuime et al. (2009)
	Ladakh Nindam Formation	Valanginian–Cenomanian	Bouilhol et al. (2011)
	Ladakh Dras 1 volcaniclastics, deformed	Albo–Cenomanian, ~79 Ma	Honegger et al. (1982)
Indus Suture Zone	Ladakh Khardung Volcanics	~53 and 56 Ma	Singh et al. (2007)
	Shangla blueschists peak metamorphism	~80 Ma	St-Onge et al. (2010)
	Sapi-Shergol mélange contains Albian radiolarians	Mid Cretaceous blueschist-bearing blocks	Weinberg and Dunlap (2000) Clift et al. (2002a)
	Spongtag Arc gabbros, over-lain by andesitic arc rocks, radiolarians, plus older basal fossils	~177 Ma (gabbros) ~88 Ma (andesites)	Robertson and Degnan (1994)
	Nidar ophiolite (eastern ISZ) dated by radiolarian fossils as well as radiometrically	Valanginian–Aptian, Triassic–Jurassic Hauterivian–Aptian ~126 Ma ~130–110 Ma	Fuchs (1982)
The Himalaya	Eastern Himalaya Syntaxis granulite metamorphism (of 89 Myr-old basaltic protolith)	~81 Ma, plus 167–86.3 Ma detrital magmatic zircons (from forearc)	Bhutani et al. (2009)
	Pakistan Himalaya Tertiary peak metamorphism	~47 Ma (20 Ma earlier than in East Himalaya)	Maluski and Matte (1984), Anczkiewicz et al. (2000)
	Himalayan amphibolite and granulite metamorphism	~36–33 Ma	Kojima et al. (2001)
		~37–32 Ma	Honegger et al. (1989)
Yarlung-Tsangpo Suture Zone	Various ophiolites generally coalesce into two age groups	Middle Jurassic or Lower Cretaceous	Pedersen et al. (2001)
	Contains the Zedong Arc, Dazhuqu ophiolitic belt, and Bainang accretionary wedge	Late Jurassic (~161 Ma)	Baxter et al. (2010)
	Andesitic detrital zircons in debris of the Xigaze Group	Aptian–Barremian	Fuchs (1981)
	Xigaze (exposed forearc) dolerite and quartz diorite intrusions	Mid-Aptian	Kojima et al. (2001)
	Xigaze Group, with a main stage of deep sea deposition, addition of continental crust	Peak at 190–150 Ma, and more so at 130–80 Ma 127–124 Ma (aka subduction initiation)	Zyabrev et al. (2008)
	Xigaze mélange age of amphibole in garnet	116–65 Ma (or Ypresian) ~107–84 Ma ~91 Ma	Maheo et al. (2004), Guo et al. (2013)
		~81 Ma (time of tectonic emplacement)	Wang et al. (2012)

Table 1 (continued)

Terranes/suture zones	Event	Age of event	Reference
Lhasa Terrane	amphibolite		
	Detrital zircons sampled near Xigaze suggest convergent magmatism until Late Eocene	~35 Ma (possibly sourced from the Linzizong Volcanics)	Aitchison et al. (2011).
	Lhasa batholiths four age-groups, including juvenile mantle-derived granite, an adakitic intrusion at ~80 Ma, peaking at ~50 Ma	~205–152 Ma ~188 Ma ~103–80 Ma ~65–45 Ma, or to 35 Ma ~33–13 Ma	Ji et al. (2009a), Chu et al. (2006) Lee et al. (2009), Wen et al. (2008), Ji et al. (2012) Ji et al. (2009a)
	Eastern syntaxis magmatic events (may match gaps in the Gangdese batholiths)	~152–103 Ma and ~80–65 Ma 165, 81, 61, 50, 25 Ma	Ji et al. (2009a) Guo et al. (2011)
	SE Lhasa Terrane charnockites with adakitic affinities, other adakites emplaced nearby	90–86 Ma (trench and ridge intersection)	Zhang et al. (2010b)
	Linzizong Volcanics erupted as subaerial andesitic subduction-related magmatism	~84 Ma (spreading ridge subduction) Between ~69 and 43 Ma, with a climax ~50 Ma	Guan et al. (2010) Coulon et al. (1986), He et al. (2003), Zhou et al. (2004), Lee et al. (2012)
	Linzizong granite intrusion then accelerated cooling, then end of arc magmatism	~52 Ma (flare-up at 50 Ma–42 Ma (slab break-off))	He et al. (2007)
	Linzizong andesites formed earlier east of ~87°E	~75–59 Ma (east) ~60–51 Ma (west)	Zhou et al. (2010a)
	Evolved rhyolitic flows and ignimbrites (continental melt)	~60 Ma (slab rollback) ~50 Ma (slab break-off)	Lee et al. (2009, 2012)
	Yeba mafic-felsic rocks erupted	190–174 Ma (arc on thin/new continental crust)	Dong et al. (2006), Zhu et al. (2008b)
	Bivalves in Yeba volcanics	~180 Ma	Yin and Grant-Mackie (2005)
Bangong–Nujiang Suture Zone	Sangri volcanics erupted	112–71 Ma	Lee et al. (2009)
	Volcanism in Northern Lhasa coeval with Takena	~110–80 Ma	Coulon et al. (1986)
	Formation andesitic dyke intrusion	~90 Ma (plus a ~52 Ma folded dyke)	He et al. (2003)
	HP metamorphic belt dividing the Lhasa Terrane east to west	~292–242 Ma	Yang et al. (2009)
	Volcanic and plutonic rocks respectively emplaced in Northern Lhasa	~143–102 Ma, ~80 Ma, with a magmatic flare-up at ~110 Ma)	Zhao et al. (2008)
	South Lhasa magmatism (from lithospheric delamination), then subduction-related adakites	135–100 Ma (upwelling asthenosphere)	Zhu et al. (2009a)
	Tibetan Plateau exhumed and cooled	90–78 Ma	K.J. Zhang et al. (2012)
	~70–55 Ma, stabilised at ~48 Ma (or ~45 Ma)		Hetzell et al. (2011)
	Granitoids in eastern Lhasa, and earlier granitic intrusion	~133–110, ~66–57 Ma, ~198 Ma	Rohrmann et al. (2012)
	Radiolarians (N-central)	Early Aptian	Chiu et al. (2009)
Qiangtang Terrane	Several ophiolites obducted onto the Lhasa Terrane's northern margin	Late Jurassic–Early Cretaceous	Baxter et al. (2009)
	The west has remnants of a subduction–accretion complex	Jurassic–Mid-Cretaceous	E.g. Girardeau et al. (1984a), Dewey et al. (1988), Pearce and Deng (1988)
	The ophiolitic belt widens further east e.g., at Donqiao	~180–175 Ma (metamorphic aureole)	Kapp et al. (2003)
	Precambrian Amdo granitoids, likely exhumed coeval/prior to the Qiangtang anticline	~185–170 Ma by the mid-Cretaceous	Zhou et al. (1997)
Southeast Asia	South Qiangtang and Lhasa terranes drifted from Gondwana	Early Permian to Late Triassic	Gwynn et al. (2006)
	Central eclogites interpreted as a Triassic suture zone (inc. intra-oceanic arc)	230–237 Ma (exhumed at ~220 Ma)	Kapp et al. (2005)
	Age of South Qiangtang granites and volcanic tuffs	~145 Ma and ~111 Ma	Schneider et al. (2003) Sciunnach and Garzanti (2012)
	Argoland rifted from Australia, likely accreted to SE Asia from Late Cretaceous time	Late Jurassic (155 Ma)	Zhai et al. (2011)
	Continental collision with Sundaland and Java	Mid-Late Cretaceous	Pullen et al. (2008)
	Woyla Arc attributed to an allochthonous terrane collision	c. 80 Ma	Kapp et al. (2005)
	Woyla Group intruded by the Sikuleh granodiorite batholith	Albian–Aptian	E.g. Metcalfe (1996, 2011b), Acharyya (1998), Heine and Müller (2005), Hall (2011)
	UHP metamorphic rocks (highly aluminous protolith) intrude southwestern Sulawesi/Celebes	~97.7 Ma	Wakita (2000)
		115–110 Ma (though not clear from which side of the trench they came)	Clements and Hall (2011)

reinterpretations of magnetic anomalies offshore Western Australia (Gibbons et al., 2012) and East Antarctica (Gibbons et al., 2013), that revise the earliest spreading history of the Indian Ocean (Late Jurassic to Early Cretaceous). To revise the spreading history of the preceding Tethys Ocean, we adapt intra-oceanic subduction from regional plate models for Eurasia and Southeast Asia (Zahirovic et al., 2012, 2014), with refinements that account for magmatic gaps and ridge subduction episodes on the overriding plate (namely the geological record of the Lhasa terrane, see Table 1), and paleomagnetic constraints for the

terranes, where available (see Table 2). The model was constructed interactively using the open-source and cross-platform GPlates software (Boyden et al., 2011).

2. Eurasian and Southeast Asian geology

Many authors describe the growth of the Southeast Asian and Eurasian regions through accretionary episodes in great detail (e.g. Allegre et al., 1984; Chang et al., 1986; Searle et al., 1987; Dewey et al.,

Table 2

Summary of paleomagnetic studies.

Terrane	Volcanics	Age	Paleolatitude	Reference
Lhasa terrane	Southern Lhasa red bed Takena Formation, the Linzizong Volcanics were deposited above	Upper Cretaceous and Paleocene, 69–43 Ma, with peak at ~50 Ma	~12.5° (with ~41.5° a/c rotation) ~13.5°N	Achache et al. (1984), Coulon et al. (1986), He et al. (2003), Lee et al. (2012), Zhou et al. (2004)
	Linzizong Volcanics (Lhasa) mafic dykes	~53 Ma	~14.4 ± 5.8°N	Liebke et al. (2010)
	Linzizong Group (above the volcanics)	Lower Paleogene	~10°N	Chen et al. (2010).
	Linzizong Volcanics inclination-corrected paleolatitudes	Lower Paleogene	21–27°N 22.8 ± 4.2°N 20 ± 4°N	Tan et al. (2010) Dupont-Nivet et al. (2010) Huang et al. (2013)
	Northern Lhasa Terrane's rhyolitic tuffs	55 Ma	13.8 ± 7.3°N	Sun et al. (2010)
Qiangtang terrane	Central Lhasa Terrane Zenong Group	~130–110 Ma	~19.8 ± 4.6°N	Chen et al. (2012) Zhu et al. (2008a)
	Volcanic rocks in South Qiangtang	~40 Ma	~28.7 ± 3.7°N, or ~20°N in Eocene	Lippert et al. (2011)
Kohistan–Karakoram	Remagnetisation in northern Kohistan Red bed formations along the SSZ	50–35 Ma	25 ± 6°N 1–2°N	Ahmad et al. (2001) Zaman and Torii (1999)
	Utror Volcanics, south of Kohistan Batholith	Mid-Late Cretaceous	9–13 ± 4°N	Ahmad et al. (2000)
Himalaya–India	Tethyan Himalaya marine sediments	55–45 My-old	~4.7 ± 4.4°S	Yi et al. (2011)
		~62–56 Ma	Recalculated to 8.7 ± 1.7 N	van Hinsbergen et al. (2012)
	Tethyan Himalaya limestones	Latest Paleocene	~5–10°N	Besse et al. (1984)
	North Indian sediments	~66 Ma, ~60 Ma	5.7°S and 4°N	Patzelt et al. (1996)
		71–65 Ma	Recalculated to 4.9 ± 2.8°S	van Hinsbergen et al. (2012)

1988; Yin and Harrison, 2000; Metcalfe, 2011b). Generally, the suture zones presently in Eurasia, demarcating Tethyan terranes (Fig. 2), are nearly east–west trending. The terranes north of the Himalaya can be divided into east and west partitions by two main faults running southeast and southwest of the Tarim Basin (Fig. 2). The Tarim Basin is underlain by the largely undeformed Tarim craton, where deformation has been focused on its boundaries, resulting in large-scale faulting and orogenesis. The sinistral Altyn Tagh Fault (ATF) forms the boundary

between the Tarim Basin and the eastern terranes (in Tibet and China), which from north to south include, Kunlun–Quaidam (Kunlun), Songpan–Ganzi–Hoh Xil (Songpan), Qiangtang, Lhasa, Himalaya (deformed India with Tethyan remnants) and India. These terranes are respectively divided from north to south by, the Anyimaqen–Kunlun–Muztagh Suture Zone (AKMSZ), Jinsha Suture Zone (JSZ), Bangong–Nujiang Suture Zone (BNSZ), Yarlung–Tsangpo Suture Zone (YTSZ), and the Main Boundary Thrust (MBT). Further west, the ATF

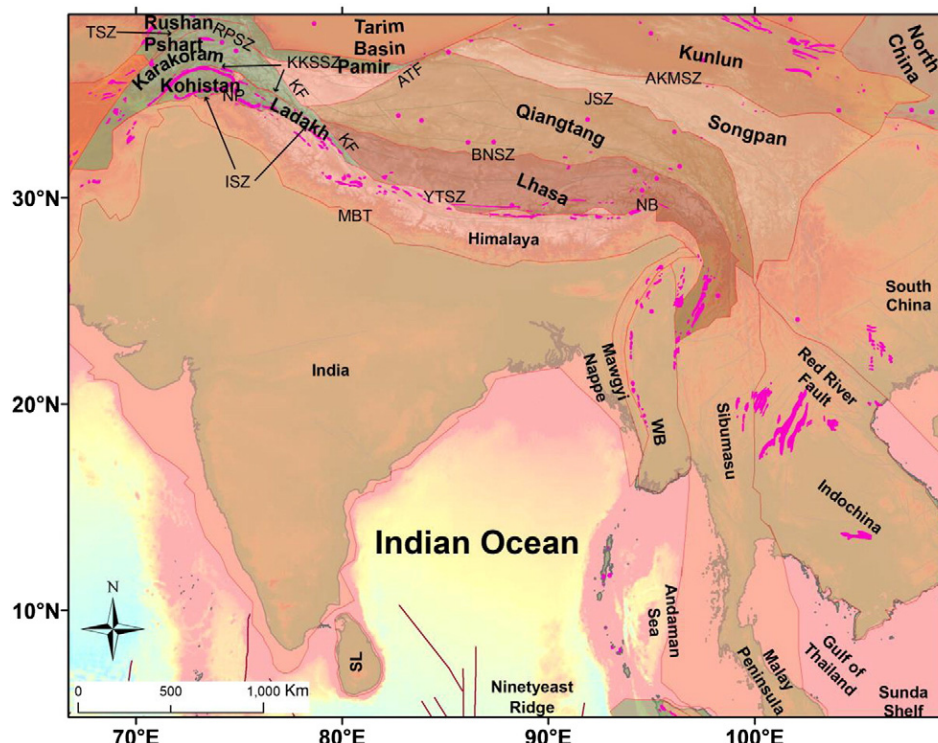


Fig. 2. Regional tectonic map of Southern Eurasia, including fracture zones (brown, Matthews et al., 2011), ophiolites (magenta, Hutchison, 1975; Zahirovic et al., 2014) and continental faults (thin grey, Hearn et al., 2003), plotted on a topography-bathymetry basemap (Amante et al., 2009). Also showing the sinistral Altyn Tagh Fault (ATF), Anyimaqen–Kunlun–Muztagh Suture Zone (AKMSZ), Bangong–Nujiang Suture Zone (BNSZ), Indus Suture Zone (ISZ), Jinsha Suture Zone (JSZ), dextral Karakoram Fault (KF), Karakoram–Kohistan–Shyok Suture Zone (KKSSZ), Main Boundary Thrust (MBT), Nanga Parbat/West Himalaya Syntaxis (NP), Namche Barwa/East Himalaya Syntaxis (NB), Rushan Pshart Suture Zone (RPSZ), Sri Lanka (SL), Tanjumas Suture Zone (TSZ), West Burma (WB), and Yarlung–Tsangpo Suture Zone (YTSZ).

terminates along the dextral Karakoram Fault (KF), which isolates terranes west of Tibet, including from north to south: Pamir, Rushan Pshart, Karakoram, Kohistan–Ladakh, Himalaya and India. These terranes are respectively divided from north to south by the Tanyemas Suture Zone (TSZ), Rushan Pshart Suture Zone (RPSZ), Karakoram–Kohistan–Shyok Suture Zone (KKSSZ, also referred to as the Northern Suture Zone, north of Kohistan), Indus Suture Zone (ISZ), and the southern thrust systems, including the Main Boundary Thrust (MBT). A study of detrital zircons (Gehrels et al., 2011) suggests that the terranes south of the Jinsha Suture Zone (JSZ, Fig. 2), at least southern Qiangtang, Lhasa and Himalaya (formerly Greater India), were derived from the Gondwanan margin, possibly rifting as part of the Cimmerian continent (e.g. Sengor, 1987). Recent radiometric dating and geochemical analysis of the Panjal Traps of Kashmir help constrain the rifting of Cimmeria from Gondwana to the Early Permian (Shellnutt et al., 2011, 2014a). For continuity, existing knowledge about the terranes and suture zones will be outlined from north to south, west of the Karakoram Fault, then from south to north, east of the Karakoram Fault, and summarised in Tables 1 and 2.

2.1. Karakoram terrane

The northern margin of the Karakoram terrane (Figs. 2, 3 and 4) records Late Devonian–Early Carboniferous rifting, which formed before it migrated north as part of the Cimmerian continent (Heuberger, 2004; Heuberger et al., 2007) in the Early Permian (Shellnutt et al., 2011, 2014a). From south to north, the terrane can be divided into a metamorphic complex, batholith, and sediments consisting of Carboniferous shales, Permian–Mesozoic carbonates, conglomerates and tuffs, with mid-late Cretaceous gneissic intrusions (Rex et al., 1988). The batholith, emplaced in stages during mid Cretaceous, lower Paleogene (with a large Paleocene tectonometamorphic event), and Upper Miocene

(Debon et al., 1987), is a subduction-related igneous crustal body of mainly massive or weakly foliated biotite–granodiorite (Pudsey, 1986). Intrusive, continental arc rocks dated at ~130–104 Ma, and arc magmatism, dated at ~112–39 Ma, identified further south in Kohistan, can be isotopically (Hf) traced to the Karakoram terrane (Heuberger et al., 2007). Other calc-alkaline granites and granodiorites aged ~120–96 Ma suggest that subduction along the southern Karakoram margin had initiated by at least ~120 Ma, before causing continental arc magmatism (Searle et al., 1990a; Fraser et al., 2001; Thanh et al., 2010). The Karakorum Metamorphic Complex is composed of meta-sedimentary sequences, felsic gneisses and migmatites, and mélange that includes ultramafic material from the KKSSZ (Rex et al., 1988). Crustal thickening from ~63 Ma formed sillimanite and kyanite-grade metamorphic rocks (Searle et al., 1999; Searle, 2011), cross-cut by leucogranite dykes dated at ~50–52 and 35 Ma (Fraser et al., 2001; Searle, 2011), and plutons dated ~36–34 Ma (Rex et al., 1988). Heuberger (2004) notes that the regional metamorphism in eastern Karakoram roughly coincided with ferriferous-alkaline intrusions and ~83–71 Ma carbonates, suggesting a shallow marine basin was present.

2.2. Kohistan–Karakoram–Shyok Suture Zone

The Kohistan–Karakoram–Shyok Suture Zone (KKSSZ, Figs. 2 and 4), also known as the Northern Suture Zone, north of Kohistan, divides Karakoram from the Kohistan (west) and Ladakh (east) terranes (Shyok Suture Zone separates Ladakh and Karakoram terranes). Southward-dipping thrusts and strike-slip faulting in the KKSSZ suggest that Kohistan has overridden the Karakoram terrane in some locations (Coward et al., 1986; Coward et al., 1987; Heuberger, 2004). The KKSSZ was interpreted to represent the tectonised remnants of a marginal backarc basin (Thakur and Misra, 1984). From north to south, the main tectonostratigraphic units of the KKSSZ include the Shyok

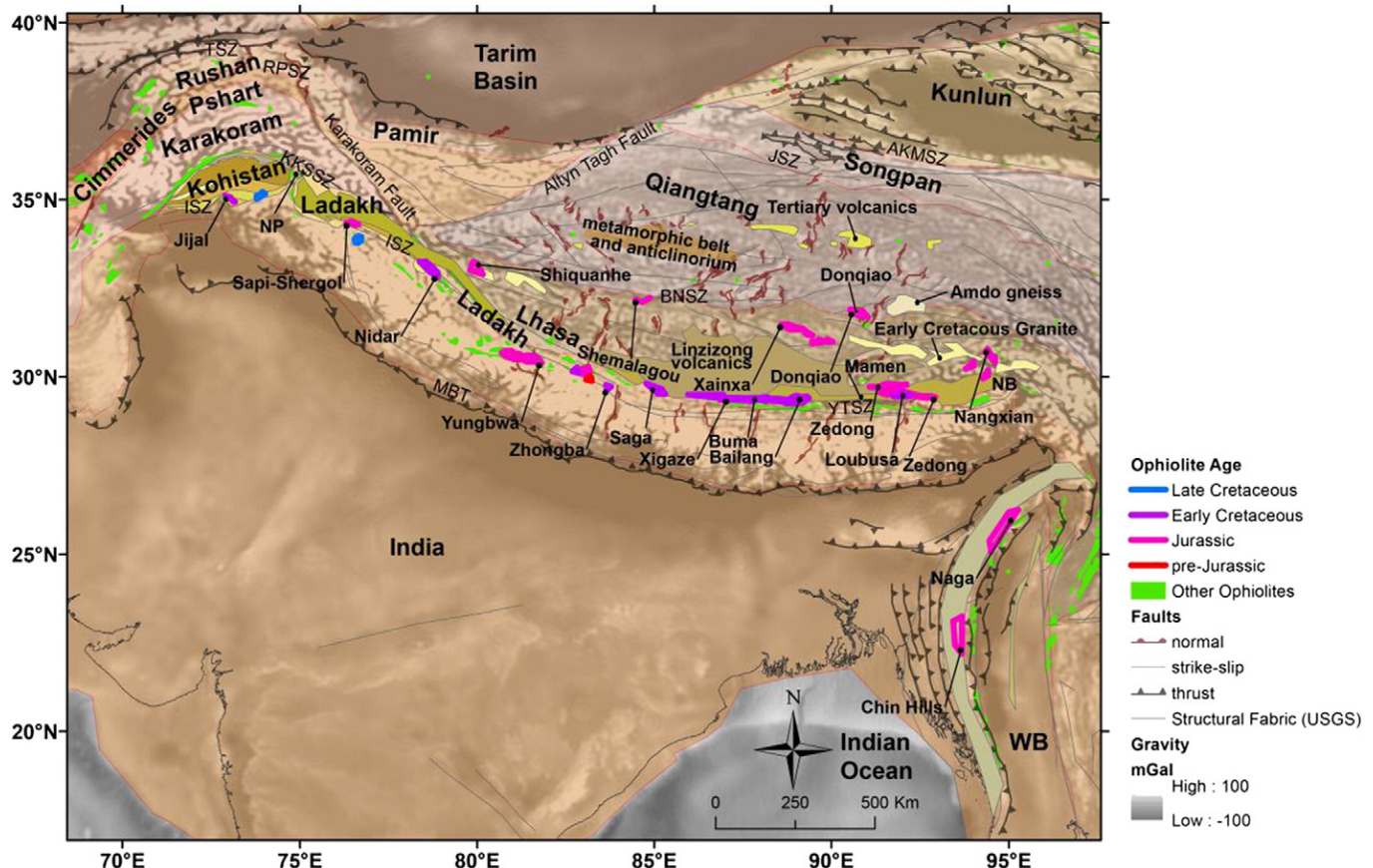


Fig. 3. Main tectonic and magmatic features of Southern Eurasia, with approximate locations of ophiolites, age colour-coded, right. Other details are as in Fig. 2.

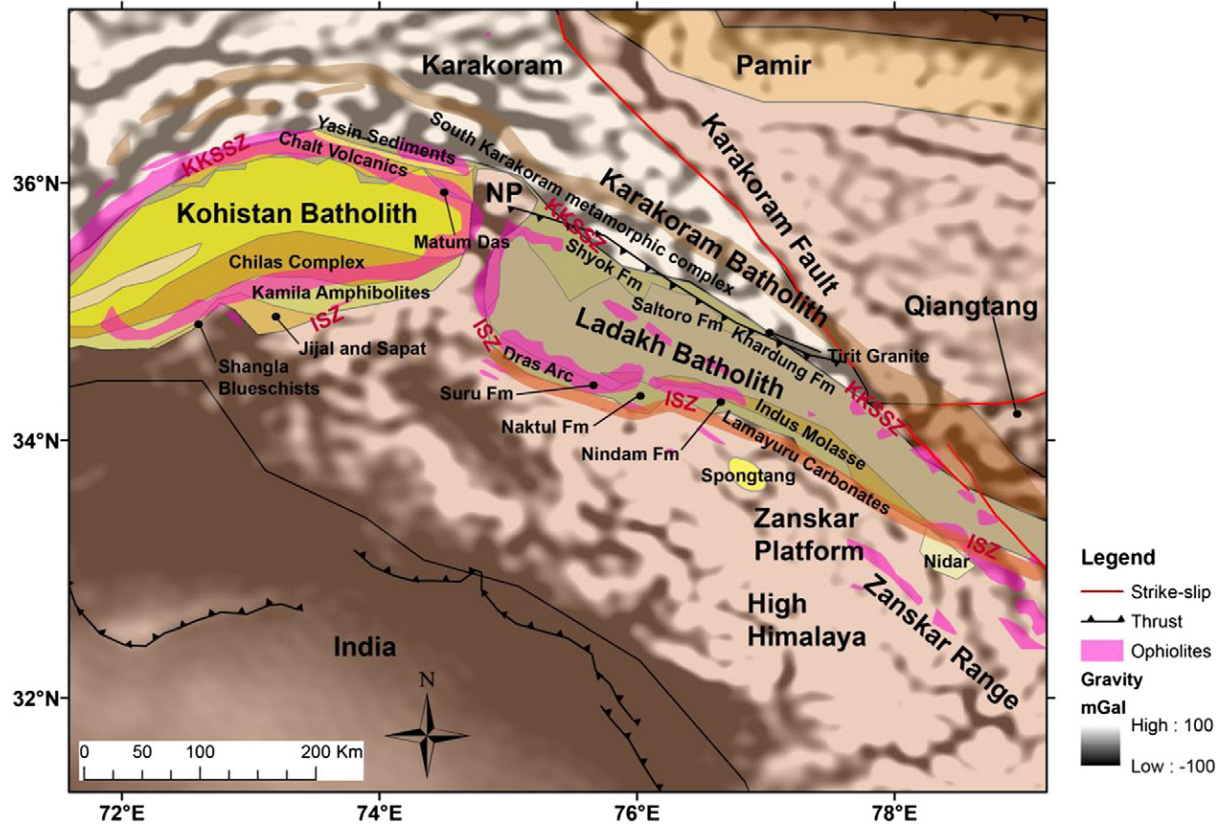


Fig. 4. Main geological units of the Kohistan–Ladakh Arc (KLA) with approximate locations of volcanic and sedimentary formations, and metamorphic features on a free-air gravity anomaly basemap (Sandwell and Smith, 2009). Ophiolites are adapted from Hébert et al. (2012) and fault geometries are from Styron et al. (2010). ISZ is the Indus Suture Zone, KKSSZ is the Karakoram–Kohistan–Shyok Suture Zone.

and Nubra ophiolitic mélange, the Shyok and Khardung Volcanics (Thakur, 1990) and the overlying Saltoro flysch, which contains upper Cretaceous to Eocene fossils (Bhutani et al., 2009). Strike-slip motion along the Karakoram Fault transported the Shyok Volcanics southward and adjacent to the rhyolitic Khardung Volcanics, which overlie the northern margin of the Ladakh Batholith and are younger, dated at ~53 and 56 Ma (Bhutani et al., 2009). This previous study (Bhutani et al., 2009) argues that a Paleocene age for the Khardung Volcanics (Dunlap and Wysoczanski, 2002) was likely derived from zircons that were inherited from continental crust or a mature-arc, thus preferring the Eocene age of at least 52 Ma. The Shyok Volcanics were dated at ~124 Ma (Coulon et al., 1986; Dunlap and Wysoczanski, 2002).

Between the Ladakh and Karakoram terranes, the KKSSZ has been divided into a western group of basaltic olistoliths with backarc mineral chemistry and more southerly andesites with island-arc tholeiite to calc-alkaline affinities, and an eastern group of basaltic-andesitic lavas, interlayered with Albian–Cenomanian siliciclastic Ladakh Arc-derived sediments (Rolland et al., 2000). This variation was explained potentially as the west to east evolution from backarc to continental arc, possibly developing after subduction of a NeoTethyan spreading centre, following India's rapid northward motion in the mid Cretaceous (Rolland et al., 2002). A weak zone of transitional crust between oceanic and continental lithosphere may have initiated the Karakoram Fault, responsible for juxtaposing the Khardung and Shyok Volcanics (Bhutani et al., 2009).

Alternatively, the eastern KKSSZ (Shyok Suture Zone) may have had no continental arc component and instead be related to a mid-Cretaceous equatorial intra-oceanic arc, also recorded in the YTSZ of southern Tibet (Abrajevitch et al., 2005). Robertson and Collins (2002) interpret the KKSSZ rocks northeast of the Ladakh Batholith as a subduction–accretion complex of distal marginal origin. They assign the

southern succession to a wider intra-oceanic basin, separating the mature arc-like rocks from Ladakh–Kohistan via the tectonic mélange, which they suggest allows correlation with a similar sequence in southern Tibet (Aitchison et al., 2000), including an Andean-type arc (southern Lhasa terrane), accreted oceanic arc (Zedong, Fig. 3) and forearc (Dazhuqu, ~150 km east of Xigaze, Fig. 3), described further in Section 2.7. The four main lithological units Robertson and Collins (2002) identify include the lower and southern-most (Askore) amphibolites, which overlie a non-terrigenous, volcano-sedimentary formation derived from the Ladakh Arc (Burje-La). The amphibolites are overlain by a volcanoclastic apron related to Ladakh backarc rifting (the Cretaceous Pakora Formation, with no terrigenous input), which may be correlated with the Yasin sediments in northern Kohistan (see Section 2.3). The volcanoclastic apron is overlain by the laterally-discontinuous Shyok tectonic mélange or by the terrigenous Ordovician–Triassic Bauma-Harel group, which borders the Karakoram margin and records its rifting from Gondwana. The Shyok Formation (Fig. 4) of deformed metasedimentary and metavolcanic rocks is in contact with the southeast margin of the Karakoram Batholith but cannot be traced east of the Karakoram Fault into Tibet (Bhutani et al., 2009). Activation of the Karakoram Fault from as early as 25 Ma (Leloup et al., 2011), and granodiorite intrusions from the Ladakh Batholith, have disturbed the age spectra of the Shyok Volcanics, but these may be Albian–Santonian in age (Coulon et al., 1986), if correlated with the Yasin Group of northern Kohistan (Pudsey, 1986) or older, as they seem continuous with ~124 Ma metasediments (Dunlap and Wysoczanski, 2002).

Further west, Robertson and Collins (2002) interpret the mixed volcanogenic and terrigenous succession between Kohistan and Karakoram as syn-deformational infill of a remnant backarc basin/foreland basin that formed prior to suturing between Kohistan and Karakoram terranes. The mélange includes a mainly Kohistan Arc-

derivedolistostrome with depositional rather than tectonic contacts, suggesting that the suture zone formed during closure of a backarc basin in the mid to Late Cretaceous, given ~111–62 Ma intrusions within Albian–Aptian limestones in the mélange (Pudsey, 1986). Burg (2011) instead suggests that under-thrusting (parts of Karakoram beneath Kohistan–Ladakh) finally closed the backarc system (at least between the Kohistan–Ladakh and Karakoram terranes) in the middle Eocene, coinciding with dacite and granodiorite intrusions in northern Ladakh (Brookfield and Reynolds, 1981). The Cretaceous–Eocene Shyok mélange (Rai, 1982), southwest of the Karakoram Batholith, was intruded by the Tirit granite (Fig. 4) at ~68 Ma, which has Andean-type characteristics (Rao and Rai, 2009) and a similar age and modal composition to the Ladakh Batholith (Weinberg et al., 2000). Two Eocene-aged (47 and 41 Ma), post-collisional granites in northern Kohistan, with isotopic links to ancient Asian crust, may link the KKSSZ to the YTSZ, the latter was dated at 51 Ma (Khan et al., 2009).

2.3. Kohistan–Ladakh Arc

Further south, Ladakh and Kohistan terranes (Fig. 4) are laterally equivalent, and typically correlated with each other, although they are not geologically identical and therefore may have undergone separate tectonic processes (e.g. Pudsey, 1986; Robertson and Collins, 2002; Burg, 2011). The terranes are divided by tectonic thinning about the Nanga Parbat (Western Himalayan Syntaxis), a large-scale, antiformal structure where regional cooling occurred at 25 ± 5 Ma (Treloar et al., 2000) and present-day uplift rates can exceed ~6 mm/yr (Treloar et al., 1991). The Ladakh and Kohistan terranes have been interpreted as the remains of a single intra-oceanic arc, the Kohistan–Ladakh Arc (KLA) (e.g. Bard, 1983; Coward et al., 1987; Khan et al., 1996; Petterson, 2010), thought to have initiated in the Early Cretaceous over a Late Jurassic–Early Cretaceous oceanic substratum (Honegger et al., 1982; Reuber, 1989). The KLA may have stretched along the Tethys but only ophiolites outcrop east of the Karakoram Fault, extensively in the YTSZ and BNSZ (Sections 2.7 and 2.9).

The Kohistan portion of the KLA can be divided into six mainly Cretaceous units (Fig. 4) including (north to south), the Yasin Sediments, Chalt Volcanics, Kohistan Batholith, Chilas Ultramafic Complex, Kamila Amphibolite Belt, and Jijal Ultramafic Complex (Petterson and Windley, 1985; Pudsey, 1986; Petterson and Windley, 1992). In northern Kohistan, the Albian–Aptian Yasin slates, turbidites and limestones formed in intra-arc basins. The Yasin Sediments and the Chalt Volcanic Group of pillow-bearing island arc tholeiitic lavas, calc-alkaline andesites and rhyolites, were intruded by the Kohistan Batholith, which has been divided into an early, deformed group and younger undeformed group. The older Kohistan Batholith group contains the ~154 Ma Matum Das tonalite (Schaltegger et al., 2003), and a ~102 Ma trondhjemite pluton (Petterson and Windley, 1985). Burg (2011) describes the ~154 Ma old Matum Das tonalite as a potential proto-arc that may document changes in plate motion between Gondwana and Eurasia. At ~134 Ma, a dike swarm of backarc affinity intruded the north-central area of the batholith, the NW–SE orientation of the dike intrusions could indicate the direction of early Cretaceous spreading (Khan et al., 2007).

The Chilas Gabbronorite Complex (Fig. 4) intruded the southern part of the Kohistan Batholith, northern sediments and more southern (Kamila) amphibolites, at ~85 Ma (Schaltegger et al., 2002; Dhuime et al., 2009). The Chilas Complex was initially thought to represent the magma chamber of the arc (Rai and Pande, 1978), but has since been attributed to intra-arc rifting (Khan et al., 1996; Burg et al., 1998). Further south, the Kamila Amphibolite Belt (Fig. 4) is mainly composed of amphibolites and metasediments that underwent ductile deformation between ~107 and 81 Ma (Yamamoto et al., 2005), and then cooling in the early Campanian (Treloar et al., 1989). The eastern portion thrusts directly onto the Tethyan Himalaya and may represent a southerly, metamorphosed equivalent of the Kohistan Arc, or an earlier accreted

arc (Searle et al., 1987). Treloar et al. (1996) ascribe the belt as the oldest unit of the arc, representing a Lower Cretaceous or older subduction basement that was intruded by arc-type gabbroic sheets and plutons.

The Jijal Complex (Fig. 4), the deepest and most southern outcrop of the Kohistan terrane, is a garnet-granulite body of ~150 km² extent, that occurs in the hanging wall of the ISZ (Jan and Howie, 1981), and formed between ~118 and 83 ± 12 Ma (Yamamoto and Nakamura, 2000). A garnet-free ultramafic body of ~40 km² area was thought to have intruded the Jijal Complex and was variously explained as a faulted slab of upper mantle/sub-oceanic crust, an orogenic diapir, or ultramafic rocks isolated from basaltic magma (Jan and Howie, 1981). The contact between the garnet-free ultramafic body and the Jijal Complex has been described as the sub-arc petrological Moho (Burg et al., 1998) or in-situ dehydration melting of plutonic rocks buried at depths exceeding 25–30 km at 900 °C (Garrido et al., 2006). High Mg, low REE basal dunites, wehrlites and clinopyroxenites of the Jijal mafic-ultramafic basal section may have been created through sampling of a metasomatised mantle wedge in the initial stages of subduction before boninitic magmas left behind a lherzolite lens (Dhuime et al., 2007). Boninites often form in association with tholeiitic arcs and are thought to originate from a depleted/refractory, metasomatised peridotite melt, such as the residue from an earlier arc, with elevated geothermal gradient and supply of hydrous fluid (e.g. Hickey and Frey, 1982) either during plume slab-window interaction (Falloon et al., 2008), or in the early stages of subduction sampling an undisrupted mantle wedge (Dobson et al., 2006). Such settings include forearcs and primitive island arcs, either with low-angle interaction between the spreading centre and volcanic arc, or a high-angle interaction between spreading centre and young subduction zone or transform fault (Deschamps and Lallemand, 2003). Underplating and thermo-mechanical erosion may also have metamorphosed the base of the Kohistan Arc (Jijal) to granulite facies at ~105–91 Ma, possibly before intra-oceanic subduction ended, leaving a 'cold blanket' at ~85 Ma, coinciding with a magmatic pulse that formed the Chilas Complex (Dhuime et al., 2009).

Further east, the Sapat mafic–ultramafic layered complex (Fig. 4) was initially identified as the base of the Kohistan Arc due to its mineral chemistry (Jan et al., 1993; Searle et al., 1999). Khan et al. (2004) suggested it may have formed in a supra subduction zone setting of forearc affinity, after analysis of chrome spinel grains from its peridotite-bearing dunite. Field relations, micro-textures and geochemistry also indicate that the Sapat rocks may have formed following reactions between primitive arc-melt and metasomatised, depleted meta-harzburgites/refractory mantle (Bouilhol et al., 2009). Geochemical tracers and Ar–Ar zircon dating suggest this may have been due to slab retreat between 105 and 99 Ma, which caused the splitting of the Kohistan Arc at ~85 Ma and intrusion of the Chilas Complex (Bouilhol et al., 2011).

Evolution of the Kohistan portion of the KLA is still debated. A recent tectonic summary (Petterson, 2010) suggests that the bulk of the island arc formed during ~134–95 Ma, with sub-crustal mantle accretion from ~117 Ma, and crustal thickening that led to wide-spread granulite-facies metamorphism by ~95 Ma, before a collision (previously suggested with Eurasia) caused intense deformation at ~90 Ma. The Kohistan Arc was then extended and intruded by ultramafic diapirs at ~85 Ma (Chilas Complex, discussed later in this section, Fig. 4), then by Andean-type gabbros, granites and diorites (Petterson, 2010). Accretion of Kohistan to Asia may have occurred from as early as ~100 and 75 Ma, based on relatively undeformed dykes intruding through the folded Kohistan Batholith at ~75 Ma (Petterson and Windley, 1992). The younger group (75 Ma undeformed dykes) is cross-cut by granodiorites dated ~54 Ma, and granites dated ~40 Ma (Petterson, 1985, unpublished Ph.D. Thesis). However, recent field mapping has identified a ~50 Ma old metagabbro intrusion with an intense fabric similar to that of a 'stage 1' (inferred as pre-collisional) pluton (Jagoutz et al., 2009). The I-type granitoids, intruding Kohistan Arc during 75–42 ± 4.5 Ma, have been attributed to mantle-derived melts that evolved through

amphibole fractionation with intra crustal assimilation (Jagoutz et al., 2009). Aplite–pegmatite sheets, derived from young oceanic crust and/or mantle, intruded the Kohistan Batholith 34 ± 14 Myrs ago, likely the time that oceanic subduction and calc-alkaline magmatism ended (Petterson and Windley, 1985).

Another recent review of the Kohistan portion of the KLA (Burg, 2011) suggests an alternative model, with two parallel north-dipping subduction zones operating between ~ 130 and 90 Ma, north and south of the Kohistan Arc. This may extend to Ladakh Arc (discussed later in this section), following evidence of supra-subduction rocks on the southern Karakoram margin, suggesting that subduction beneath the Karakoram terrane must have initiated by ~ 104 Ma (Thanh et al., 2012). Closure of the KKSSZ need not have occurred prior to 75 Ma, due to evidence of continued tectonic and (Karakoram-derived) magmatic activity well into Eocene time (e.g. Heuberger et al., 2007). Simultaneous north-dipping subduction along the Kohistan Arc and Eurasian continental margin is suggested to have continued until arc-normal rifting and extension formed the Chilas Complex at ~ 85 Ma (Burg et al., 1998, 2006; Jagoutz et al., 2006), and tilted and exhumed the Kamila Amphibolites at ~ 80 Ma (Treloar et al., 1989). This ended magmatic activity and restricted marine basins to form where intra-arc crustal thickness was reduced from ~ 50 to 25 km (Burg, 2011). Burg (2011) suggests that the (Kohistan) intra-arc rifting, attributed to trench rollback (Treloar et al., 1996; Burg et al., 2006), may have removed the need for subduction along the southern Karakoram margin (post- 96 Ma) as India's faster northward motion i.e., faster subduction of the Tethys, then formed most of the Kohistan Batholith. Continued closure between India and Eurasia resulted in locking of the intervening Kohistan Arc (or KLA) during the Eocene–Miocene (Brookfield and Reynolds, 1981; Reynolds et al., 1983), as convergent thrusting created unconformable Eocene lavas, 30 Ma old plutons, and mainly north-vergent/south-dipping structures in the KKSSZ (Burg, 2011).

Further east, the Ladakh terrane (Figs. 2, 3 and 4) can be divided into three main belts, which from north to south include the Khardung Volcanics, Ladakh Batholith and Dras Arc (Fig. 4) – the latter is considered analogous to the Kohistan Arc (Reuber, 1989). The acidic, Early Eocene Khardung Volcanics (Thakur and Misra, 1984; Virdi, 1987; Bhutani et al., 2009), resting unconformably on the northern margin of the Ladakh Batholith, are LREE enriched and Nd depleted, which suggests that they contain more continental crust contamination (45%) than the Dras volcanics (20%), south of the Ladakh Batholith (Clift et al., 2002b). Zircon analysis from the batholith indicate ages as old as ~ 103 Ma (Honegger et al., 1982) with other granitic intrusions dated at ~ 58 Ma (Singh et al., 2007) and 47 Ma (St-Onge et al., 2010). Isotopic evidence and the lack of inherited zircons suggest that the Ladakh Batholith is mantle-derived and experienced its last major magmatic pulse at ~ 50 Ma (Weinberg and Dunlap, 2000). Early Eocene zircon ages suggest that magmatism continued until at least 47 Ma, with a compositional shift to adakitic rocks, derived from the lower crust, at 49.2 ± 1.2 Ma, and convergence slowdown linked to an increase in magmatism (White et al., 2011; Shellnutt et al., 2014b). Apatite fission-track data indicate rapid cooling took place from 49 to 44 Ma (Clift et al., 2002a), which may have been related to the end of intra-oceanic subduction along the KLA.

The Dras Formation (of the Dras Arc) is composed of tholeiites, alternating with calc-alkaline dacites (Honegger et al., 1982), in three north-verging, stacked structural nappes (Fig. 4) that, from east to west, include the Nindam volcaniclastic turbidites, Naktul volcaniclastics, and Suru volcanics (Dras 1 and 2), which reach lower greenschist facies as the basal unit (Reuber, 1989; Robertson and Degnan, 1994; Clift et al., 2000). The orbitoline-dated, Albo-Cenomanian Dras 1 volcaniclastics (Fuchs, 1982) were intruded by gabbro, diorite and granite, then deformed and unconformably overlain by the poorly-dated, mainly acidic Dras 2 tuffites and southerly volcanic breccia (Reuber, 1989). The Dras 1 sub-unit is thought to represent the Chalt basalts or Jutal dikes of

the Yasin Group, northern Kohistan Arc (Clift et al., 2000), or the upper crustal equivalent of lower crustal gabbros and mantle peridotites of the Kohistan Arc (Clift et al., 2002b).

Further east, serpentised harzburgite, wehrlite, pyroxenite and dunite ultramafics outcrop within the Dras Arc and at the base of the Naktul nappe, further north, but with no metamorphic contacts, they may constitute the oceanic substratum (Reuber, 1989). The folded and imbricated volcaniclastics and reworked carbonates of the Upper Cretaceous Naktul unit (Reuber, 1989) are interpreted as the proximal forearc apron (Robertson and Degnan, 1994). Still further east, deep-water volcaniclastic turbidites, tuffaceous sediments and pelagic carbonates of the Valanginian–Cenomanian Nindam Formation are interpreted as the forearc basin (distal succession) with tectono-magmatic (Robertson and Degnan, 1994) or glacio-eustatic processes causing large-scale depositional variation. The Nindam Formation may be the extrusive reworked equivalent of the Kohistan Chalt basalts (Clift et al., 2000), if the Dras Arc correlates accordingly. While the Nindam Formation underwent no deformation until Eocene time (Robertson and Degnan, 1994), the Dras 1 unit (Fuchs, 1982) was deformed at ~ 79 Ma, a similar timing to the Chilas intrusion. Robertson and Collins (2002) suggest that the KLA formed in near-equatorial latitudes, far from Eurasian terrigenous material, which is not present in the Suru, Naktul and Nindam formations (Robertson and Degnan, 1994), as is also the case in the Chilas–Jijal units of Kohistan (Petterson, 2010; Burg, 2011).

2.4. Indus Suture Zone

The Indus Suture Zone (ISZ, Figs. 2, 3 and 4) separates the KLA from the Tethyan Himalaya, further south. Robertson (2000) describes the suture zone as a composite of relatively coherent passive Indian margin thrust sheet successions (e.g. Lamayuru, Fig. 4), mid Cretaceous oceanic arc volcanics and sediments (KLA-derived), with serpentinite mélange in the north and south. In the hanging wall of the ISZ southwest of Kohistan, the Shangla Blueschists (Fig. 4) could represent thrust slices of metamorphosed volcanic or deep-sea sedimentary rocks (Robertson, 2000). The blueschists underwent peak metamorphism by ~ 80 Ma before being exhumed following arc-parallel extension, similar in timing to the formation of the Chilas Complex in the Kohistan Arc (Maluski and Matte, 1984; Anczkiewicz et al., 2000). Further east, the ophiolite fragments south of Ladakh (Sapi-Shergol gabbros and the Spongtag and Nidar basic rocks; Fig. 3), exhibit geochemical signatures that suggest they are co-genetic and could be relicts of Ladakh's (intra-oceanic) Dras Arc (Maheo et al., 2006). The Sapi-Shergol mélange contains mid Cretaceous blueschist-bearing blocks of alkaline affinity (Honegger et al., 1989), some with calc-alkaline protoliths suggesting melt derived from a supra subduction zone setting (Maheo et al., 2006), and Albian-aged radiolarians (Kojima et al., 2001), suggest an oceanic (backarc) basin existed during the mid Cretaceous.

The north-dipping Spongtag Ophiolite (Figs. 3 and 4) rests on an accretionary thrust sheet and the Tethyan Lamayuru Complex, overlying the Palaeocene–Eocene Zanskar Indian carbonate shelf (Fuchs, 1982; Corfield et al., 1999; Clift et al., 2000; Corfield and Searle, 2000). Mapping of the ophiolite reveals a complete upper mantle sequence of harzburgite, gabbro, sheeted dykes and pillow lavas, overlain by a volcano-sedimentary sequence with no clearly defined contact between them (Pedersen et al., 2001). There are some rare Triassic–Jurassic fossils underlying the Spongtag (Dras) unit with the sequence inverted at the root zone (Fuchs, 1981). Further east, the Nidar ophiolite complex (Fig. 3) consists of basal ultramafic rocks, overlain by gabbroic rocks and then volcano-sedimentary assemblages, attributed to an intra-oceanic setting, dated at $\sim 140 \pm 32$ Ma (Ahmad et al., 2008). High Mg-olivine chromites in the ophiolite suggest boninitic parentage (Ravikant et al., 2004). Other age constrains include chert-bearing Hauterivian–Aptian radiolarian fossils (Kojima et al., 2001) and a more recent radiolarian-derived age of ~ 126 Ma (Zyabrev et al., 2008). The Nidar radiometric

age of ~130–110 Ma is similar to that of the Spongfang Ophiolite, which shares similar tholeiitic compositions so that both may have formed during backarc extension (Maheo et al., 2004).

2.5. Trans-Himalayan batholith(s) and igneous bodies

Northward subduction of Tethyan or back-arc seafloor caused Andean-type calc-alkaline magmatism during the Cretaceous and early Tertiary, forming the extensive Gangdese batholiths, a granitoid belt running along SE Asia, West Burma, and southern Lhasa, Ladakh and Kohistan terranes. Known by several names depending on location (e.g. Gangdese Plutonic Complex, Kailas Tonalite, and Kohistan and Ladakh Batholith), the 2500 km-long, mainly uniform biotite-hornblende granodiorite bodies incorporate both mantle and lower continental crustal melts (e.g. Searle et al., 1987; Wen et al., 2008; Ji et al., 2009a). Though the batholiths are subduction-related, some formed along the southern Eurasian mainland (Karakoram, Lhasa and Qiangtang), while others (Kohistan-Ladakh) may have formed along an intra-oceanic subduction zone, possibly initiating from the Eurasian margin in Jurassic time, which may be seen in their temporal and geochemical variation, as outlined in Table 1, Sections 2 and 3.3, and below.

The axial Karakoram Batholith has been classified into Mid-Cretaceous (110–95 Ma), Paleogene (to 43 Ma), and Late Miocene calc-alkaline to sub-alkaline magmatic stages, most of which are matched by the ages of intrusives and dykes of northern Kohistan (Debon et al., 1987). The Kohistan Batholith was dated at ~102, 54 and 40 Ma, with aplite–pegmatite intrusions at ~34 and ~29 Ma (Petterson and Windley, 1985), while the Ladakh intrusives range from 74 to 36 Ma (Honegger et al., 1982), with ~47 Ma old leucocratic granitic dykes that intruded ~58 Ma old granodiorite in a supra subduction zone setting (St-Onge et al., 2010). The Dras volcanics (of Ladakh) were intruded by a 103 Ma old granodiorite, with chemical compositions differing from the parental magma of ~38 Ma old intrusives, further east in Tibet (Honegger et al., 1982). Along Southern Tibet (Lhasa terrane), a magmatic gap identified in the Gangdese at ~152–103 Ma by Ji et al. (2009b) may not persist in the KLA, given intrusion by the Matum Das tonalite at ~154 Ma (Schaltegger et al., 2003), a dyke swarm at ~134 Ma (Khan et al., 2009), Late Cretaceous sub-crustal accretion (Petterson, 2010), and the Valanginian–Cenomanian Nindam Formation and Albo-Cenomanian Dras 1 volcanics of the Ladakh Arc (Fuchs, 1982).

Isotopic analyses of the batholiths along Southern Tibet (Lhasa terrane) by Ji et al. (2009b) revealed four age-groups: ~205–152 Ma (Ji et al., 2009a), with a ~188 Ma old granite likely sourced from juvenile mantle (Chu et al., 2006); ~103–80 Ma, which ended with an adakitic intrusion (Wen et al., 2008; Lee et al., 2009); ~65–45 Ma, the most prominent stage with a peak at ~50 Ma; ~33–13 Ma (Ji et al., 2009a), and more recently, continuous magmatism from 65 to 35 Ma (Ji et al., 2012). Mantle-like high/positive Hf ratios in the batholith southwest of Lhasa suggest links to a juvenile/backarc crust (Ji et al., 2009a). Ji et al. (2009b) summarise the batholith formation in three main stages: 1) Mesozoic magmatism induced by Tethyan subduction, peaking in the Late Jurassic and Early Cretaceous, 2) intensive Paleocene–Eocene magmatism with subduction, rollback and slab break-off, and 3) Oligocene–Miocene magmatism attributed to the convective removal of thickened lithosphere following India–Eurasia collision. Recent sampling of magmatic zircons also reveal a Paleogene departure from the depleted Mesozoic mantle-type Hf ratios, attributed to subduction of Himalayan sediment or binary mixing between it and juvenile Gangdese sediments (Chu et al., 2011).

Magmatic gaps of ~152–103 Ma and ~80–65 Ma, identified in the Gangdese by Ji et al. (2009b), may also persist at the Eastern Syntaxis (Namcha Barwa, Fig. 2), where zircon ages from the batholith highlight magmatic or anatexic (crustal melt) events at 165, 81, 61, 50 and 25 Ma (Guo et al., 2011). Geochemical analysis suggests several emplacement mechanisms and magmatic sources here, for example, Hf values for the

Jurassic granitic gneiss and Cretaceous granite indicate that binary mixing took place between juvenile and old crust, possibly due to the intersection of a spreading centre with the trench resulting in the formation of a slab window (Guo et al., 2011). Negative Hf values and (adakitic) geochemical characteristics of Oligocene samples may be related to the break-off of Indian continental crust (Guo et al., 2011). A suite of nearby high-temperature charnockites, with adakitic affinities, is also attributed to the intersection of a trench and mid-oceanic ridge between 90 and 86 Ma (Z.-M. Zhang et al., 2010a). Other nearby adakites, emplaced at ~84 Ma, were attributed to Neo-Tethyan spreading ridge subduction (Guan et al., 2010). MORB, sediments and fluid, hybridised by peridotite in the mantle wedge, can form adakitic melts at temperatures above 700 °C and depths greater than 70–85 km, such as the ~136 Ma old Mamen adakitic andesites (Fig. 3) (Zhu et al., 2009b). The Eastern Himalayan Syntaxis also contains marble with detrital magmatic zircons, isotopically linked to the Gangdese batholiths, dated between 167 and 86.3 Ma, and granulite that records high-temperature metamorphism at ~81 Ma, with geochemical evidence of melting of a 90 Ma basaltic protolith, formed in a continental-margin arc setting, also supporting the subduction of a backarc spreading centre (Guo et al., 2013). An amphibolite facies event at ~36–33 Ma, and granulite facies metamorphism in the High Himalaya between ~37 and 32 Ma, were attributed to subduction of the Indian margin (K.-J. Zhang et al., 2010).

2.6. The Himalaya

Along the northern margin of India, the Himalaya (Fig. 2) can be divided along strike into the Tethyan Himalaya, High Himalaya, and Lesser Himalaya, from north to south. The Lesser Himalaya consists of weakly metamorphosed and deformed Late Proterozoic–Paleozoic carbonates, slates, phyllites, quartzites, flysch and tillites, thrusting southwards in slices that are overridden by nappes of the High Himalaya, which have been transported to the south by up to 100 km (Stocklin, 1980; Fuchs, 1981; Windley, 1988). Previous studies (Stocklin, 1980; Fuchs, 1981; Windley, 1988) describe the crystalline nappes of the High Himalaya as a 4–10 km-thick Precambrian–Paleozoic ‘slab’ of pelitic schists, marbles, paragneisses, orthogneisses, amphibolites and migmatites, with peraluminous leucogranite intrusions, such as the ~22–24 Ma Makalu granite, south of Mt Everest (Scharer, 1984). Age data suggest that rocks in the Pakistan Himalaya reached peak metamorphism ~47 Ma, some 20 Ma earlier than the metamorphic rocks in central and eastern Himalaya (Searle and Treloar, 2010). Lu–Hf ages (54.3 ± 0.6 Ma) of garnet from middle crustal rocks exposed in the north Himalaya, south of Tibet, were interpreted as a product of crustal thickening (Smit et al., 2014).

In the west (of the Karakoram Fault terminus), the crystalline Himalaya grade up northwards into Campanian–Maastrichtian flysch and shelf limestones, which continued to form locally until the Lower Eocene, such as in Zanskar (south of Ladakh, Fig. 4), where Maastrichtian carbonates evolve into shales and siltstones (Thakur and Misra, 1984). These are overthrust to the north by the Lamayuru unit (Fig. 4), comprised of turbidites, shales and deep-water radiolarian cherts (Windley, 1988), which record the early Jurassic subsidence of the Zanskar Platform, before mid-late Jurassic extensional collapse and related alkaline volcanism, overlain by Cretaceous carbonates, volcanoclastics, and the Spongfang Ophiolite (Robertson and Degnan, 1993). The Lamayuru (passive margin of India), Jurutze (forearc basin to the Eurasian active margin), and Khalsi (Eurasian forearc sequence, recording the collapse of Indian continental margin and ophiolite obduction) units are unconformably overlain by the fluvial sandstones of the Ypresian Chogdo Formation (Clift et al., 2002a). This Zanskar Valley formation (Searle et al., 1990b) has been classified as mostly Asian-derived, and is thought to contain the first evidence of mixed Indian and Asian provenance (Clift et al., 2002a), matching cessation of marine facies at 50.5 Ma (Green et al., 2008), though sedimentary

contact or input from the underlying Indian plate here is debated (Henderson et al., 2011). The crystalline Himalaya grade up into the Cambro-Ordovician to Aptian marine sediments of the Tibetan succession, further north (Stocklin, 1980; Fuchs, 1981).

The Tibetan sequence is exposed between the hanging wall of the South Tibet detachment system, a network of low-angle faults and shear zones that formed coeval to and parallel with north-dipping thrusts during lithospheric shortening (Leloup et al., 2010), and the south-dipping Great Counter/Renbu-Zedong thrust (e.g. Yin et al., 1999), further north, merging with the Karakoram Fault termination. The Tibetan Himalaya have been described as three regions, from north to south (Liu and Einsele, 1994): the Cretaceous Xigaze forearc (southern Lhasa terrane), the Tethyan sedimentary zone (between Lhasa terrane and Himalaya), and the Tethyan Himalaya (the continental shelf-rise). The southern Tethyan depositional zone, overlying Precambrian basement of the High Himalaya, is comprised of 13 km of Cambrian–Eocene mostly marine deposits (Willems et al., 1996). The older formations record transition from pelagic to upper slope to delta-plain deposition, while a Palaeocene–lower Eocene carbonate ramp, overlain by deep-water sediments, records shallowing into outer shelf environment, and finally fluvial deposits (Hu et al., 2012).

2.7. Yarlung-Tsangpo Suture Zone

The Yarlung-Tsangpo Suture Zone (YTSZ, Fig. 3), between the High Himalaya and Lhasa terrane, has been described as a collage of pre- and syn-collisional geological objects that formed at different latitudes across oceanic basins up to ~4000 km wide, now squeezed into a narrow belt of a few hundred metres to 25 km width (Hébert et al., 2012). The suture zone incorporates what is left of the NeoTethys Ocean and backarc basins, and is traditionally linked with the more westerly ISZ, though there are differences along strike (e.g. Burg and Chen, 1984; Murphy et al., 2000). South of the southward-dipping Great Counter Thrust, which marks the southern margin of the Lhasa terrane and associated Lower Miocene Gangrinboche conglomerates (Aitchison et al., 2002b), three sub-units can be defined in the Tethyan Himalaya (of the YTSZ). From north to south they include (Liuqu) conglomerate and Cretaceous (Xigaze) flysch, a discontinuous (Dazhuqu) ophiolitic belt, associated tectonic (Yamdrok) mélange, and flysch from India's leading margin (e.g. Aitchison et al., 2011).

Outcropping along the southern YTSZ, the Yamdrok mélange (Searle et al., 1987), also referred to as 'wildflysch with exotic blocks' (Tapponnier et al., 1981) or Upper Jurassic to Lower Cretaceous red radiolarites (Girardeau et al., 1984b), contains huge sediment rafts floating in a mud-matrix, which formed in an intra-oceanic subduction system that overrode India's water-saturated leading edge sediments (Aitchison et al., 2000). The sediment rafts include Permian–Cretaceous limestones, Campanian–Maastrichtian micrites and Aalenian–Aptian cherts (e.g. Matsuoka et al., 2002; Dupuis et al., 2005b), Maastrichtian–Paleocene fossils (Burg and Chen, 1984; Liu and Aitchison, 2002), and radiolarian stratigraphy that suggests accretion during late Aptian to late Cretaceous time (Zabrev et al., 2004). Further north, the Yamdrok mud-matrix is truncated by the Liuqu Conglomerates.

The Liuqu conglomerates outcrop in a series of oblique-slip basins within Late Jurassic–Cretaceous intra-oceanic arc terranes (Davis et al., 1999). The different deformation styles (strike-slip versus thrusting along the massifs) might be explained by paleo-ridge-transform intersections (Guilmette, 2005). The conglomerates may have formed penecontemporaneously with the Yamdrok mélange (Aitchison et al., 2000) and are not considered to have derived from terranes north of the YTSZ, but rather from between an intra-oceanic arc and India's leading margin, given coarse-grained, immature clast textures and stratigraphic relationships (Davis et al., 1999, 2002). Provenance studies of the Liuqu conglomerate clasts, with both Indian and Asian sources, identify an erosional record from the Middle Eocene for the Asian sources (Wang et al., 2010). Another recent palynological study (Wei

et al., 2011), suggests that the Liuqu conglomerates were actually deposited during Oligocene time, above sea-level and within warm-temperate climates.

East of Xigaze (Fig. 3), the Dazhuqu terrane (Zabrev et al., 2003; Abrajevitch et al., 2005) contains ultramafic blocks that can be divided into transitional harzburgites (depleted/supra subduction zone peridotites), harzburgites and dunites (mantle–residue interactions), and lherzolites and cpx-harzburgites (fertile abyssal peridotites), as part of an ophiolitic belt (Dupuis et al., 2005a). The ophiolites (Fig. 3), occur as either non-dismembered, tectonically reworked sections, such as at Spongta and segments between Dazhuqu and Xigaze, or as dismembered sections, such as at Nidar, Kiogar, Jungbwa, Saga, Sangsang, Xiugugabu, and Luobusa (Hébert et al., 2012). Hébert et al. (2012) suggest that the ophiolites formed close to the Eurasian margin within short-lived (30 Ma) basins, though some might have evolved for over 70 Myrs. They invoke a scenario where interaction between MORB (mid-ocean ridge), OIB (ocean island) and arc-type basalts, generated Jurassic ophiolites in a nascent arc along the eastern and western segments. These were then incorporated into a mid to Late Cretaceous arc running along the entire subduction zone until major arc splitting created a remanent and active arc, as suggested for KLA (e.g. Burg, 2011). Andean-type subduction resumed beneath the Lhasa terrane, causing the back-arc to stop spreading and arc to recede towards Eurasia, with obduction of the YTSZ ophiolites occurring during ~90–70 Ma, roughly 30 Myr after most had formed.

The ophiolites generally coalesce into Middle Jurassic and Lower Cretaceous age groups (Fig. 3), plus those older around the Eastern Syntaxis at ~200 Ma (Geng et al., 2006), Naga, dated as Upper Jurassic (Baxter et al., 2011), Chin Hills, dated at ~160 Ma (Mitchell, 1981), Zedong and Loubusa, dated at ~161 Ma (McDermid et al., 2002) and ~177 Ma (Robinson et al., 2004; Mo et al., 2008), respectively, though zircons from gabbros at Loubusa recently gave U–Pb ages of ~150 Ma (Chan et al., 2013). Further west, ophiolites at Kiogar (Fig. 3) and Jungbwa date at ~160 and ~123 Ma, respectively (Chan et al., 2007b; Xia et al., 2011; Chan et al., 2013), though the latter was also dated at 152 Ma (Miller et al., 2003). Even older ages have been reported, such as at Naju (~100 km east of Zhongba, Fig. 3), where a typical OIB gabbro with little or no continental affinity was dated at ~364 Ma, and explained as a PaleoTethys embayment (Dai et al., 2011a). However, this gabbro occurs as a tectonic block within melange matrix (Zhu et al., 2013). Similar ages were reported for gabbros at Dangqiong, near Xiugugabu (Fig. 3) (Zhou et al., 2010b), but this is at odds with previous studies dating the ophiolitic material at ~126–123 Ma for Dangqiong (Chan et al., 2007a; Mo et al., 2008; Chan et al., 2013) and Xiugugabu (Wei et al., 2006). A gabbroic dyke from the latter was also dated to ~173 Ma (Mo et al., 2008).

Cretaceous ophiolites are also abundant around Xigaze (Fig. 3), where a pegmatitic gabbro was dated at 131.8 Ma (Chan et al., 2013). Nearby are the Barremian–Aptian Dazhuqu forearc terrane (Zabrev et al., 2003; Dai et al., 2013), the Triassic–Aptian Bainang intra-oceanic island arc subduction complex (Zabrev et al., 2004), and the Buma ophiolitic mélange, with amphibolites dated at 130–125 Ma (Guilmette et al., 2009). The Saga mélange (Fig. 3), yields a metamorphic sole that reached peak conditions between 132 and 127 Ma (Guilmette et al., 2012). Further west, the Zhongba ophiolite (Fig. 3) is dated at ~126 Ma (Dai et al., 2012, 2013) while the Bainang amphibolites, initially dated at ~88 Ma (Malpas et al., 2003) were revised to ~123–128 Ma, which overlaps with the magmatic and sedimentary ages of the overlying ophiolite (Guilmette et al., 2009). These ages also correspond with the Albian Sapi-Shergol mélange (Kojima et al., 2001) and ~126 Ma old Nidar ophiolite (Zyabrev et al., 2008), further west near Ladakh (Fig. 3).

Recent geochemical analysis suggests that a variety of tectonic environments, including intra-oceanic arc, backarc basin, forearc basin, oceanic island, and mid-ocean-ridge fragments, became trapped within the YTSZ (Mo et al., 2008). For example, the Early Cretaceous Saga and

Sangsang massifs (Fig. 3) are incomplete sequences of prominent ophiolitic mélange overlain by a thin mantle section (Bedard et al., 2009). Given their along-strike correlation and age relationships, both could belong to the same ophiolitic backarc segment but their geochemistry differs such that the Saga peridotites are more enriched/primitive (Iherzolitic) than the Sangsang (harzburgitic) peridotites, so that the Saga peridotites represent the abyssal backarc end-member while the Sangsang peridotites, and other massifs further east, are closer to the forearc subduction-related end-member (Bedard et al., 2009).

Upper and lower sections of a metamorphic sole can have peak metamorphic age differences of up to 50 Ma, which might not convey the age of final obduction but rather the initiation of subduction, which the inverted ocean-floor sequences suggest may have been initiated by an overturned fold in young oceanic crust (e.g. Malpas, 1979; Wakabayashi and Dilek, 2003; Guilmette, 2005). The Saga sole's metamorphic peak at ~127–132 Ma may have followed an Early Cretaceous tectonic event, such as India's early drift from Gondwana, possibly transforming the backarc spreading ridge into a subduction zone (Guilmette et al., 2012). Geodynamical modelling (Bedard et al., 2009), suggests that the back arc and island arc rocks at Saga formed in a supra subduction zone setting between 155 and 130 Ma, before a new subduction trench initiated at ~127 Ma and buried the rocks, scraping off the upper crust, as was proposed for the Xigaze ophiolites (Guilmette et al., 2009).

The Early Cretaceous Xigaze ophiolitic massifs form a nearly continuous belt over 175 km long and 25 km wide, where sections are mostly north-side up and repeated across dextral strike-slip faults (Ziabrev et al., 2003). Mineral chemistry suggests that the ophiolitic massifs originated in a supra-subduction environment with superimposed backarc and arc signatures that were overprinted by complex magmatic processes, such as melt–mantle interaction (Hébert et al., 2003). The ophiolitic sequence from base to top consists of mantle peridotite, cumulates, sheeted sill dike swarms (with boninitic affinity), and basic lavas with radiolarian chert dated to Late Jurassic–Cretaceous time (Bao et al., 2013). Bao et al. (2013) also report an age of 81 Ma for amphibole in garnet amphibolite in the mélange, suggesting this as the time of tectonic emplacement/obduction, and surmise that the Xigaze ophiolites formed in a mid-ocean ridge before initiation of forearc extension and subduction-related melting intruded the oceanic crust as dykes, resulting in a close association of mid-ocean ridge basalt and boninitic rock. Another recent study of the dolerite and quartz diorite intrusions, dated between 127 and 124 Ma, suggests that the forearc-type ophiolites crystallised in a forearc setting via rapid slab rollback, which followed subduction initiation during 130–120 Ma (Dai et al., 2013). Paleomagnetic studies of dolerite dykes, which have undergone anticlockwise rotation to trend 85°N, indicate that the original spreading centre may have been located ~10–20° north of the equator (Pozzi et al., 1984).

Further east, the Loubusa ophiolite (Fig. 3) contains a well-preserved mantle section and transition zone sequence above a tectonic mélange, containing these blocks as well as amphibolite, basaltic-andesite, andesite and siltstone blocks in a serpentinite matrix, thrust northwards onto the Lhasa terrane's batholith (Aitchison et al., 2000). The chromite nodules in the mantle residue may have formed after interaction between old-MORB and new boninitic magmas, during a second stage of melting above a subduction zone (Zhou et al., 1996). Geodynamic modelling of the ophiolite suggests that the backarc spreading centre was subducting beneath the Lhasa terrane at ~120 Ma such that the Loubusa forearc formed in the wedge overlying a second north-dipping subduction zone (Hébert et al., 2003). Analysis of the Loubusa chromite reveals the presence of reduced deep mantle (>300 km) UHP rocks (Yang et al., 2007; Dobrzhinetskaya et al., 2009), while mineral and petrological evidence suggests that other YTSZ massifs underwent polybaric exhumation from at least 50 km depth (Hébert et al., 2003).

A terrane-based nomenclature has also been proposed for the YTSZ (e.g. Aitchison et al., 2002a, 2003; Ziabrev et al., 2003), though it has not been adopted by all studies because of laterally divergent ages and geochemistry. Yet, the consistent occurrence and north–south distribution of the broadly coeval, Late Jurassic Zedong Arc (McDermid et al., 2002), Aptian–Barremian Dazhuqu ophiolitic belt (Ziabrev et al., 2003; Abrajevitch et al., 2005), and the overturned mid-Aptian Bainang accretionary wedge (Ziabrev et al., 2004), supports the interpretation for a north-dipping intra-oceanic subduction system, operating by mid Cretaceous time (Aitchison et al., 2000). The hemi-pelagic, siliceous mudstone and fine-grained clastics of the Bainang terrane, overlying the Indian plate (Aitchison et al., 2002a), are in fault contact with the southern margin of the Dazhuqu terrane (Aitchison et al., 2000), which paleomagnetic studies suggest formed at sub-equatorial latitudes and underwent counter-clockwise rotation (Abrajevitch et al., 2005). These are in tectonic contact with the Zedong terrane, interpreted as the overturned remnant of an intra-oceanic arc, active from at least Late Jurassic time, given a dacite breccia dated at ~161 Ma (McDermid et al., 2002), as well as Lhasa terrane volcanics and batholith, to the north (Aitchison et al., 2000). Further north, the Xigaze volcaniclastic turbidites overlie and truncate the highly fragmented Dazhuqu ophiolitic sequence, though their contact is faulted or not exposed (Aitchison et al., 2000, 2002a).

The Xigaze terrane (Fig. 3) is considered a prime example of an exposed forearc basin associated with a northward-dipping subduction zone, comprised of mid-late Cretaceous siliciclastic turbidites with plutonic and volcanic pebbles, thought to derive from the more northerly Gangdese Belt (Windley, 1988) and Lhasa terrane, from as early as Aptian–Albian time (e.g. Einsele et al., 1994; Durr, 1996; Wu et al., 2010). Facies architecture of the Xigaze Basin suggests that an accretionary wedge slowly grew during the Albian–Cenomanian stages of initial forearc basin infill (Einsele et al., 1994), which may have arisen from a high degree of plate coupling (Schneider et al., 2003). The Xigaze forearc facies were recently divided into the flysch-dominated Xigaze Group and a shallow marine group, the latter containing andesitic debris sourced from volcanics of the southern Lhasa terrane during ~112–49 Ma (Wang et al., 2012). The Xigaze Group, deposited between ~116 and 65 Ma, or to Ypresian time (Wang et al., 2012), had a main stage of deep marine deposition between ~107 and 84 Ma, and is comprised of several formations with isotopic values similar to those of the Gangdese Batholith, their likely source (Wu et al., 2010). Provenance studies suggest other sources that include the Jurassic–Lower Cretaceous Yeba and Sangri formations in the Lhasa terrane (Wang et al., 2012). Younger formations contain pre-Mesozoic zircons and negative Hf values, implying the addition of older (continental) crust from ~91 Ma (Wu et al., 2010). While younger sediments have been eroded (Aitchison et al., 2000), those remaining record basin inversion into the Eocene, with detrital zircon peaks at ~120 and 170 Ma that could not be traced to the Lhasa terrane, possibly due to lateral translation (Aitchison et al., 2011).

The transition from Upper Cretaceous Xigaze marine flysch to Eocene Qiuwa conglomerates, the latter originating from the Gangdese batholith, was interpreted as a product of the India–Eurasia collision (Searle et al., 1987). The Qiuwa conglomerates may be counterparts to the coeval Kargil conglomerates, overlying the southern margin of the Ladakh pluton (Virdi, 1987). The Kailas, Qiuwa, Dazhuqu and Loubusa formations, which outcrop unconformably along the southern Lhasa basement for 1500 km and are collectively termed the Gangrinboche conglomerates, contain Early Miocene felsic tuffs and older and younger sediments, respectively sourced from the Lhasa then more southern terranes, after India–Eurasia collision (Aitchison et al., 2002a,b, 2009). Detrital zircons as young as 37 Ma, sampled from the conglomerates near Xigaze, suggest that subduction-related convergent magmatism continued until Late Eocene time, though the zircons may have been sourced from younger Linzizong Volcanics in the southern Lhasa terrane (Aitchison et al., 2011).

2.8. Lhasa terrane (South Tibet)

The Great Counter Thrust marks the boundary where the Lhasa terrane rocks dip southward beneath the Tethyan Himalaya (Figs. 2 and 3), including the Xigaze, Dazhuqu and Bainang terranes (Aitchison et al., 2002a). The Lhasa terrane may have separated from Gondwana during Triassic–Jurassic (Metcalfe, 2011a,b), or Early Permian time (Shellnutt et al., 2011, 2014a), as part of the Cimmerian continent (Allegre et al., 1984; Metcalfe, 1988). The rocks of the Lhasa terrane include Precambrian gneisses, overlain by Carboniferous glacio-marine shelf deposits, Triassic breakup volcanics, shallow marine shelf carbonates, the Late Cretaceous shallow marine-fluvial Takena Formation, and the Early Tertiary Linzizong (and older) volcanics to the south, considered the extrusive component to the batholith (Chang et al., 1986).

The subaerial andesitic Linzizong Volcanics erupted between ~69 and 43 Ma as subduction-related magmatism reached its climax at 50 Ma (Coulon et al., 1986; He et al., 2003; Zhou et al., 2004; Lee et al., 2012). These volcanics, as the extrusive component of the Gangdese Batholith, may correlate with the Late Cretaceous–Eocene Khardung Volcanics at the northern margin of the Ladakh Batholith (Virdi, 1987). The Linzizong Formation is located in the footwall of a north-dipping thrust system with Triassic–Jurassic strata in the hanging wall that contain a 52 Ma old granite intrusion that underwent accelerated cooling at ~42 Ma, coincident with cessation of voluminous arc magmatism, attributed to slab break-off, tertiary thrusting or crustal thickening (He et al., 2007). Sequence distribution of the basal Linzizong member reveals that the eastern portion ceased volcanism earlier; andesites east of ~87°E were dated at ~75–59 Ma while the more westerly acidic tuffs continued to form during ~60–51 Ma (Zhou et al., 2010a). Several lines of evidence also suggest that the upper Linzizong member experienced a ‘flare-up’ at ~50 Ma, with geochemical variations that include melts from several sources, attributed to subduction rollback at ~60 Ma then slab break-off at ~50 Ma (Lee et al., 2009, 2012).

The 190–174 Ma old Yeba mafic–felsic rocks, outcropping among the Linzizong Volcanics and Gangdese Batholith, are interpreted as an arc built on thin, immature continental crust since Jurassic time (Dong et al., 2006; Zhu et al., 2008b). The broadly coeval Sangri Group, outcropping 200 km east of Xigaze, is dominated by adakite-like andesitic lavas (from ‘hot’ subduction zones), derived from volcanic island arc rocks (Zhu et al., 2009b). Provenance studies suggest that the Yeba and Sangri volcanics, the latter erupted during 112–71 Ma (Lee et al., 2009), may correlate with the earlier magmatic activity identified from detrital zircons in andesitic debris of the Xigaze Group, peaking between 190 and 150 Ma, and more so at 130–80 Ma (Wu et al., 2010).

The Cretaceous Takena Formation, with major and minor detrital zircon peaks at 160–100 Ma and 220–180 Ma, respectively (Leier et al., 2007b), consist of Aptian–Albian orbitolinid limestones, overlain by clastic red bed, fluvial lithic and volcanic fragments, likely derived from the Gangdese volcanic arc (Leier et al., 2007a) and/or the unconformably overlying Linzizong Volcanics (Pan and Kidd, 1999). The Takena Formation was attributed to a north-verging fold and thrust belt, with the passage of a flexural fore-bulge causing deposition in a retro-arc foreland basin (Leier, 2005; Leier et al., 2007a). Andesitic dykes intruded the formation at ~90 Ma, coinciding with volcanism in the northern Lhasa terrane between ~110 and 80 Ma (Coulon et al., 1986). Deposition of the Takena Formation may have continued until ~69 ± 2.4 Ma, given the oldest zircon age for the overlying Linzizong Formation (He et al., 2003). While the regional unconformity between the folded and eroded Takena Formation and the gently-dipping Linzizong Volcanics (e.g. Maluski et al., 1982; Allegre et al., 1984; Coulon et al., 1986) suggests that the majority of crustal thickening and shortening may have occurred before final India–Eurasia collision (e.g. Burg and

Chen, 1984; Leier et al., 2007a), detailed mapping shows that the Linzizong Volcanics are folded to sub-vertical in places and may have accommodated more shortening (Pan and Kidd, 1999). Other ‘post-collisional’ deformation is indicated by a folded ~52 Ma old dyke (He et al., 2003).

Yang et al. (2009) divide the Lhasa terrane into north and south segments based on a narrow HP (high pressure) metamorphic belt, dated at ~292–242 Ma, with an oceanic basaltic protolith proposed for the eclogites and associated outcrops, identified as dismembered ophiolite units. Ophiolites obducted onto the Lhasa terrane’s northern margin have been interpreted to mark the end of north-dipping subduction and accretion (e.g. Zhou et al., 1997). Ophiolites trending northwest to southeast through the terrane (Matte et al., 1996), such near Xainxa (Fig. 3), could represent remnants from one giant ophiolite nappe originating from over a hundred km further north at the Bangong–Nujiang Suture Zone, rather than from another suture zone, e.g. YTSZ (Girardeau et al., 1984a). The dichotomous crustal thickness of the Lhasa terrane, increasing from ~65 to 80 km from west to east across the dextral Jiali Fault (Fig. 3), may also support the presence of two blocks but this observation has been linked to the ongoing convergence between India and Eurasia, and extrusion of the Qiangtang terrane (Zhang and Klempner, 2005).

The Lhasa terrane has also been divided into three northwest-trending ‘ribbons’ according to different sedimentary cover rocks (Zhu et al., 2011). The southern portion contains limited sedimentary cover, including the Sangri and Yeba formations (Dong et al., 2006; Zhu et al., 2008b, 2009b), interspersed by plutonic rocks. The central portion contains Permo-Carboniferous metasediments, with minor pre-Jurassic limestones and Jurassic–Cretaceous volcaniclastics (Zhu et al., 2011). The northern area contains limited Jurassic–Cretaceous cover rocks, including exposed plutonic and volcanic rocks, respectively emplaced at ~80 Ma (Zhao et al., 2008) and between ~143 and 102 Ma, with a magmatic flare-up at ~110 Ma (Zhu et al., 2009a).

A recent review of the Tibetan Plateau (Zhang et al., 2012a) describes two coeval, north-directed subduction zones, the northern one produced a Jurassic–Middle Cretaceous magmatic arc along the southern Qiangtang margin, which may have remained open (marine) until Late Cretaceous time, given the occurrence of 132–108 Ma old ophiolites with mid Cretaceous radiolarians (Baxter et al., 2010). The southern subduction zone produced a belt of Early Jurassic adakitic rocks along the southern Lhasa terrane until Jurassic–Early Cretaceous uplift and denudation formed up to 15 km of Jurassic turbidites and molasse-type sediments on the northern Lhasa terrane (Zhang et al., 2012a). The previous authors (Zhang et al., 2012a) suggest that the orogen ended with lithospheric delamination and asthenospheric upwelling, causing widespread magmatism during 135–100 Ma, extensional deformation and marine transgression, before subduction resumed in the Late Cretaceous (90–78 Ma) producing more adakitic rocks further south. Fission track ages from Cretaceous granitoids and Jurassic metasediments in the Tibetan peneplain indicate that cooling and exhumation occurred between 70 and ~55 Ma before the plateau stabilised at ~48 Ma (Hetzell et al., 2011). Another recent thermo-chronological study also found that the Tibetan plateau grew locally from the Late Cretaceous, spanning the region by 45 Ma (Rohrmann et al., 2012).

In the eastern Lhasa terrane, S-type granitoids correlate better with the northern plutonic belt rather than the I-type Gangdese Batholith, and show two periods of magmatic arc emplacement, at ~133–110 Ma and ~66–57 Ma, after an earlier granitic intrusion at ~198 Ma, with Hf values that suggest they were derived from Lhasa and Qiangtang collision (Chiu et al., 2009). Compositions of granitoids and volcanics from similar locations indicate that the eastern batholiths are not the eastern equivalent to those of the Gangdese but rather the northern Lhasa Plutonic Belt, which may also extend further southeast to the Cretaceous–Paleocene western Yunnan and Jurassic–Paleocene Burmese batholiths (Lin et al., 2012).

2.9. Bangong–Nujiang Suture Zone

The Bangong–Nujiang Suture Zone (BNSZ, Figs. 2 and 3) bisects the Lhasa and Qiangtang terranes. It contains mainly Mesozoic shallow to deep marine sedimentary sequences, overlain by younger terrestrial and volcanic rocks and mélange (e.g. Schneider et al., 2003; Kapp et al., 2005). Several ophiolites were obducted onto the Lhasa terrane's northern margin in the Late Jurassic–Early Cretaceous (e.g. Girardeau et al., 1984a; Dewey et al., 1988; Pearce and Deng, 1988). In the west, Mid-Cretaceous strata unconformably overlie ophiolitic mélange and Jurassic flysch, which was interpreted as the remnants of a forearc basin and subduction–accretion complex (Kapp et al., 2003). The more central ophiolites exhibit a southward-trending regional chemical zonation, which Pearce and Deng (1988) attribute to backarc, island arc and forearc rocks. The ophiolitic belt is anomalously wide further east near Xainxa (Girardeau et al., 1985a) and Donqiao (Girardeau et al., 1984a), the latter has a metamorphic aureole dated at ~180–175 Ma (Zhou et al., 1997).

Also along the eastern BNSZ, the Precambrian Amdo crystalline basement (Fig. 3), exhumed in the hanging wall of an Early Cretaceous south-directed thrust system, incorporates high-grade metamorphic and magmatic rocks. It has been identified as an isolated microcontinent that underwent deep subduction before its collision with either Qiangtang or the Lhasa terrane (Zhang et al., 2012b), or as the remnants of a continental arc, which rifted south from the Qiangtang terrane (Guynn et al., 2006). The latter thermochronological study dated the granitoids at ~185–170 Ma and noted that their exhumation was coeval with (or just prior to) the formation of the Qiangtang Anticline, where mid-Cretaceous volcanic rocks unconformably overlie Carboniferous strata (Kapp et al., 2005). Guynn et al. (2006) suggest that the arc was present all along the margin but was either buried or underthrust with the Lhasa terrane (beneath Qiangtang terrane).

A review of extensive mapping in Tibet incorporates an extended BNSZ where unconformities in age between the underlying strata and BNSZ ophiolitic mélange, from Upper Triassic in the east to Upper Cretaceous in the west, suggest that the Bangong–Nujiang Ocean may have existed from Carboniferous to Early Cretaceous time and closed from east to west (Pan et al., 2012, and the references therein). This indicates that there may have been large intra-oceanic backarc system(s) in the preceding Tethys ocean, also supported by the Shan-Thai Sukhothai zone in SE Asia (Metcalfe, 2011b; Sone et al., 2012). The Triassic–Jurassic bivalves in the Yeba volcanic sediments, northeastern Lhasa terrane, also show that marine conditions were extant between the Lhasa and Qiangtang terranes ~180 Ma (Yin and Grant-Mackie, 2005). Radiolarian fossil assemblages indicate that deep marine conditions prevailed until Early Aptian time (Baxter et al., 2009).

2.10. Qiangtang terrane (North Tibet)

The Qiangtang terrane (Fig. 2) lies north of the Lhasa terrane. Stratigraphic succession suggests that both terranes drifted from Gondwana by Early Permian time (Sciunnach and Garzanti, 2012), and that Lhasa and southern Qiangtang terranes were a continuous platform until Late Triassic time (Schneider et al., 2003). South Qiangtang contains Permian fusilinids, Jurassic limestones and shales, interbedded with lava flows (Matte et al., 1996). These are unconformably overlain by Cretaceous–Tertiary red sandstones and conglomerates containing Tertiary porphyries (Norin, 1946). Volcanic tuffs and granitic intrusions in South Qiangtang, respectively yielding Ar–Ar ages of ~145 Ma and ~111 Ma, intrude or unconformably overlie folded Triassic–Jurassic turbiditic sandstone and limestone deposits, indicating that Central Tibet was already above sea level and deformed by ~111 Ma (Kapp et al., 2005).

The Qiangtang terrane has been divided into south(west) and north(east) sections according to an east-plunging anticlinorium with blueschist-bearing mélange, Permo-Carboniferous strata outcropping

at its core, and Mesozoic strata along its limbs (Yin et al., 1998; Kapp et al., 2005). Glaucomphane schists (Hennig, 1915), with volcanics and Mesozoic granite running through central Qiangtang, were also attributed to a Mid Triassic to Early Jurassic collision between North and South Qiangtang, from west to east (Zhang and Tang, 2009). Eclogites dated at 230–237 Ma were also interpreted as a Triassic suture zone, exhumed at ~220 Ma (Zhai et al., 2011). Zircon affinities for the high-pressure rocks suggest that the Qiangtang Metamorphic Belt (Central Uplift Zone) could also be attributed to an arc terrane (Pullen et al., 2008).

Late Carboniferous glacio-marine sequences (e.g. Metcalfe, 1988) and Gondwanan facies (Norin, 1946; Sun, 1993; Jin, 2002) in South Qiangtang also support a distinction between it and North Qiangtang, as suggested by deep seismic profiles, which show that the northern and southern parts of the terrane have different upper-crustal structures (Lu et al., 2009). The presence of Carboniferous dykes, gabbros, pillow basalts and radiolarian-bearing rocks with warm water fauna in North Qiangtang suggest that it was Cathaysian (e.g. Kidd et al., 1988), and part of an island arc-basin tectonic composite, whose basins continued to subduct until Late Triassic collision with the Kunlun composite terrane, further north (Pan et al., 2012).

2.11. West Burma (Myanmar)

West Burma (Fig. 5) was separated from the West Sumatra block, further south, by the Andaman Sea from Miocene time (Barber and Crow, 2009). Fan and Ko (1994) define West Burma as Arakan Yoma and Central Burma (Fig. 5), the latter consists of Upper Triassic flysch basement, unconformably overlain by Cretaceous limestone and over 10 km of Late Oligocene to Quaternary sediments. Volcanic materials in the Lower Eocene deposits come from the Central Burmese volcanic arc (Fig. 5), a Mid Cretaceous granodioritic pluton running from north to south (Mitchell, 1981). Fan and Ko (1994) attribute Arakan Yoma, consisting of Mesozoic–Early Cretaceous flysch, to an Oligocene-uplifted, eastward-dipping subduction system, which led to the formation of the Arakan Yoma Ranges and Central Burmese volcanic arc. The plutonic (Mergui) arc extending north from SW Thailand, was attributed to the Cretaceous–Paleocene allochthonous collision between Arakan Yoma and Central Burma (Fan and Ko, 1994). Arakan Yoma was then transported ~450 km north along the dextral Sagaing fault (Mitchell, 1981) as Lower Cretaceous I- and S-type granites intruded the marine clastic rocks and the eastward-dipping subduction zone migrated west (Fan and Ko, 1994).

2.12. Southeast Asia

Southeast Asia (Fig. 5) is a collage of continental, exotic and intra-oceanic terranes that have accreted or grown during continuous subduction (e.g. Şengör et al., 1988; Metcalfe, 2011a; Hall, 2012). Mapping, biostratigraphy and petrology indicates strong evidence of a mid-Late Cretaceous continental collision with the SE Asian margin, then called Sundaland (Wakita, 2000), while zircon ages also suggest collision of a Gondwana-derived microcontinent along Java by ~80 Ma (Clements and Hall, 2011). Sibumasu (Fig. 5) composed of the western Malay peninsula and East Sumatra, contains Late Carboniferous–Early Permian glaciogenic diamictites, and can be traced into southern China (Barber and Crow, 2009). West Sumatra has Cathaysian fauna and flora, and was emplaced against western Sibumasu via dextral faulting along a Triassic–Jurassic tectonic zone (Barber and Crow, 2009). It was overthrust in the mid Cretaceous by the Woyla nappe (Woyla Arc, Fig. 5), an intra-oceanic arc that can be correlated with the Mawgyi nappe (Fig. 5), west of Burma (Barber and Crow, 2009). The Woyla Group includes fragments of volcanic arc and imbricated oceanic crust, attributed to a marginal basin formed by subduction (Cameron et al., 1980) and collision of an allochthonous terrane during Albian–Aptian time (Barber, 2000; Barber and Crow, 2009). The Woyla Group was intruded at ~97.7 Ma by the

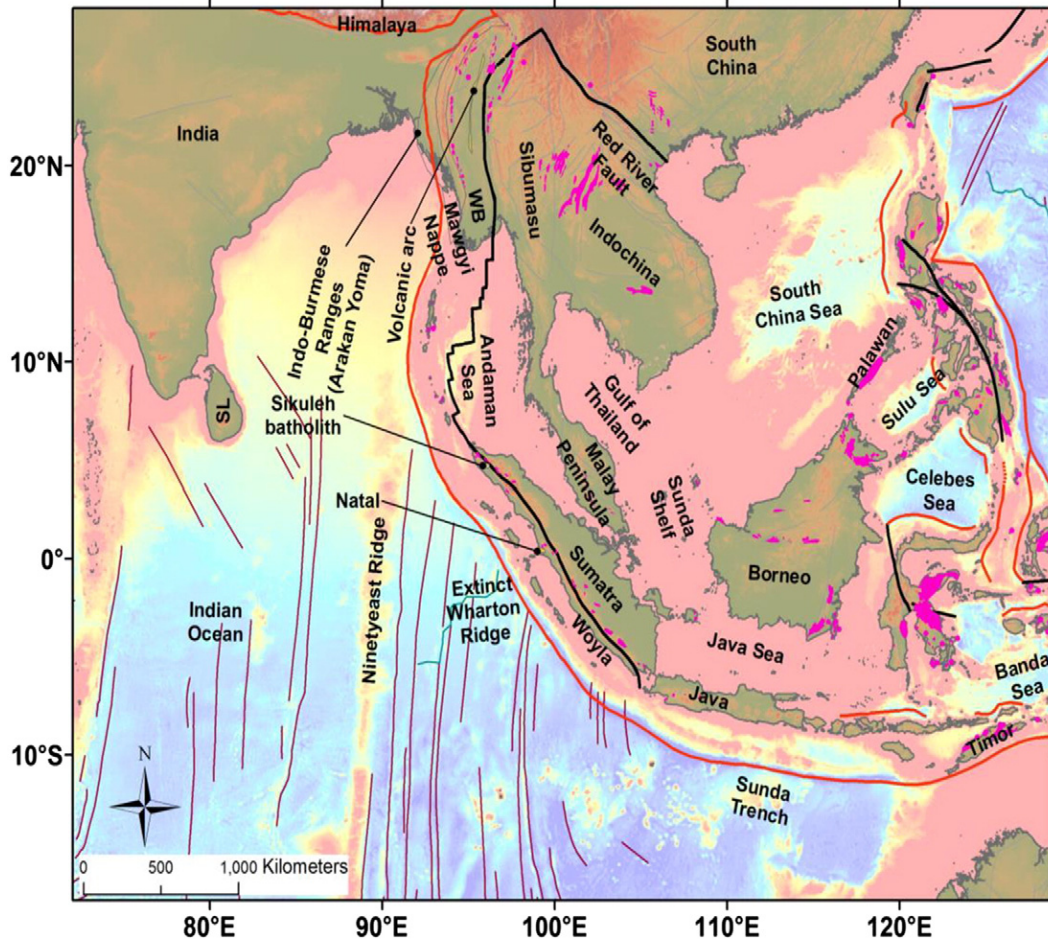


Fig. 5. Regional tectonic map of Southeast Asia, including West Burma (WB) and Sri Lanka (SL). Plate boundaries and subduction zones (black and red, respectively; Bird, 2003). Other details are as in Fig. 2. Woyla, Natal, Sikuleh batholith, and West Burma may be the best candidates for remnants of Argoland.

Sikuleh Batholith (Fig. 5), a complex of homogenous, unfoliated, biotite-hornblende granodiorite (Bennett et al., 1981).

3. Methodology, data and kinematic constraints

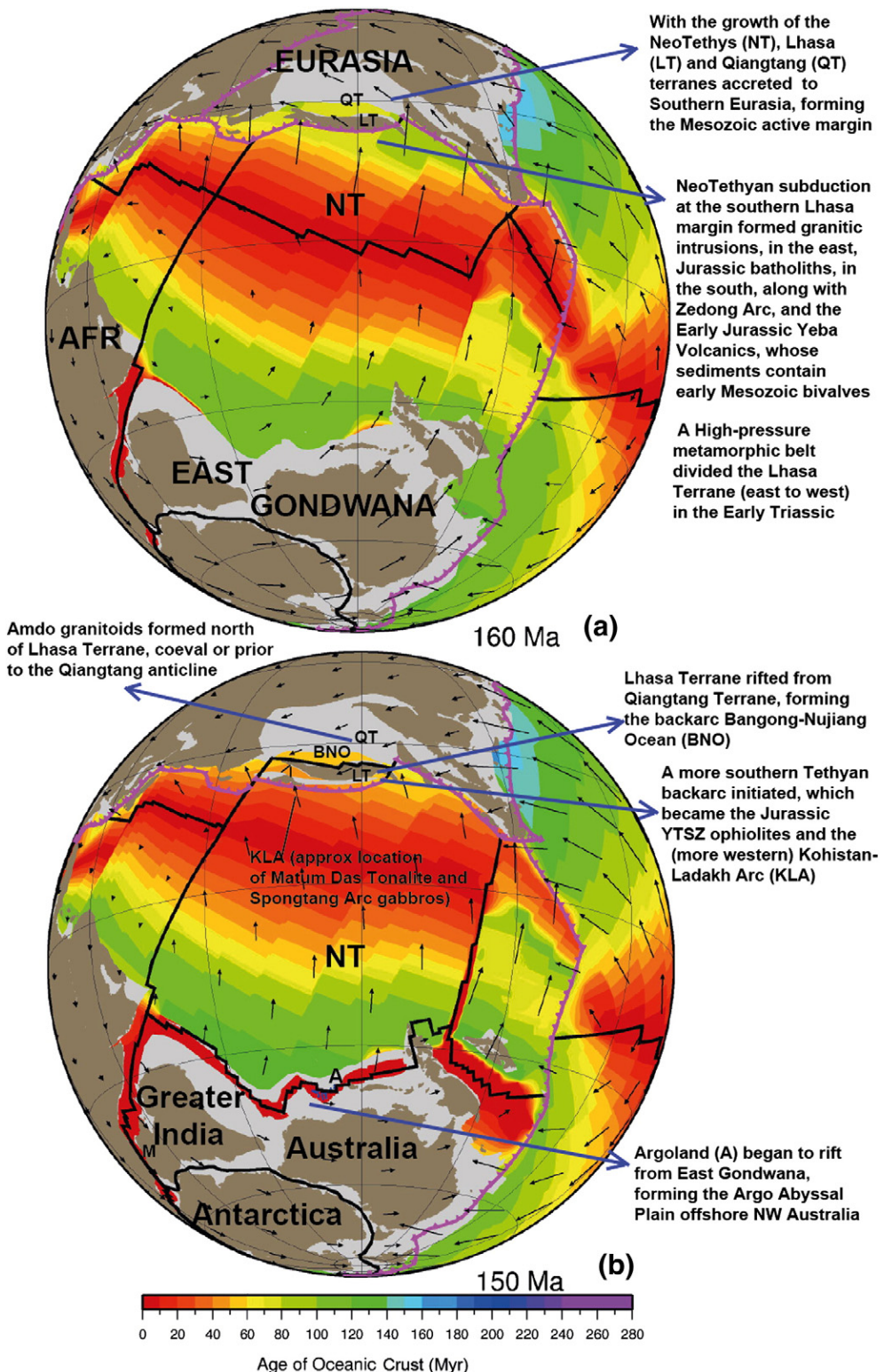
We construct a plate tectonic model encompassing the evolution of the Tethyan and Indian Oceans from 200 Ma to the present day (Fig. 6).

We construct the plate model interactively using the open-source and cross-platform plate reconstruction software, GPlates (Boyden et al., 2011), to create a regionally-constrained global plate model based on combining the seafloor-spreading histories from ocean basins (Seton et al., 2012) and our extensive review of the regional onshore geology, outlined in the previous section. The global plate model uses a hybrid absolute reference frame, combining a moving (Indo-Atlantic) hotspot

Fig. 6. Plate reconstructions (orthographic projection on centre co-ordinate 15°S, 90°E) showing oceanic lithosphere age, transforms/MORs (black), subduction zones (magenta), continental extents (grey) and reconstructed present-day coastlines (khaki). Blue triangles in oceanic crust indicate magnetic picks, outlining preserved seafloor. A = Argoland, ANT = Antarctic Plate, AFR = Africa, AUS = Australian Plate, BNO = Bangong–Nujiang Ocean, EG = East Gondwana, EUR = Eurasian Plate, GB = Gascoyne Block (north Greater India), GI = Greater India, IND = Indian Plate, I-A = Indo-Australian Plate, J = Java, KLA = Kohistan–Ladakh Arc, LT = Lhasa terrane, M = Madagascar, MT = MesoTethys, NT = NeoTethys, QT = Qiangtang Terrane (as part of the Southern Eurasian margin), S = Sumatra, TIA = Tethyan intra-oceanic arc (including the YTSZ ophiolites), WB = West Burma (Argoland), WA = Woyla Arc. a) 160 Ma: continental rifting along northern Gondwana margin coincided with Tethyan subduction along southern Eurasia (including Lhasa terrane) via a north-dipping subduction zone. Soon after, PaleoTethys seafloor spreading ceased, which leads to increased slab-pull along the northern Gondwana margin, promoting the onset of slab rollback. b) 154 Ma: continued slab-rollback generated a forearc at the southern Lhasa margin, the embryonic Kohistan–Ladakh Arc (KLA) and its eastern continuation, the Tethyan intra-oceanic arc (TIA). Continental rifting along northern Gondwana and a southward jump in seafloor spreading detached a number of continental fragments, including Argoland. The Lhasa terrane also begins to drift obliquely from the Eurasian margin (Qiangtang terrane), forming a narrow seaway (Bangong–Nujiang Ocean, BNO). c–d) 130–112 Ma: KLA, Dazhuqu and other Cretaceous arc remnants from the TIA currently situated along Southeast Asia, formed a continuous intra-oceanic subduction system, which approached its maximum north-south extent of near-equatorial latitudes by mid-Cretaceous time. Seafloor spreading in the Tethys was synchronous to rifting between India and Australia–Antarctica, resulting in a triple junction forming off the NW Australian shelf during Early Cretaceous time. The Lhasa terrane (re)accretes to southern Qiangtang terrane, closing the Bangong–Nujiang Ocean (BNO). e) 103 Ma: north-dipping Andean-style subduction initiated south of the Lhasa terrane, in parallel with the TIA. The (re)initiation of subduction beneath the Lhasa terrane coincides with the onset of diachronous collision between western Argoland and the KLA part of the TIA (black star), the latter may have already collided with SE Asia, further east. f–g) 90–84 Ma: Andean-style subduction along southern Lhasa became inactive between ~85 and 65 Ma, possibly due to the TIA spreading axis resisting subduction. h) 75 Ma: Argoland sutured to Sumatra by ~70 Ma though its westward extent was likely subducted (or accreted in presently-obscure geology) earlier along the TIA, if the continental sliver extended that far west. i) 61 Ma: Andean-style subduction re-initiated along southern Lhasa by 65 Ma, forming the batholith and Linzizong Volcanics. The Indus suture zone (ISZ) formed as the KLA obducted onto the leading edge of Greater India. j) 52 Ma: buoyant Indian continental crust stalls intra-oceanic subduction, the remnant backarc oceanic basin now a narrow seaway between Greater India and Eurasia. k) 44 Ma: continent-continent collision has begun forming the Karakoram–Kohistan–Shyok suture zone (KKSSZ) and Yarlung–Tsangpo suture zone (YTSZ), resulting in a second significant drop in India–Eurasia convergence rates and a reorganisation of seafloor spreading in the Indian Ocean, followed in a few million years by the cessation of spreading in the Wharton Basin off NW Australia, combining Indian and Australian plate motion. l) 34 Ma: coincides with the youngest marine sediments found in the YTSZ, as Greater Indian lithosphere continued to subduct, delaminate or break off beneath Eurasia.

model until 100 Ma and a true-polar wander-corrected paleomagnetic model from 200 to 100 Ma. We have incorporated more recent relevant regional reconstructions into the global plate model, updating basins around the western and northwestern Australian shelf (Gibbons et al., 2012) and East Antarctica (Gibbons et al., 2013), and incorporate a revised model for Australian–Antarctic separation (Whittaker et al., 2013).

The main tectonic elements used in our reconstructions are Argoland, Greater India, a Tethyan intra-oceanic arc (TIA), comprised of the KLA, ophiolitic fragments from the YTSZ, and WA, and the post-Triassic Eurasian margin, comprised of the Karakoram, southern Qiangtang and Lhasa terranes. All but the intra-oceanic arc originated from East Gondwana, with Karakoram, Qiangtang and Lhasa drifting earlier, as part of the Cimmerian continent that accreted to Eurasia around Late



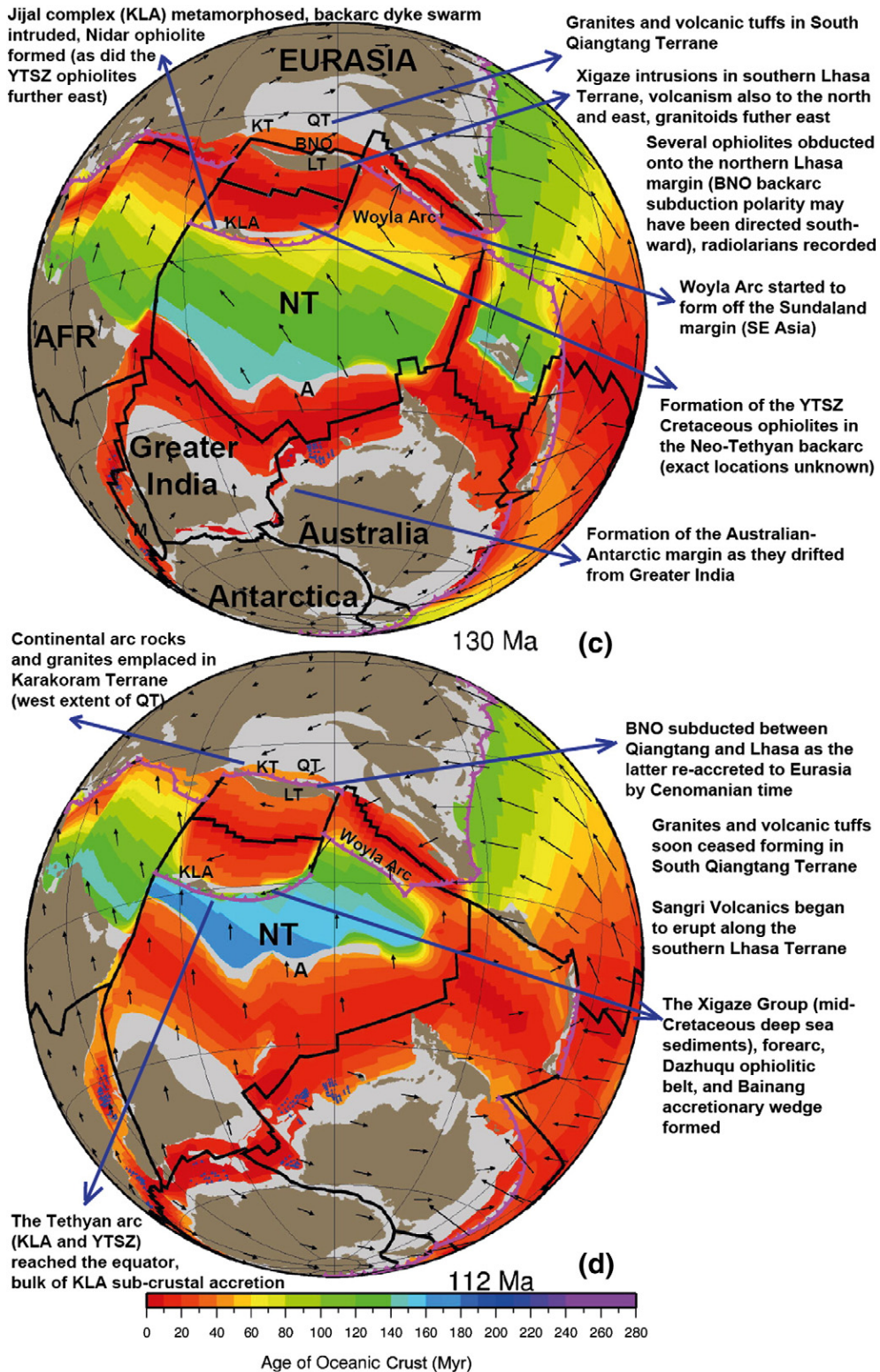


Fig. 6 (continued).

Triassic–Jurassic time (e.g. Sengor, 1987). The extents of the continental terranes are based on available potential field data and tectonic constraints. Subduction polarities are inferred from subduction-related volcanism on the overriding plate, as discussed in Section 2. We use the combined timescales of Cande and Kent (1995) and Gradstein et al. (1994) for Cenozoic and Mesozoic times, respectively. For more information regarding competing GPTS models, please refer to

Section 2.3 of Seton et al. (2012), our preferred global plate reconstruction model.

Time-dependent, intersecting topological features (e.g. mid-ocean ridges, subduction zones, transforms) have been created in order to model the continuous evolution of the plate boundary system, forming continuously closing plates (CCP), which enables global sampling of plate velocities, using previously established methodology (Gurnis

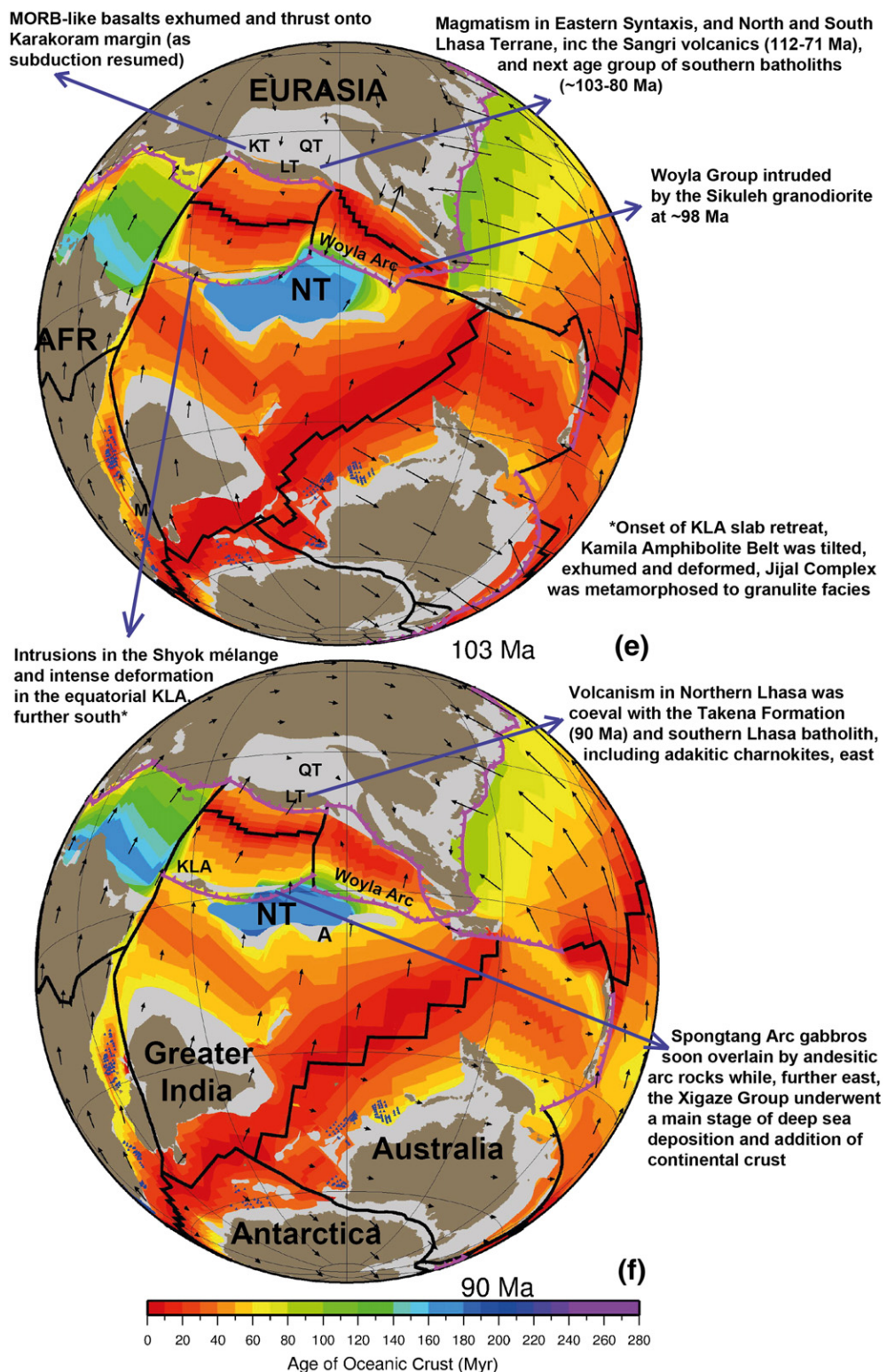


Fig. 6 (continued).

et al., 2012). The CCP functionality, built into the plate reconstruction software GPlates (Boyden et al., 2011), assigns an Euler rotation to each boundary of a dynamic plate polygon, derived from a series of intersecting plate boundaries that is user-defined, to ensure global coverage of plates and conservation of surface area through time. Each plate boundary feature is attributed with metadata, for example, the life-span of a mid-ocean ridge, the duration of a subduction zone, including its polarity and dip angle (if known), or the sense of motion on transforms.

The plate boundaries of our base model (Seton et al., 2012) were based on present day plate boundaries (Bird, 2003), geological evidence for island and magmatic arcs, suture zones and major faults through time, as discussed above in Section 2. Plate motion vectors were derived from a global set of finite rotations for relative motions. Subducted oceanic crust was restored by assuming seafloor spreading symmetry where only one flank of the spreading system was preserved. In addition, evidence from subduction, slab windows and anomalous volcanism from

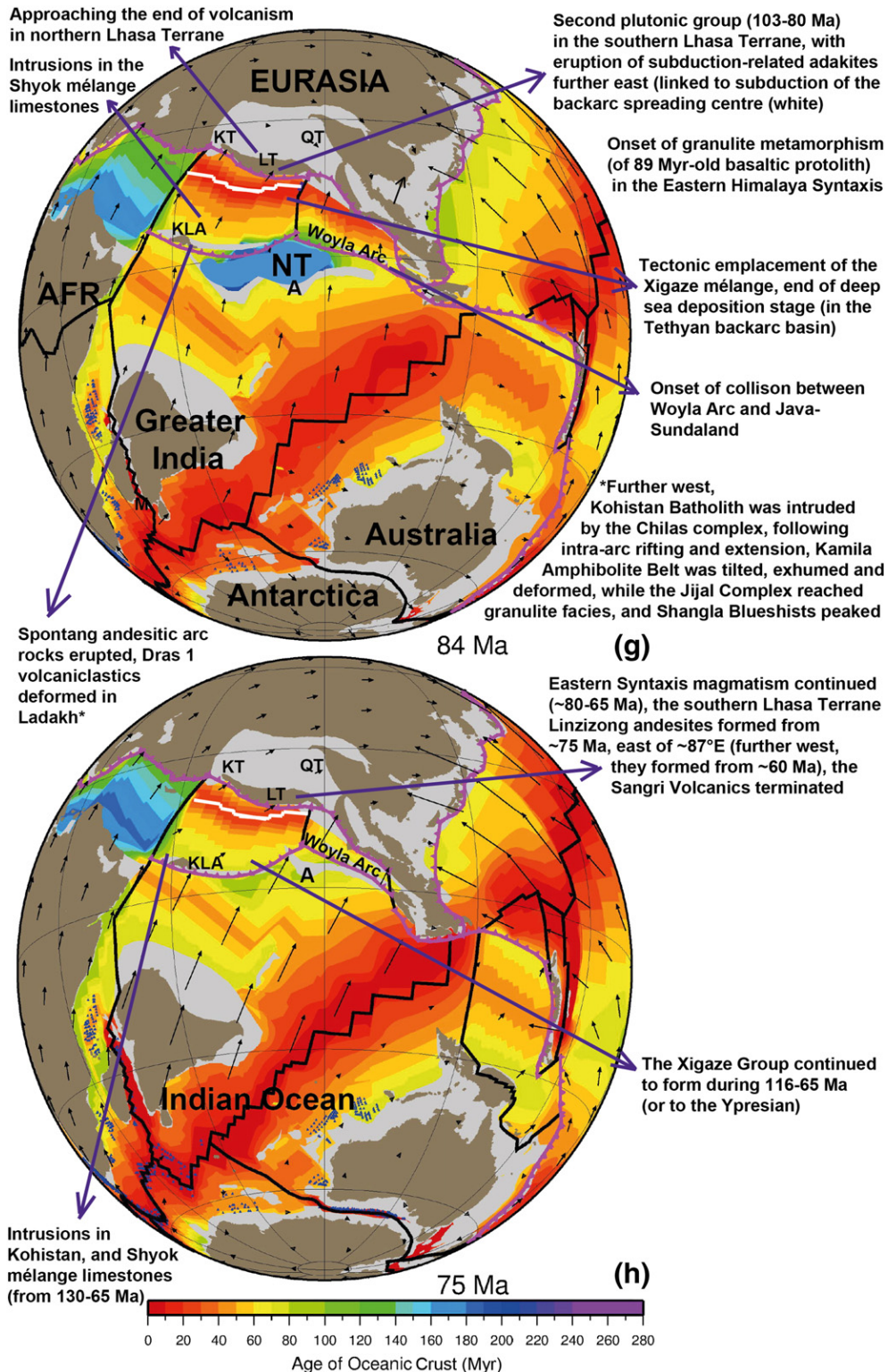


Fig. 6 (continued).

onshore geology, were incorporated into the model within established plate kinematic constraints (Müller et al., 2008). The resolved topological plate boundaries, block outlines and model rotation files are included in the Supplementary material. Quality-checked magnetic anomaly identifications (age picks) from all ocean basins were taken from a recently published, open-source, community-driven online repository (Seton et al., 2014).

3.1. Argoland and Greater India

Argoland was juxtaposed with East Gondwana's northern margin during Jurassic time — we suggest that it stretched from NE Arabia to New Guinea, where the pre-existing strike-slip boundary (Owen Transform, Fig. 1) accommodated northward motion of India relative to Africa, towards Eurasia from the Late Cretaceous. The evolution of

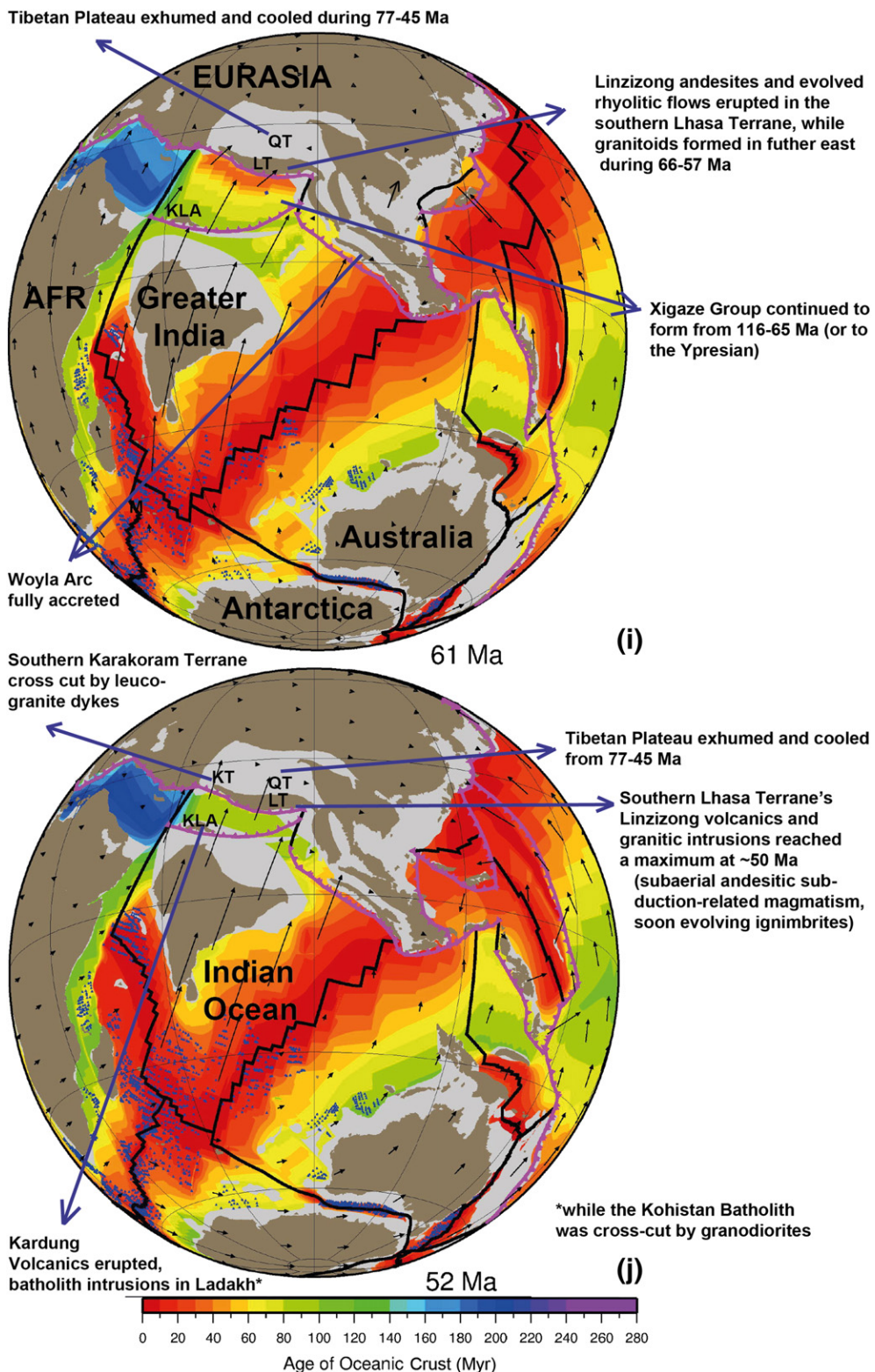
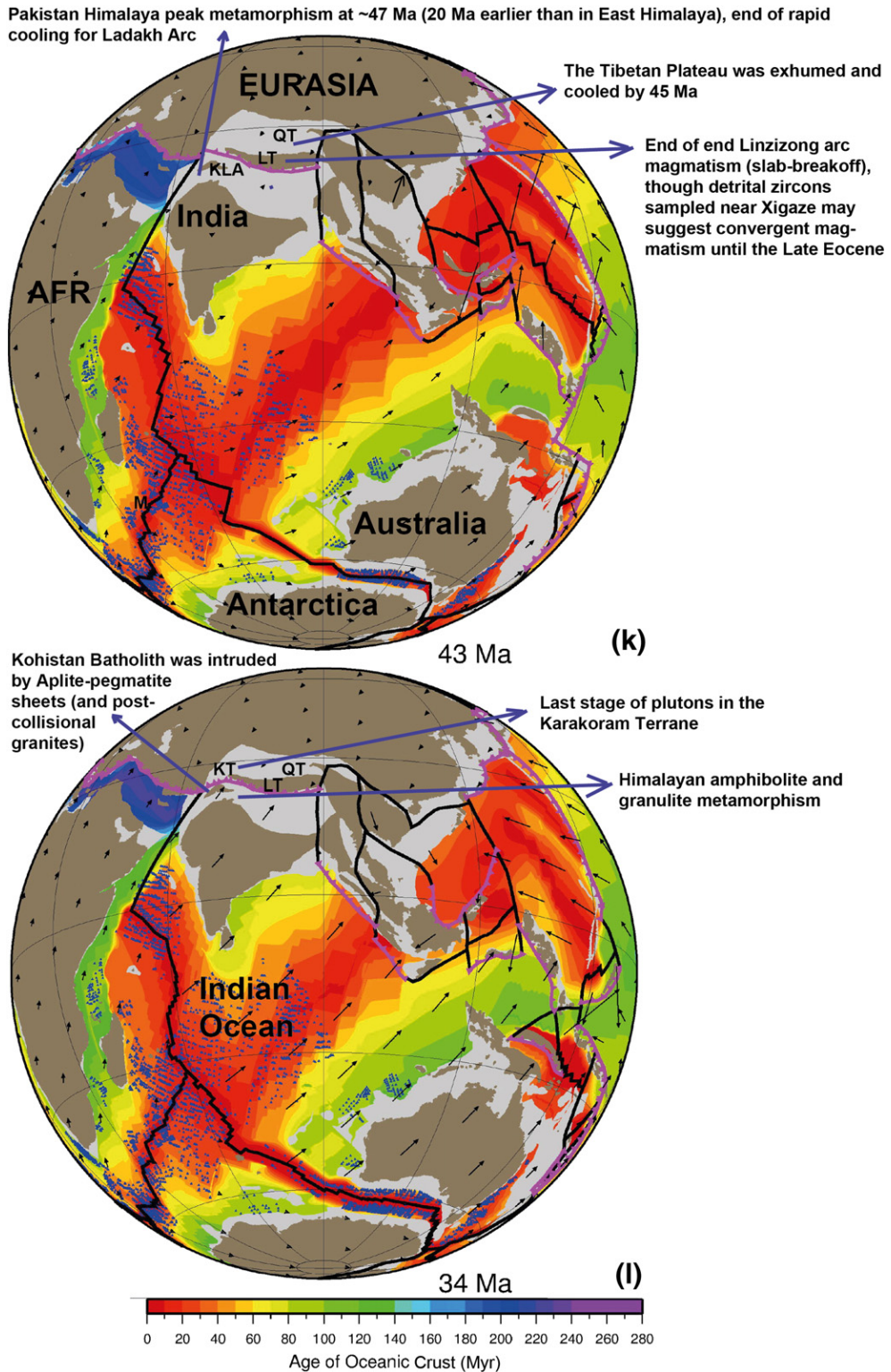


Fig. 6 (continued).

Argoland–Australia–India breakup and early seafloor spreading was recently revised when a Jurassic gabbro, dredged ~1000 km off West Australia (Gibbons et al., 2012), necessitated an extended Argoland (reaching further southwest, almost to the Zenith Plateau off western Australia, Fig. 1) as well as a reduced northern extent for Greater India, including the Gascoyne Block (GB, Fig. 6), which was a strip of continental crust originally conjugate to the Exmouth Plateau, offshore

NW Australia (Fig. 1). The geometry of the southern margin of eastern Argoland mirrors the NW Australian continent-ocean boundary (Müller et al., 2005). The remaining extent of Greater India (conjugate to the southern half of the Australian margin), reaching ~600 km and 1000 km in western and central regions, respectively, is a reasonable match to mass-balanced cross-sections that give crustal shortening estimates of ~670 km (DeCelles et al., 2002) and 1100 km (Guillot et al.,

**Fig. 6 (continued).**

2003), respectively for western and central Himalaya. The timing of collisions between India and an intra-oceanic arc and Eurasia is constrained by the outlines of these blocks, the position of the Eurasian margin, including any intra-oceanic terranes, and their relative motion through time.

Early motion for Argoland is based on the magnetic anomaly identifications in the Argo Abyssal Plain, which encompass ~155–136 Ma, coinciding with a 136 Ma ridge jump (Gibbons et al., 2012), before the

seafloor is truncated by the Sunda–Java trench. The onset of seafloor spreading separating Greater India from East Gondwana began at 136 Ma. Our previous study implies a transient triple junction between Argoland, Greater India, and Australia–Antarctica, allowing Argoland to continue along its original trajectory during India's initial 'unzipping' from Australia–Antarctica, from north to south from ~136 to 120 Ma (Gibbons et al., 2012). The 'unzipping' motion is invoked because Greater India initially drifted within a giant vice, whose 'jaws' (constraining

boundaries) consisted of the eastern edge of Madagascar and the Wallaby-Zenith Fracture Zone (WZFZ, Fig. 1), a prominent linear bathymetric feature, perpendicular to the western Australian passive margin (Gibbons et al., 2013). During the Cretaceous Normal Superchron (CNS), a period of no magnetic reversals from ~120 to 83 Ma, we fix Argoland to Greater India and maintain a similar speed for India at ~70 mm/yr for both flanks (Australia and India) along a trajectory that can recreate major fracture zones, including those offshore NW Australia (Wharton Basin) and East Antarctica (Kerguelan Fracture Zone, Fig. 1), which prominently bend towards north (Matthews et al., 2011; Gibbons et al., 2012, 2013). This bend signifies the onset of India's dextral motion from Madagascar from ~100 Ma, before India's northward motion resulted in their separation from south to north from 94 to 83 Ma (Gibbons et al., 2013). The latter timing is similar to the onset of seafloor spreading offshore east Madagascar, in the Mascarene Basin (Fig. 1), with oldest magnetic anomaly picks of 34n (Dymont, 1991; Bernard and Munschy, 2000; Eagles and Wibisono, 2013) dated at 83 Ma, but possible initiation of seafloor spreading at ~86.5 Ma (Yatheesh et al., 2006). From Paleocene time, Greater India (and Argoland) motion is constrained by the magnetic anomaly picks surrounding the Southwest Indian ridge (Central Indian Basin/Capricorn-Somalia) until Early Eocene time (Cande et al., 2010), then by a statistical best fit between magnetic anomalies and fracture zone traces from the Southeast, Southwest, Central Indian and the Carlsberg ridges, also considering the Neogene deformation of the Indo-Australian (Capricorn) plate (Royer and Chang, 1991).

3.2. The Eurasian margin

The geometry of the southern Eurasian continental margin is taken from the retro-deformed model proposed by van Hinsbergen et al. (2011b). Several lines of evidence indicate that the post-Triassic Eurasian margin likely consisted of the Karakoram, Qiangtang and Lhasa terranes (Fig. 6a), as discussed in Section 2. The Karakoram terrane can be linked to Gondwana based on its fossil assemblages (Sharma et al., 1980; Xingxue and Xiuyuan, 1994; Srivastava and Agnihotri, 2010). The latter authors identify Karakoram sediment source links to the Qiangtang terrane but it is also proposed as a counterpart to the dextrally-offset Lhasa block (Rolland, 2002). Correlating the Triassic–Jurassic Aghil carbonates, north and east of the Karakoram terrane, suggests an offset of ~149–167 km along the Karakoram fault, with slip-rates reaching 11 (or 7) mm/yr and fault initiation at ~15 (or 23) Ma, implying that Karakoram and Qiangtang had been one continuous terrane (Robinson, 2009). Exhumed, dextrally sheared gneisses, intruded by syn-kinematic leucogranites with U/Pb on zircon ages of ~23 Ma, suggest that activation of the Karakoram fault may have occurred by the Early Miocene (Lacassin et al., 2004; Leloup et al., 2011). However, only the Karakoram terrane shows high uplift-exhumation of deep crustal rocks after crustal thickening from latest Cretaceous time (Searle, 2011). The Karakoram fault, with up to ~150 km offset between exhumed granites (Searle et al., 1998) and regional rock sequences (Weinberg et al., 2000), also suggest that the Karakoram and southern Qiangtang terranes are lateral equivalents (Robinson, 2009). We support the distinction between South Qiangtang, with Gondwanan facies (Norin, 1946; Sun, 1993; Jin, 2002), and North Qiangtang, with Cathaysian facies (Kidd et al., 1988), and attribute the latter to a preceding accretion.

Stratigraphic studies indicate that the Lhasa and South Qiangtang terranes were a continuous platform until the Late Triassic (Schneider et al., 2003) but Triassic–Jurassic bivalves in the Yeba volcanic sediments of the NE Lhasa terrane show that marine conditions prevailed by ~180 Ma (Yin and Grant-Mackie, 2005). The intervening Bangong-Nujiang Suture Zone (BNS) is dated as Late Jurassic (Dewey et al., 1988; Metcalfe, 2006) and Early Cretaceous, based on clastic strata in the north Lhasa terrane (Zhang, 2004), coeval deformation forming the Qiangtang anticline (Kapp et al., 2003) and ~120 Ma plutonism

(Xu et al., 1985). Field mapping and geochronological studies near Shiquanhe (Fig. 3), far-west Lhasa terrane, uncovered the remnants of a subduction-accretion complex and forearc basin, attributed to the closure of the Late Jurassic–Early Cretaceous ocean (Kapp et al., 2003), or the BNS, while up to 500 km of lateral translation has been suggested by a detrital zircons provenance study from Xigaze forearc basin sediments (Aitchison et al., 2011). Given that marine deposition in the BNS (Fig. 6c) has been reported for Late Triassic–Jurassic (Yin and Grant-Mackie, 2005) and Aptian times (Baxter et al., 2009), we incorporate minor, oblique seafloor spreading between South Qiangtang and Lhasa terranes (QT and LT, Fig. 6b–e) forming the BNS from Late Jurassic to Aptian time, with subduction/closure of the BNS, and collision by Late Cretaceous time.

In the southern Lhasa terrane, uniform magnetisation across the red bed Takena Formation yielded paleolatitudes of ~12.5°N during Upper Cretaceous and Paleocene time, with a ~41.5° counter-clockwise rotation, potentially hinting at an oblique margin to the northwest (Achache et al., 1984). Achache et al. (1984) suggests that the Takena Formation was located at ~13.5°N when the Linzizong Volcanics were extruded over them during 69–43 Ma, peaking at ~50 Ma (Coulon et al., 1986; He et al., 2003; Zhou et al., 2004; Lee et al., 2012). Similar latitudes of ~14.4 ± 5.8°N were reported from 53 Ma-old mafic dykes, intruding the volcanics (Liebke et al., 2010). Another recent paleomagnetic study for the Linzizong Group (sediments overlying the Linzizong Volcanics) reported paleolatitudes of ~10°N, without rotation or latitudinal variation during their extrusion (Chen et al., 2010). However, (volcano-) sedimentary facies can be affected by inclination shallowing, leading to overestimates of crustal shortening, recent tilt-corrected paleolatitudes for the Linzizong Volcanics include 21–27°N (Tan et al., 2010), 22.8 ± 4.2°N (Dupont-Nivet et al., 2010) and 20 ± 4°N (Huang et al., 2013), with similar paleolatitude reported by further work (Huang et al., in review). Lower paleolatitudes of 13.8 ± 7.3°N were recorded for 55 Ma-old rhyolitic tuffs in the northern Lhasa terrane (Sun et al., 2010). In the central Lhasa terrane, the ~130–110 Ma-old volcanic-sedimentary Zenong Group (Zhu et al., 2008a) yield a paleolatitude of ~19.8 ± 4.6°N (Chen et al., 2012). A recent re-evaluation of published paleomagnetic data suggest that between ~110 and 50 Ma, the Lhasa terrane was located at ~20 ± 4°N, before drifting to 29°N, its latitude since early Eocene time (Lippert et al., 2014), which fits with our modelled location for the Lhasa terrane.

Paleomagnetic data compiled from volcanic rocks in the South Qiangtang terrane suggest that it was located at ~28.7 ± 3.7°N at ~40 Ma, so that the southern margin of the Lhasa terrane may have been located as far south as ~20°N throughout Eocene time (Lippert et al., 2011). Accordingly, we locate the BNSZ at a paleolatitude of ~28°N at ~40 Ma, but position it further south at ~55 Ma, so that the mid-southern Lhasa terrane margin is coevally located at ~20°N. Northward subduction beneath the Lhasa terrane is documented by magmatism along the Trans-Himalaya Batholith, dated at ~205–152, ~109–80, ~65–41 and ~33–13 Ma (Ji et al., 2009a). The gap between 152 and 109 Ma could coincide with the formation of an intra-oceanic arc, discussed below.

3.3. Intra-oceanic arc(s)

The KLA has been identified as part of a Tethyan-wide intra-oceanic arc (TIA) (e.g. Khan et al., 2009; Burg, 2011; Bouilhol et al., 2013), which may have stretched further east along the Eurasian margin but does not outcrop as definitively beyond the Karakoram Fault (Pudsey, 1986), except for the ophiolitic fragments in the YTSZ. The intra-oceanic arc may also have reached further west, into the Mediterranean Tethysides, or alternatively initiated along a transform (Reuber, 1986), which must have existed offshore NE Africa, allowing the northward passage of India (relative to a relatively stationary Africa) from mid-Cretaceous time. Jurassic oceanic substratum (or earliest backarc seafloor) along Kohistan–Ladakh (Honegger et al., 1982; Reuber, 1989) and at

Spongfang (Fuchs, 1981; Pedersen et al., 2001), also outcrops further east along the YTSZ, at the Eastern Syntaxis (Geng et al., 2006), Naga (Baxter et al., 2011), Chin Hills, near Burma (Mitchell, 1981), and Zedong and Loubusa ophiolites (McDermid et al., 2002; Robinson et al., 2004; Mo et al., 2008). The earliest formation of the intra-oceanic arc, which we suggest consisted of both the KLA and YTSZ, may have occurred at ~154 Ma based on the Matum Das tonalite (Schaltegger et al., 2003), which is either related to an earlier arc or the onset of trench roll-back from the Karakoram margin. Early Cretaceous radiolaria near the Spongfang ophiolitic massif, south of Ladakh (Baxter et al., 2010) may also record the initial stages of KLA formation. Here, gabbros, dated at ~177 Ma, are overlain by andesitic arc rocks dated at ~88 Ma, which may indicate Turonian–Maastrichtian obduction (Pedersen et al., 2001). Two Valanginian–Aptian radiolarian faunal assemblages associated with the Spongfang ophiolite suggest that this was a long-lived (Jurassic–Cretaceous) island arc system, which sutured at post-Aptian times (Baxter et al., 2010), possibly forming in a transform setting, given relationships between two mylonite shear zones in the upper mantle sequence (Reuber, 1986).

Further evidence for the intra-oceanic arc system along the YTSZ includes the overturned Late Jurassic arc volcanic rocks named the Zedong terrane (McDermid et al., 2002), the Mid Cretaceous Bainang accretionary wedge (Ziabrev et al., 2004), and the Barremian Dazhuqu ophiolite, generated at near-equatorial latitudes (Ziabrev et al., 2003; Abravitch et al., 2005). The obduction of the Barremian–Aptian Dazhuqu (Ziabrev et al., 2003), Bainang (Ziabrev et al., 2004), Xigaze (Guilmette et al., 2009), Buma (Guilmette et al., 2009), Saga and Sangsang (Guilmette et al., 2012), Zhongba (Dai et al., 2011b), and Xiugugabu (Wei et al., 2006) ophiolites was suggested to have occurred due to changes in motion between Africa and India, causing intra-oceanic thrusting/fracture zone imbrication at ~110–85 Ma (Girardeau et al., 1985b), the timing of which may be related to the 105–100 Ma global plate reorganisation (Matthews et al., 2012).

If the intra-oceanic arc formed via rollback during Late Jurassic to Barremian time, northwards subduction beneath the Lhasa terrane is likely to have ceased. This is supported by the magmatic gap in the southern Lhasa terrane between 150 and 109 Ma (Ji et al., 2009a), when the intra-oceanic arc reached the equator (and in our model was soon to collide with Argoland). Northwards subduction beneath Eurasia (Lhasa and Karakoram) then resumed until there was a second magmatic gap at 80–65 Ma (Ji et al., 2009a), which coincides with a second phase of KLA growth i.e., the arc-normal rifting and extension that formed the Chilas Complex of Kohistan at ~85 Ma (Burg et al., 1998, 2006; Jagoutz et al., 2006). The subduction of young and buoyant crust at the intersection of the backarc mid-oceanic ridge and southeast Lhasa terrane (i.e. Andean-style margin along southern Eurasia/Lhasa) at ~81 Ma, may have impeded further subduction of the backarc for a time (Guo et al., 2013), with convergence between India and Eurasia mostly accommodated by subduction and roll-back at the intra-oceanic arc. Subduction beneath Eurasia again resumed from ~65 Ma, forming the Linzizong Volcanics (Coulon et al., 1986; He et al., 2003; Zhou et al., 2004; Lee et al., 2012), when our modelled Greater India and the intra-oceanic arc are within 500 km of each other but over 1500 km from the Eurasian continental margin (Fig. 6h and i).

The timing of collision between Eurasia (Karakoram) and the intra-oceanic arc (including KLA), forming the KKSSZ, has been controversial because the suture zone was initially dated as Late Cretaceous based on 111–62 Ma intrusions within Albian–Aptian limestones (Pudsey, 1986). Two magmatic stages identified for the Kohistan Batholith, where a ~104 Ma-old deformed group was intruded by an undeformed group at ~75 Ma, also initially suggest that the KLA accreted to Eurasia between ~100 and 75 Ma (Petterson and Windley, 1985). The first evidence of obduction may be the appearance of ophiolitic detritus in sedimentary units, including the Palaeocene Chogdo Formation in Ladakh's Zanskar Valley (Searle et al., 1990b), though this formation has since been classified as mostly Asian-derived and therefore not

related to India–Eurasia collision (Wu et al., 2007; Henderson et al., 2010a). Khan et al. (2009b) instead date the KKSSZ to ~47–41 Ma, linking it to the YTSZ, which they dated at ~51 Ma. Other recent in situ geochronological and isotopic studies of zircons in the Kohistan granitoids indicate that the KLA collided with Greater India at ~50 Ma, then with Eurasia at ~40 Ma, forming the KKSSZ (Bouilhol et al., 2013). Field observations of foliated rocks within older non-foliated rocks in the batholith (Jagoutz et al., 2009), as well as evidence of continued tectonic and magmatic activity well into Eocene time (e.g. Heuberger et al., 2007), may also preclude a simple one-phase collision model.

With this evidence in mind, we initiate the intra-oceanic arc (encompassing both the KLA and YTS), from 155 Ma with rollback to the equator until ~125 Ma to match the estimated paleolatitude of the Barremian Dazhuqu ophiolite (Ziabrev et al., 2003; Abravitch et al., 2005) and the Trans-Himalayan Batholith magmatic gap, when there was no subduction beneath the southern Lhasa margin between ~152 and 109 Ma (Ji et al., 2009a). The intra-oceanic arc then gradually receded north from the equator as subduction reinitiated beneath the Eurasia mainland (coinciding with our collision between the intra-oceanic arc and Argoland, from ~100 Ma). Subduction beneath Eurasia continued until the 80–65 Ma magmatic gap (Ji et al., 2009a), when a second phase of intra-oceanic arc growth formed the Chilas Complex at ~85 Ma (Burg et al., 1998, 2006; Jagoutz et al., 2006). Subduction reinitiated beneath the Lhasa terrane forming the Linzizong Volcanics from ~65 Ma with a climax at ~50 Ma (Coulon et al., 1986; He et al., 2003; Zhou et al., 2004; Lee et al., 2012). Our model features coeval, parallel northward subduction beneath both Eurasia mainland (Karakoram–Lhasa) and the intra-oceanic arc from 103 to 85 Ma, and from 65 to 42 Ma.

Our model features a diachronous collision between Greater India and the intra-oceanic arc (starting near the KLA portion) by ~54 Ma thereby matching isotopic changes in the source rocks of the KLA granitoids at ~50 Ma (Bouilhol et al., 2013), the cessation of arc volcanism in the KLA at 61 Ma (Khan et al., 2009), and the significant drop in India–Eurasia convergence rates by 58 Ma, an indicator of initial collision and the arrival of buoyant continental crust at the intra-oceanic arc to impede subduction (Zahirovic et al., 2012). The ~50 Ma slab break-off (Lee et al., 2009, 2012) marginally postdates our timing for collision between India and the intra-oceanic arc (~60 Ma). The ~42 Ma cooling of a granite, intruding the southern Lhasa terrane's Linzizong Volcanics at 52 Ma, is attributed to the end of arc magmatism, slab break-off, thrusting or thickening (He et al., 2007), and is also a good match for our modelled onset of collision between Eurasia and Greater India (~44 Ma) and a significant drop in convergence rates at ~43 Ma (Fig. 7b), accompanied by the onset of high P–T metamorphism (Zahirovic et al., 2012, and the references therein), initiating the KKSSZ (Bouilhol et al., 2013). The second-stage collision propagated eastward, with abandonment of the Wharton Ridge, final suturing, and the end of marine sedimentation in the Indus–Tsangpo Suture Zone occurring by 34 Ma further east (Aitchison et al., 2007).

A remagnetisation event in northern Kohistan plutonic and volcanic rocks during 50–35 Ma, yielding a paleolatitude of $25 \pm 6^\circ\text{N}$ (Ahmad et al., 2001), which is within the limits of our location of the KLA at that time. However, equatorial paleolatitudes of 1–2°N (and considerable counter-clockwise rotation) reported for Mid-Late Cretaceous red bed formations along the KKSSZ (Zaman and Torii, 1999), can only match our position for the KLA, not Karakoram. Geological evidence suggests that Karakoram and Qiangtang, were likely continuous terranes, and the latter was likely located at ~20°N in Early Cretaceous time, as discussed in Section 3.2. South of the Kohistan Batholith, paleolatitudes of $9–13 \pm 4^\circ\text{N}$ were acquired from the 55–45 Ma-old Utror Volcanic Formation (Ahmad et al., 2000). Our reconstruction can only match the lower age and northern paleolatitude, unless the KLA was already accreted to Eurasia at that time.

The geometry and motion of the intra-oceanic arc, matching Early Cretaceous equatorial paleolatitudes (Abravitch et al., 2005),

combined with our motion and extent for Argoland (Gibbons et al., 2012), suggests that Argoland and the intra-oceanic arc may have had an oblique collision, initiating in the west (KLA) from ~100 Ma (black cross, Fig. 6e), which did not begin in the east (around Timor) until ~20 Myr later.

4. Tectonic model and discussion

Our tectonic model aims to satisfy the key geological events (tectonic, magmatic, metamorphic and sedimentary) of Southern Eurasia and the Indian Ocean, as summarised in Figs. 6, 7 and 8, and Table 1. In our preferred model, the Karakoram, South Qiangtang and Lhasa terranes rifted from Gondwana during the Triassic or earlier, as part of Cimmeria, and

accreted to Eurasia by Jurassic time, followed by initiation of northward-directed subduction beneath these newly accreted terranes (Fig. 6a). Shortly before ~155 Ma, possibly due to the subduction of a mid-oceanic ridge, slab rollback along Eurasia (possibly due to subduction of a mid-oceanic ridge) may have generated a forearc at the southern Lhasa margin, which may have incorporated the embryonic KLA, further west (Fig. 6b). The KLA does not have continental basement, so a forearc origin is likely with progressive backarc spreading separating it from the Eurasian continental margin, following the model of Stern (2010). The Matum Das (northern Kohistan) tonalite age of 154 ± 0.6 Ma (Burg, 2011) may represent the inception of KLA. We interpret that the KLA, Dazhuqu and other Cretaceous arc remnants formed a continuous intra-oceanic subduction system approaching near-equatorial latitudes

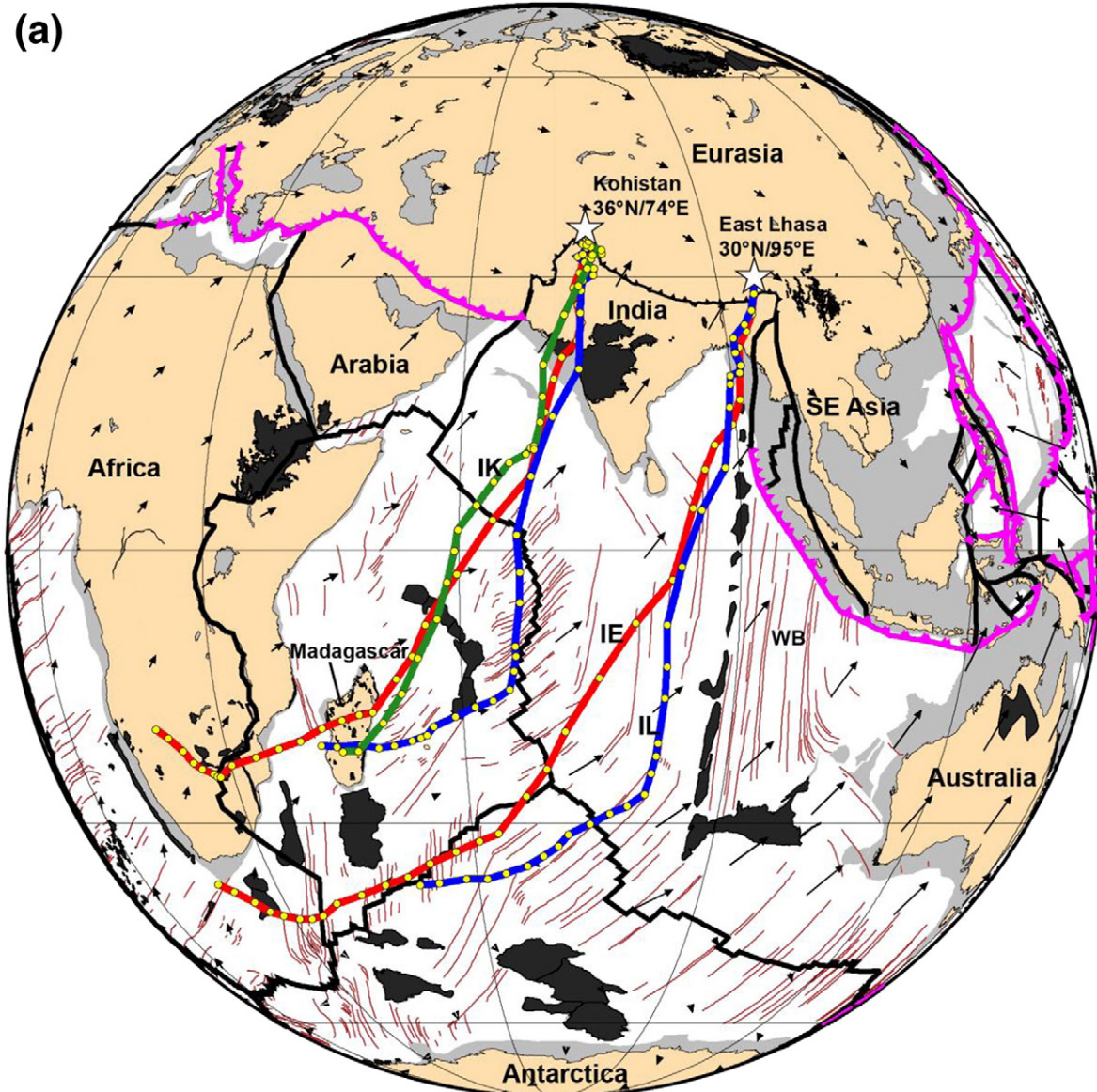


Fig. 7. a. Map showing the motion paths shown for two present-day reference points India–Eurasia (red), India–Lhasa (blue), India–Kohistan (green), with present-day plate boundaries (same symbology as in Fig. 1, except fracture zones as thin brown lines), coastlines filled in apricot, continental crust filled in light grey, and LIPs filled in dark grey. b. Relative convergence rates and direction calculated between India and stable Eurasia, India and Lhasa, and India relative to Kohistan (intra-oceanic arc) and plotted in 5 Myr intervals, using points in the Western and Eastern Syntaxis (white stars). Eurasia, Lhasa and Kohistan were taken as the fixed plate. Full lines on the graphs represent convergence rates derived from the western point, and dashed lines represent those from the eastern point (only the western point was plotted for Kohistan as the eastern portion of the arc is entirely synthetic). Notably, the acceleration related to Reunion eruption is only observable in the India–Kohistan convergence rates for 65 to 60 Ma. The initial arc–continent collision reduces convergence rates between India and Kohistan significantly, but only slightly for India–Eurasia (60 to 55 Ma). The continent–continent collision likely occurs sometime between 45 and 40 Ma, which is consistent with also the Wharton Ridge spreading cessation and the changes in the spreading rates and directions of the Indian Ocean (see text). c. Comparison of seafloor spreading rates plotted in 5 Myr intervals for 1) India–Antarctica from 125 Ma to present, with Antarctica anchored and seed point on the Southeast Indian Ridge (33.1783° S, 76.6478° E), 2) India–Madagascar (Africa) from 90 to 0 Ma, with Madagascar fixed and seed point at the Carlsberg Ridge (7.8820° S, 67.7773° E), 3) Australia–India (Central Indian Basin) from 130 to 45 Ma, with Australia fixed and seed point at the extinct Wharton Ridge (1.1747° N, 99.6213° E), note that the northern (Indian) flank has been mostly subducted and is therefore omitted.

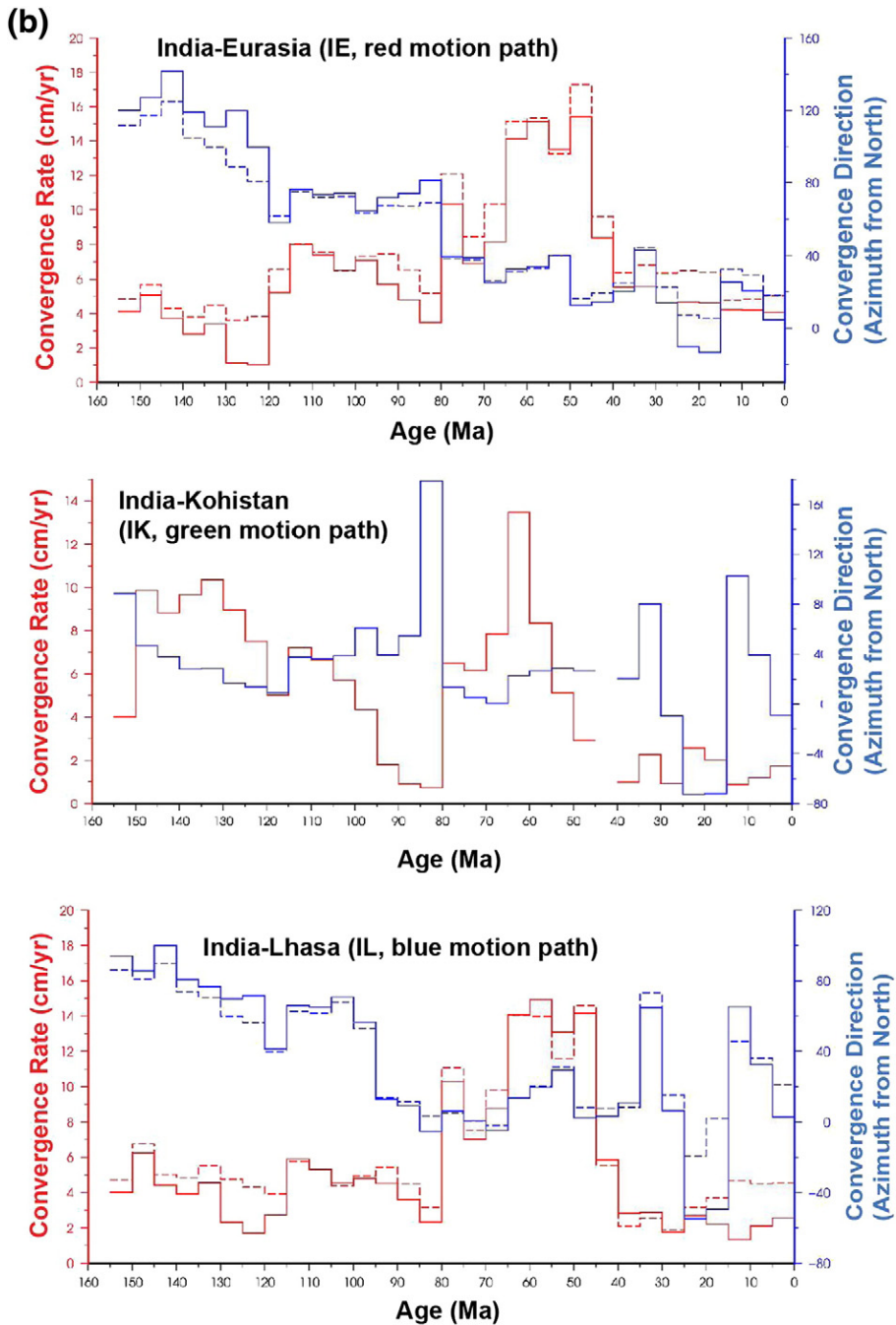


Fig. 7 (continued).

(via trench roll-back) by the mid-Cretaceous (Abrajevitch et al., 2005), which marks the maximum north-south extent of the Tethyan backarc sea (Fig. 6c-d). Supra subduction zone ophiolites and volcanic arcs obducted onto Sumatra also indicate that intra-oceanic subduction was established in the eastern Tethys during the mid Cretaceous, and we interpret a largely continuous intra-oceanic subduction zone extending across the Tethys, as per the recent study of Zahirovic et al. (2014). To avoid an intra-oceanic arc being larger than most observed today, we infer that there was one intra-oceanic subduction zone composed of two arcs originating respectively from SE Asia (Woyla) and Eurasia (KLA and YTSZ ophiolitic remnants). Their inherent arcuate geometry would imply a northward indentor at their nexus, which we locate east of the Lhasa terrane (roughly half-way between their distant terminals at KLA and Java). The indentation of India within Asia is supported by

analogue and numerical models (e.g. Peltzer and Tapponnier, 1988; Bajolet et al., 2013; Capitanio and Replumaz, 2013), and tomography (e.g. Richards et al., 2007; Replumaz et al., 2014). The nexus between the Woyla and YTSZ intraoceanic arcs is not necessarily a precursor to that indentation, our model suggests that NE Greater India initially docked further east, at roughly where Burma was located, prior to its northward relocation (as the Andaman Sea formed).

In the south, Jurassic continental rifting along northern Gondwana progressed to seafloor spreading via a southward jump that began to open the Argo Abyssal Plain, detaching Argoland (Fig. 6b), as well as fragments of Java, eastern Borneo and West Sulawesi, and blocks potentially belonging to Sumatra (Zahirovic et al., 2014). The oldest seafloor in the Argo Abyssal Plain, sampled by ODP Leg 123, Site 765, was dated at 155 ± 3.4 Ma (Gradstein and Ludden, 1992). Argoland drifted

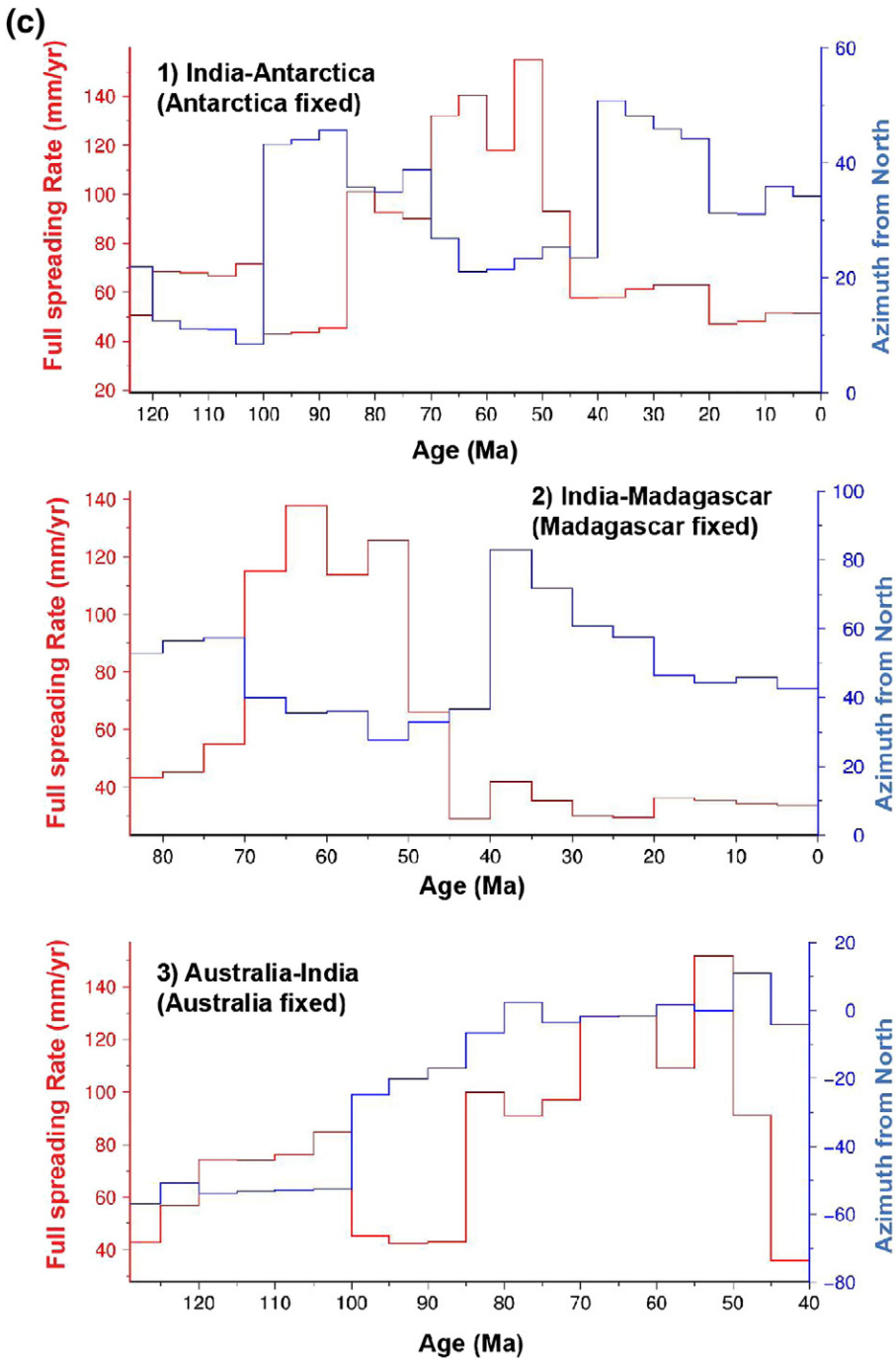


Fig. 7 (continued).

north and was likely offset from the western Tethys (north of Africa) via a north-trending transform fault (the potential precursor to the Owen Transform), offshore eastern Arabia. East Gondwana continued to disperse in the Early Cretaceous when Greater India, including the Gascoyne Block (GB, Fig. 6, originally conjugate to the Exmouth Plateau, Fig. 1) began to move northward. This led to the formation of a triple junction offshore NW Australia between Australia, India and Argoland (Fig. 6c), until mid-Cretaceous time, when the arm between India and Argoland was abandoned (Gibbons et al., 2012). Seafloor spreading between Australia and Antarctica slowly initiated from 83 Ma (chron 34) (Mutter et al., 1985), following rifting that probably initiated as early as 160 Ma (Totterdell et al., 2000) and experienced two significant changes in direction at 100 Ma and 50 Ma (Veevers, 2000; Whittaker

et al., 2007, 2013). Greater India also began to separate from Madagascar from Albian–Cenomanian time (Fig. 6f), as it slowly changed motion from west to north (Gibbons et al., 2013).

Meanwhile along the Eurasian margin, the Lhasa terrane rifted from the southern Qiangtang terrane during the Jurassic (Fig. 6b) to form the Bangong–Nujiang Ocean (a backarc sea) but resumed its northward motion during the Early Cretaceous until it (re-) collided with the Qiangtang terrane (Fig. 6e), forming the BNS in the Albian (Baxter et al., 2009). Andean-style northward subduction of backarc oceanic crust, beneath the Lhasa terrane, initiated sometime in the mid-Cretaceous (110–95 Ma), marked by the onset of emplacement of Karakoram Batholith (Debon et al., 1987) and Gangdese Batholith from 103 to 80 Ma (Wen et al., 2008). We interpret that Andean-style

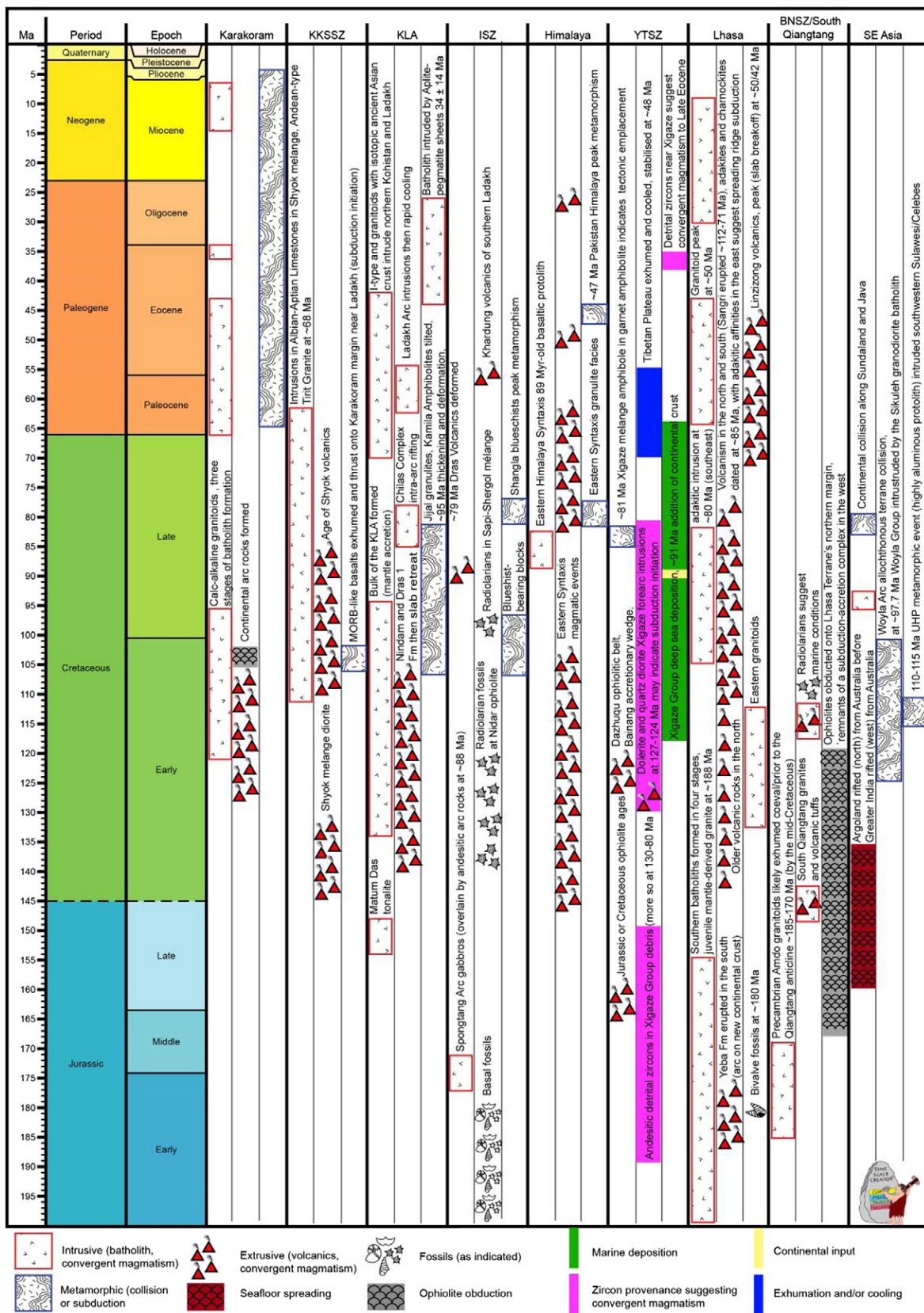


Fig. 8. Summary of first-order tectonic events related to the latest Jurassic evolution of the Tethys and Indian oceans. Showing magmatic (left column), volcanic or sedimentary (middle column), and metamorphic (right column) events documented for each region and suture zone, as per the key. For more details and references please see Table 1 (abbreviations and locations are as per Fig. 2).

subduction was initiated at least by 103 Ma (based on the age of pluton emplacement on the overriding plate), and that there were two north-dipping subduction zones in the Central Tethys, south of the Lhasa terrane and intra-oceanic arc (Fig. 6e). This is comparable to the present-day simultaneous subduction polarities observed along the Philippine and Izu-Bonin-Mariana trenches (Bird, 2003). Andean-style subduction along Eurasia (Lhasa and Karakoram terranes) continued until ~80 Ma, then became inactive until 65 Ma (Fig. 6g–h), possibly due to the approach of warmer, buoyant crust from the backarc mid-ocean ridge, resulting in the Gangdese magmatic gap (Chung et al., 2005; Wen et al., 2008; Ji et al., 2009a; Lee et al., 2009) (Fig. 6f–g). High-temperature metamorphism at ~81 Ma of a 90 Ma-old basaltic protolith, in the Eastern Himalayan Syntaxis, supports this subducting ridge scenario (Guo et al., 2013).

If Argoland extended across the Tethys to East Arabia, the (re-) initiation of northward subduction beneath the Lhasa terrane's southern margin coincides with the onset of diachronous collision between West Argoland and the KLA part of the intra-oceanic subduction zone, that likely spanned the entire Tethys (Fig. 6e–f). Further east, geological evidence suggests that Java, easternmost Borneo and West Sulawesi had collided with the intra-oceanic arc by 115 Ma, while collisions between Argoland fragments and the Woyla Arc (Figs. 5 and 6g) portion of the Tethyan intra-oceanic arc, likely followed in the Late Cretaceous (Zahirovic et al., 2014). Having accreted to the intra-oceanic arc, Argoland fragments may have finally reached Burma during Campanian–Maastrichtian time (Fig. 6h). The westward extent of Argoland may have been subducted or accreted in a region that is presently geologically obscure (such as between the Himalaya and KLA, southern Lhasa terrane or West Burma), or perhaps did not extend this far west. Evidence for the accretion of Argoland is also controversial along West Burma, Sumatra, East Java, and Borneo, as the blocks have both intra-oceanic and continental origin signatures, with inherited zircons and alluvial diamonds provenances that may be attributed to northwestern Australia (Smyth et al., 2007; Metcalfe, 2011b; Hall, 2012).

The fastest convergence recorded between India and Eurasia is a full rate of up to 20 cm/yr at ~70–60 Ma (Fig. 7b) (Lee and Lawver, 1995; Acton, 1999). Paleomagnetic constraints and changes in arc volcanism suggest that contact between the KLA and Greater India occurred by at least ~50 Ma (Bouilhol et al., 2013). This coincides with the significant drop in India–Eurasia convergence from 60 to 50 Ma (India-Kohistan/KLA, Fig. 7b) (Zahirovic et al., 2012) and was likely due to the buoyancy of Indian continental crust impeding subduction at the intra-oceanic arc. Andean-style subduction re-initiated along southern Lhasa by 65 Ma (Fig. 6i), resulting in the onset of plutonism in the Gangdese and eruption of the Linzizong Volcanics, between 69–43 Ma, peaking at around 50 Ma (Wen et al., 2008; Lee et al., 2009; Ji et al., 2012; Lee et al., 2012). Lu-Hf ages (54.3 ± 0.6 Ma) of garnet formed during thickening of middle crustal rocks in the north-central Himalaya (Smit et al., 2014), coincide with our modelled collision between Greater India and the intra-oceanic arc (Fig. 6j). Northern Greater India (Gascoyne Block) accreted to the intra-oceanic arc near West Burma during Ypresian time (Fig. 6i). Slab break-off likely occurred at ~50 Ma (Lee et al., 2009, 2012), with the remnant backarc oceanic basin becoming a narrow seaway separating Greater India and Eurasia (Fig. 6j). At this time, significant changes in seafloor spreading rates and directions (Fig. 7c) occurred in the Indian Ocean (Patriat and Achache 1984; Chaubey et al., 2002; Cande et al., 2010), while the chemistry of magmatism on KLA indicates the arrival of magma contaminated with a continental source (Bouilhol et al., 2013). The ISZ formed when the KLA was obducted onto the leading edge of Greater India at ~55 Ma (Fig. 6i–j).

In our model, continent–continent collision between Eurasia and Greater India (bearing the intra-oceanic arc) began in the Middle Eocene (Fig. 6k), and coincides with a second significant drop in India–Eurasia convergence rates at ~43 Ma (Fig. 7b) and reorganisation of seafloor spreading in the Indian Ocean (Lee and Lawver, 1995; Zahirovic et al., 2012), coupling Indian and Australian plates (Liu et al.,

1983), which began to move to north-eastward. The youngest marine sediments in the YTSZ with an age of ~34 Ma (Aitchison et al., 2007), suggest that suturing was complete and the YTSZ, with the KKSSZ as its western continuation, was raised above sea-level after Eocene time (Fig. 6l). Greater Indian mantle lithosphere may have continued to subduct and delaminate (Capitanio et al., 2010) or breakoff beneath Eurasia at ~15 Ma (Replumaz et al., 2010; Capitanio and Replumaz, 2013). Oligocene–Miocene metamorphic rocks of the Mogok metamorphic belt, exposed along the Sagaing Fault, where Burma travelled dextrally from the Early Miocene at present-day slip-rates of 18 mm/yr (Maurin et al., 2010), suggest that the Eastern Himalayan Syntaxis migrated northward (Bertrand et al., 1999), forming the pull-apart central Burmese basins within a transtensional shear zone.

4.1. Argoland

The Argo Abyssal Plain (Fig. 1) is Jurassic–Early Cretaceous seafloor, situated adjacent the passive margin of NW Australia, as well as the volcanic Joey and Roo Rises (e.g. Fullerton et al., 1989; Heine and Müller, 2005; Gibbons et al., 2012). There is no evidence for Late Jurassic south-dipping subduction along northern Gondwana, or that this oceanic crust formed as a backarc basin — the two drillsites in the Argo Abyssal Plain (ODP 261 and 765) reach a Jurassic tholeiitic basalt sill, overlying basement, and pillow basalt (Veevers et al., 1974; Gradstein, 1992). Two-dimensional numerical stochastic basin modelling suggests that a yield-strength minimum, thermally enhanced by heating from a mantle plume (of which Joey and Roo Rises could be a potential remnant), may cause a passive-margin segment to become isolated as a spreading ridge relocates to a zone of weakness along the landward edge of a rifted margin, thereby isolating another microcontinental terrane (Müller et al., 2002), in this case Argoland.

Argoland has been considered to form part of the Sikuleh (Fig. 5), West Burma and West Sulawesi continental fragments, which supplied sediments to northwest Timor during the Triassic and Jurassic until it separated from NW Australia (Metcalfe, 1996). Geochronological studies show that the Malay Peninsula, Thailand and Indochina have remained uplifted throughout the Cenozoic following a thermotectonic event at ~90 Ma (Hall, 2002), which precedes our modelled accretion of East Argoland there by ~10 million years. Also, at ~87 Ma, the volcanic and imbricated oceanic Woyla Group was intruded by the Manunggal Batholith, a composite of leucogranodiorite, granodiorite, granite and pyroxene-quartz diorite, at Natal in southwest-central Sumatra (Kanao, 1971, unpublished but quoted in Barber, 2000). This may correspond to our modelled accretion of eastern Argoland, as the fragment became trapped in the eastern part of the SE Asian intra-oceanic subduction trench from ~85 Ma. A Late Cretaceous oblique collision between the intra-oceanic arc and west-central Argoland may also account for the Dazuqu metamorphic soles, dated at ~90–80 Ma (Malpas et al., 2003), as our model shows Greater India almost 3000 km south of the equator at that time.

The accretion history along West Burma and Sumatra are poorly constrained and controversial, and West Burma has been referred to as Argoland (Metcalfe, 2006) and previously considered to have accreted to Burma in the Late Cretaceous (Heine and Müller, 2005). However, a more recent study (Metcalfe, 2011b) suggests that West Burma had already accreted by Triassic times and therefore cannot be Argoland. The Mesozoic Gondwanan origin for West Burma is disputed by recently identified Permian Cathaysian facies in northwest Burma, resulting in an alternative kinematic reconstruction that places Argoland's final destination along Java and east Borneo (Metcalfe, 2011b; Hall, 2012). However, these models require the initiation of a 1500 km transform fault across pre-existing Tethyan seafloor, and several closely-spaced parallel subduction zones with alternating polarities through time. We do not adopt this model since such a configuration of plate boundaries is arguably overly complex and unlikely, as such large areas of oceanic

crust are too rheologically robust to spontaneously develop into a large transform cross-cutting pre-existing tectonic fabrics.

The Late Jurassic uplift erosional unconformity shared between the Indo–Burman Ranges (Mitchell, 1993) and NW Australian shelf (Gradstein, 1992; von Rad et al., 1992), and Triassic Halobia bivalve affinities between Timor and NW Australia (Charlton et al., 2009), may yet support a link to Argoland. We propose that Argoland was probably a thinned, continental fragment, that became obliquely embedded in the intra-oceanic arc trench from ~100 to 85 Ma which, if it existed further west, collided with Greater India from the Mid-Paleocene, then with Eurasia during the Mid-Eocene, possibly destroying any remaining direct evidence of the continental fragment.

4.2. Implications of the 100 Ma global plate reorganisation on Tethyan evolution

Fracture zone bends in the Wharton Basin (Fig. 1) indicate a significant change in seafloor spreading directions and up to 50° clockwise rotation of the spreading system between India and Australia in the mid Cretaceous (Müller et al., 1998). The age of the resulting fracture zone bends in the Wharton Basin has been constrained by assuming constant seafloor spreading rates during the Cretaceous Normal Superchron, and interpolating the ages along the fracture zones to obtain an estimate of ~97 Ma (Müller et al., 1998), while microfossil evidence at nearby DSDP Site 256 indicates a minimum uppermost Albian age, representing basement age of 101 ± 1 Ma (Davie et al., 1974). The fracture zone bends in the Wharton Basin have been constrained to ~102 to 97 Ma, a time that is consistent with other globally-contemporaneous fracture zone bends at ~100 Ma (Matthews et al., 2011, 2012). Similarly, by assuming constant seafloor spreading rates during the Cretaceous Normal Superchron whilst incorporating geological and geophysical data from the western Indian Ocean (Fig. 1) to model the breakup between India and Madagascar, the bend can be modelled at 100 Ma via an anticlockwise component to India's rotation, which continued until their final breakup at ~83 Ma (Gibbons et al., 2013).

The tectonic driving mechanism for the significant change in seafloor spreading direction at ~100 Ma in the Indian Ocean has been poorly explored. In the context of our plate motion model, we suggest that the change in India's trajectory was likely a result of changing plate boundary configurations along southern Eurasia in the mid Cretaceous. Based on geological evidence, outlined in Sections 2.5, 2.8 and 2.9, we model intra-oceanic subduction of the MesoTethys in the Early Cretaceous, and invoke the inception of an additional subduction zone along southern Lhasa from ~103 Ma (Fig. 6e), increasing northward slab pull and suction forces on the Indian Plate due to the descending Bangong–Nujiang slab in the upper mantle. The renewed subduction along southern Lhasa at this time resulted in two contemporaneous north-dipping subduction zones in the NeoTethys, much like the present-day Pacific–Eurasia convergence across the Philippine Sea Plate in Southeast Asia. The two north-dipping subduction zones in the central Tethys may have generated an increased northward slab pull on the Indian Plate during mid Cretaceous time to result in a change of seafloor spreading orientation from NW–SE to dominantly N–S, observable in the bending motion path between India and Eurasia (Fig. 7a), as well as in the fracture zone bends of the Wharton Basin (Matthews et al., 2012).

Further east in the Woyla segment along the West Burma and Sumatra blocks, we propose a similar scenario for two contemporaneous north-dipping subduction zones. The renewal of Andean-style subduction and forearc formation along West Burma and Sumatra is interpreted to have occurred soon after onset of subduction along southern Lhasa, and is constrained by the 95 ± 2 Ma supra-subduction zone Andaman ophiolites (Pedersen et al., 2010). We invoke the collision of Gondwana-derived continents (corresponding in our model to Argoland) along the Woyla Arc from ~100 Ma, which may have propagated compressive stresses northward to drive Woyla

back-arc closure from this time. Hence we interpret that the global plate reorganisation event at ~100 Ma manifests itself most strongly in the Indian Ocean, as a major reorganisation of seafloor spreading resulting from increased slab pull driven by contemporaneous double north-dipping subduction zones along southern Eurasia.

4.3. Greater India and its collision(s)

A recent review paper (Chatterjee et al., 2013) summarising the evolution of India since it was part of Gondwana favoured collision with the KLA at ~85 Ma, closing the 'IndoTethys' (which we interpret as the Tethyan backarc sea) and forming the ISZ, before a final collision with the Eurasian mainland at ~50 Ma, inline with a drastic slowdown of India around the Early Eocene. The ~85 Ma suturing between KLA and India would be contemporaneous with the mid Cretaceous obduction of the Semail ophiolite in Oman (Smewing et al., 1991), supporting an east–west continuous intraoceanic subduction zone during Cretaceous time (Chatterjee et al., 2013). The mid Cretaceous obduction of the Semail ophiolite may instead be related to the change in plate motion of Greater India as it rifted away from Madagascar (from south to north) and began migrating north towards Eurasia. The Late Jurassic–Early Cretaceous ages for the Masirah ophiolite ages (Smewing et al., 1991) generally match the breakup between India and Australia–Antarctica. Another rationale for the ~85 Ma KLA–India collision model (Chatterjee et al., 2013) was that it may have formed a land bridge for the migration of several groups of Maastrichtian dinosaurs between India and Africa (Chatterjee and Scotese, 2010). Our geometric configuration of the KLA allows it to come within 500 km of the Arabian COB at ~80 Ma, but only Western Argoland (if it extended that far west) was close enough to collide with KLA, as India was nearly 2000 km further south at this time, though only within ~700 km of the Somali plate (the closest part of Africa at that time, Fig. 6g–h) and may have come within ~300 km of Arabia at ~58 Ma (Fig. 6i–j). Though we support the notion of a continuous east–west-trending Cretaceous intraoceanic subduction zone, other recent studies of the KLA magmatism suggest that collision between Greater India and KLA took place by either ~61 Ma (Khan et al., 2009) or at ~50 Ma (Bouilhol et al., 2013). Our model, which is also based on the paleolatitudes and geometric/tectonic of Greater India and KLA (described in this section, and Sections 2.3 and 3.3, Fig. 8 and Tables 1 and 2), accordingly features a diffuse collision between 61 and 50 Ma (more certainly by ~54 Ma).

Many studies date the onset of India–Eurasia continent–continent collision to ~55–50 Ma (e.g. Garzanti et al., 1987; Leech et al., 2005; Sciunnach and Garzanti, 2012; Searle et al., 1987). An abrupt change from Upper Cretaceous Xigaze marine flysch to Eocene Qiuwa conglomerates, the latter originating from the Gangdese Batholith, was interpreted as a product of the India–Eurasia collision (Searle et al., 1987). However, stratigraphic relationships indicate an Upper Oligocene–Lower Miocene age for the conglomerates (Aitchison et al., 2002b). Early evidence of India–Eurasia collision could be the appearance of ophiolitic detritus in sedimentary units, including the Palaeocene Chogdo Formation in the Zanskar Valley (Searle et al., 1990b), yet this formation has been classified as mostly Asian-derived and therefore not related to Indian collision (Wu et al., 2007; Henderson et al., 2010a). Aitchison et al. (2007) suggested a 34 Ma India–Eurasia collision with the identification of Lower Eocene marine sediments in the Pengqu Formation, central YTSZ (Wang et al., 2002). The lack of Indian-plate input in the ~50 Ma-old Indus Basin sedimentary rocks, between India and KLA (Henderson et al., 2010b), may also support a younger collision.

We suggest that the initial continent–continent collision, based on the paleolatitudes and configurations of Greater India and the Eurasia mainland (described in this section, Sections 3.1 and 3.2, Fig. 8 and Tables 1 and 2), began by 44 ± 2 Ma, as supported by several lines of evidence. Constraints from marine geophysical data shed light on the collision, with significant slowdown in seafloor spreading from ~52 to

43 Ma on the Central and Southeast Indian Ridge and a significant change in spreading direction from ~43 Ma (Cande et al., 2010), which may be linked to continent–continent collision impeding subduction and changing the stress field acting on the Indian plate. Earlier magnetic investigations (Liu et al., 1983; Krishna et al., 1995) in the Wharton Basin inferred that the seafloor spreading in the Wharton Basin ceased shortly after Anomaly 20 (~42 Ma) and the spreading centre jumped south between Australia (Broken Ridge) and Antarctica (Kerguelen Plateau), creating a single Indo-Australian Plate. Recent magnetic investigation in the Australian Southern Ocean (Whittaker et al., 2013) revealed an acceleration in the spreading rate of Australia–Antarctica seafloor spreading system at ~43 Ma, suggesting extinction of Wharton spreading centre at this time so that the northward slab pull from subduction along the Java–Sunda trench was transferred across the entire Indo-Australian Plate to drive faster Australia–Antarctica seafloor spreading. These events of extinction in the Wharton Basin and acceleration of Australia–Antarctica spreading rate, which occurred during ~42–44 Ma, were generally considered as a response of continent–continent collision between India and Eurasia.

Two recent publications (Krishna et al., 2012; Jacob et al., 2014) used detailed and improved magnetic anomaly identifications of the Wharton Basin from an updated compilation of magnetic profiles. Both these studies confirm that Anomaly 20n (42.5–43.8 Ma) is the youngest identifiable magnetic anomaly in the Wharton Basin, but they differ in the interpreted timing of spreading cessation in the Wharton Basin. While Krishna et al. (2012) inferred the timing of extinction of Wharton Basin spreading as ‘soon after middle Eocene anomaly 19’, Jacob et al. (2014) inferred the timing of extinction specifically at 36.5 Ma. Jacob et al. (2014) used the analytic signal technique and plate reconstructions to determine precise locations of younger and older boundaries of each normal-polarity blocks, and therefore provided an age map with higher resolution. Their seafloor age map clearly shows that Anomaly 20ny (42.5 Ma) is the youngest magnetic anomaly which can be identified and delineated in the Wharton Basin but that a considerable area of crust exists between the younger bound of Anomaly 20n in the southern flank of the Wharton Basin (Australian Plate) and its conjugate in the northern flank of the Wharton Basin (Indian Plate). Due to the decreasing spreading rate and increasing tectonic and magmatic complexity, it is difficult to decipher magnetic anomalies at the fossil spreading centre. Consequently, they interpreted the extinct axis as Anomaly 18ny (38 Ma), although it is possible to consider a reduced spreading activity up to Anomaly 15 (35 Ma).

Though the exact timing of spreading cessation proposed by Jacob et al. (2014) is not very well constrained, Wharton Basin spreading appears to have continued for a few million years after Anomaly 20ny (42.5 Ma), which is younger than our proposed continent–continent collision timing of 44 ± 2 Ma, derived from several lines of geological evidence from the collision zone, and marine geophysical evidence. This observation necessitates a reassessment of the relationship between the Wharton Basin spreading extinction (considerably younger than 42.5 Ma), accelerated motion between Australia and Antarctica (43 Ma) (Whittaker et al., 2013) and our proposed onset of India–Eurasia continent–continent collision at 44 ± 2 Ma. All these pieces of information are compatible when we consider a two-stage continent–continent collision between India and Eurasia, i.e., ‘soft (initial continent–continent) collision’ by 44 ± 2 Ma and ‘hard (complete continent–continent) collision’ by ~38–35 Ma, due to the increasing presence of buoyant cratonic crust in the collision zone (and/or a slab detachment event that caused a slowdown in India’s northward motion).

Our study differs from the more conventional concept of a single India–Eurasia collision, in favour of a multistage collision (e.g. Guillot et al., 2003; Hafkenscheid et al., 2006; Zahirovic et al., 2012), where the arc–continent and continent–continent collisions both need to be considered as gradual processes, composed of different stages. Greater India–Eurasia collision is likely to have had two (or more) stages,

starting when only the west-central part of northern Greater India collided with continental Eurasia at 44 ± 2 Ma, resulting a slowing down of spreading in the central Indian and southeast Indian ridges (and perhaps the Wharton Basin spreading centre), and accelerating spreading centre in the Antarctica–Australia spreading system. During this time, part of the NeoTethys Ocean still existed, leaving a gap in the east between Greater India and southeastern part of Eurasia (roughly where Burma or the Eastern Himalayan Syntaxis is today). The northeastward movement of Greater India might have continued after 44 ± 2 Ma in the same direction and arrived at a stage of final continent–continent collision, completing the continental contact between Greater India and Eurasia. This final stage of collision and the end of marine sedimentation in the Indus–Tsangpo Suture Zone might have occurred by 34 Ma in the east (Aitchison et al., 2007). The inferred timing of extinction for Wharton Basin spreading (Jacob et al., 2014) is several million years younger than Anomaly 20ny (42.5 Ma) and therefore, the cessation of spreading in the Wharton Basin likely occurred during ‘hard’ (near complete) continent–continent collision stage sometime between 44 ± 2 Ma and 34 Ma. This timeframe may also represent an episode of continental lithosphere subduction as proposed by Capitanio and Replumaz (2013).

Independent of the marine geophysical observations, the history of deformation on the continents also supports a continental collision underway by 44 ± 2 Ma. The majority of crustal thickening in the Tethyan Himalaya occurred by 44.1 ± 1.2 Ma based on the age of younger undeformed granitoid bodies constrained by U–Pb zircon dating (Aikman et al., 2008). We postulate the same for the Tibetan Plateau, where exhumation and cooling of Tibetan peneplain granitoids occurred between 70 and ~55 Ma (Hetzell et al., 2011), and the plateau likely spanned the entire margin by 45 Ma (Rohrmann et al., 2012). The Bengal fan system became active (albeit with lesser channel activity) as early as Eocene time (Bastia et al., 2010), and the influx of clastic sediment from the Himalayas and Indo-Burman Ranges, signalling a major switch in sedimentation pattern over the Bengal Basin during the Mid Eocene, may also be a result of that final collision (Alam et al., 2003). Late Eocene (~38 Ma) Himalayan-derived sediments found in the Bengal Basin (onset of vigorous Himalayan erosion), makes a diachronous collision seem less likely, unless older Himalayan-derived sediments were deposited earlier in the west, and the authors point out that older material may have deposited elsewhere (Aikman et al., 2008). The Late Eocene Himalayan-derived sediments, being the oldest identified, may preclude a younger India–Eurasia hard collision, as does the ~35 Ma onset of extrusion tectonics (Leloup et al., 2001, 2007), with activation of the NW–SE trending Red River–Ailao Shan shear zone between Indochina and South China, accommodating several hundred kilometres of sinistral motion (Tappognier et al., 1990; Lee and Lawver, 1995). In addition, the oldest eclogites reported in the Eastern Himalayan Syntaxis bear ages of ~38 Ma, which likely indicate that continental collision was well under way by the Late Eocene (Kellett et al., 2014).

Further west, Petterson and Windley (1985) dated the ISZ as forming in the Eocene, based on Eocene fossils, sediments and calc-alkaline lavas overlying the Kohistan Batholith, but they also dated layered aplite–pegmatite sheets intruding the batholith at ~34 and 29 Ma, suggesting they were post-collisional. In our model, their Eocene ISZ coincides with the collision between India and the intra-oceanic arc, and then their final collision with Eurasia. The ~54–40 Ma calc-alkaline plutons forming two thirds of the Kohistan Batholith (Petterson and Windley, 1985) suggests that oceanic subduction continued here until 40 Ma, which post-dates our modelled Early Eocene KLA–India collision, unless there was southward subduction of the backarc basin beneath Kohistan (the plutons were described in northern Kohistan). The cessation of Linzizong volcanic and granitoid emplacement by ~43 Ma (Coulon et al., 1986; He et al., 2003; Zhou et al., 2004; Lee et al., 2012) supports the end of Andean-style volcanism along southern Lhasa and the onset of continent–continent collision by ~ 44 ± 2 Ma. If the calc-alkaline Linzizong Volcanics represent Andean-style subduction of

oceanic lithosphere (Coulon et al., 1986; Zhou et al., 2001), then the cessation of magmatism by ~43 Ma would indicate the completion of oceanic subduction and initiation of continental lithosphere subduction and underthrusting of Indian crust. Treloar et al. (1996) also reported that plutons intruded the KLA (extruding basaltic through to rhyolitic volcanic rocks) until 40 Ma, before the Indus confluence granite sheets were emplaced at $\sim 34 \pm 14$ Ma. Our model features a two-stage collision between Greater India and intra-oceanic arc by ~54 Ma, though it may have been ongoing until the initial continental collision between Greater India and Eurasia at ~44 Ma, which respectively coincide with a spreading rate decrease and minima in the convergence rates (Fig. 7b and c), as recorded in the seafloor spreading histories (e.g. Cande et al., 2010). The convergence rate decrease, starting ~52 Ma and resulting in the ~43 Ma spreading rate minima, is a good match to our collision between Greater India and the KLA, and then Eurasia (Fig. 6i–j). We interpret that collision between Greater India (bearing KLA) and Eurasia formed the ISZ and the second phase of the YTSZ, the latter having already partly formed in the west, following Early Eocene collision between Greater India and the intra-oceanic arc.

Notwithstanding the KLA, India's northern margin (Zanskar Himalaya, Fig. 4), has no stratigraphic record of ophiolite detritus before Eocene time (Garzanti et al., 1987), but ~500 m uplift is recorded in the distal Tertiary succession preserved beneath the Spongfang Ophiolite in the Early Eocene (Sciunnach and Garzanti, 2012). Our model also features an Early Eocene collision between NE Greater India's promontory, called the Gascoyne Block (Gibbons et al., 2012), and West Burma, which matches the emplacement of a ~50 Ma granitic batholith (Fan and Ko, 1994), though the Gascoyne Block may have accreted to the intra-oceanic arc instead. The Gascoyne Block would likely have been consumed by Greater India's collision with Burma, featured in our model at ~43 Ma, and now may underlie the Eastern Himalayan Syntaxis. The considerable reduction in India's northward motion at ~52 Ma (Cande and Stegman, 2011) corresponds in our model not only to collision between the KLA and Greater India but also collision between Burma (or the intra-oceanic arc) and the Gascoyne Block (Fig. 6i–j).

The reduced extent of Greater India and the paleolatitudinal difference between it and the Eurasian margin through time, as explained in Sections 3.1 and 3.2, can also constrain the timing of final collision. Indian northern margin sediments, dated at Late Maastrichtian (~66 Ma) and mid-late Paleocene (~60 Ma), give paleolatitudes between 5.7°S and 4°N (Patzelt et al., 1996), which were recalculated to 4.9 ± 2.8 °S (van Hinsbergen et al., 2012). Paleocene marine sediment paleopoles imply that the Tethyan Himalaya were located around $\sim 4.7 \pm 4.4$ °S between ~62 and 56 Ma (Yi et al., 2011), which were recalculated to 8.7 ± 1.7 °N (van Hinsbergen et al., 2012). Latest Paleocene limestones in the Tethyan Himalaya (near Tingri, Mt Everest), record paleolatitudes between ~5 and 10°N (Besse et al., 1984). These are all considerably further south than the majority of paleolatitudes reported for the Eurasian margin for the same time period, indicating that India and Eurasia did not collide in pre-Eocene times. For example, the Linzizong Volcanics along the southern Lhasa terrane record paleolatitudes of 21–27°N (Tan et al., 2010), 22.8 ± 4.2 °N (Dupont-Nivet et al., 2010) and 20 ± 4 °N (Huang et al., 2013), or even ~ 12.5 °N (Achache et al., 1984) and $\sim 14.4 \pm 5.8$ °N (Liebke et al., 2010). These results suggest that the Lhasa terrane was further north than the Tethyan Himalaya during the Paleocene–Eocene. The most recent re-evaluation of published paleomagnetic data suggest that the Lhasa terrane was located at $\sim 20 \pm 4$ °N between ~110 and 50 Ma (Lippert et al., 2014). This matches our motion for the Lhasa terrane and a collision with Greater India from 44 Ma ± 1 Ma.

Complete closure of the Tethys at the Eocene–Oligocene boundary (~34 Ma) would coincide with several significant climatic events, including abrupt cooling and glaciation in Antarctica (DeConto and Pollard, 2003; Zachos and Kump, 2005), the disappearance of playa lake deposits in the northeastern Tibetan plateau (Dupont-Nivet et al.,

2007), and cooling and aridification in Asia (Ivany et al., 2000). Tibetan uplift was previously invoked to explain these events but was likely already concluded by 38 Ma (Dupont-Nivet et al., 2008), or over 10 million years earlier (Hetzel et al., 2011). Amphibole data from the western Nanga Parbat (Western Himalayan Syntaxis) indicate regional cooling through 500 °C at 25 ± 5 Ma (Treloar et al., 2000). This coincides with a peak in metamorphism at the Namche Barwa (Eastern Syntaxis), though the age range for the metamorphic zircons is 30–8 Ma, followed by retrograde metamorphism at ~18 Ma (Su et al., 2012; Z.M. Zhang et al., 2012b). Though not obvious in our model, this age range may suggest a diachronous collision between India and Eurasia, progressing from west to east over 8 Myr, and coincides with an anti-clockwise component to India's motion as well as a 40% Indian plate deceleration between 20 and 10 Ma (Molnar and Stock, 2009), and initiation of Burma's northward transfer. There may have been a north-bound transform fault offsetting/dividing the intra-oceanic arc between the Central Tethys and SE Asian portions, so that the Gascoyne Block (NE Greater India), then Greater India's eastern edge were subducted (eastward) somewhere near West Burma.

4.4. Implications of India–Eurasia convergence for mantle structure

The long-term India–Eurasia convergence consumed the equatorial Meso- and Neo-Tethyan ocean basins, leaving slab remnants in the upper- and mid-mantle that can be imaged using mantle seismic tomography (Van der Voo et al., 1999; Replumaz et al., 2004; Hafkenscheid et al., 2006). The first-order interpretations aim to characterise the active Eurasian margin as a purely Andean-style convergent margin with a single subduction zone consuming Tethyan lithosphere, or alternatively as one requiring an additional intra-oceanic subduction zone. Based on the number of interpreted discrete slab volumes in P-wave seismic tomography (Bijwaard et al., 1998), and the large latitudinal spread of interpreted slabs ranging from equatorial latitudes to the present-day suture zone at ~40°N, led Van der Voo et al. (1999) to infer intra-oceanic subduction of the NeoTethys with a two-stage collision between Greater India and an island arc, followed by the terminal continent–continent collision. The numerical analysis of slab volumes by Hafkenscheid et al. (2006) also supported an intra-oceanic subduction scenario, and suggested an average slab sinking rate of 3 cm/yr in the upper mantle, and 2 cm/yr in the lower mantle. The reconstructed positions of Eurasia and Southeast Asia superimposed on P-wave tomography depth slices by Replumaz et al. (2004) suggested a sinking rate of 5 and 2 cm/yr in the upper and lower mantle, respectively. Global mantle flow models, with a kinematic surface boundary condition, were used by Zahirovic et al. (2012) to test the two competing hypotheses of long-term Andean subduction consuming Tethyan lithosphere as opposed to a scenario that invokes both intra-oceanic and Andean-style subduction in the NeoTethys. The results of the numerical modelling indicated that the large latitudinal spread of slab material in the mid-mantle can better be accounted for by intra-oceanic subduction, as well as reconciling geological evidence of island arc volcanism (Burg, 2011; Bouilhol et al., 2013), intra-oceanic supra-subduction zone ophiolites (Aitchison et al., 2000; McDermid et al., 2002; Aitchison et al., 2007) and a two-stage slowdown in India–Eurasia convergence.

Age-coding of horizontal tomography slices using average vertical sinking rates is presented in Fig. 9 using end-member sinking rate estimates of 3 and 1.2 cm/yr in the upper and lower mantle, respectively, following Zahirovic et al. (2012), and 5 and 2 cm/yr for the upper and lower mantle, respectively, following Replumaz et al. (2004). The slab material (blue regions) in the P-wave seismic tomography model (Li et al., 2008) highlights the Eurasian slab burial grounds from long-term subduction of Tethyan and (proto-) Pacific lithosphere that is largely beneath the reconstructed position of east and southeast Asia when applying the faster sinking rates (right column, Fig. 9). Geological evidence for established intra-oceanic arc volcanism in the Cretaceous, as well as a larger latitudinal range of slab material at mid-mantle

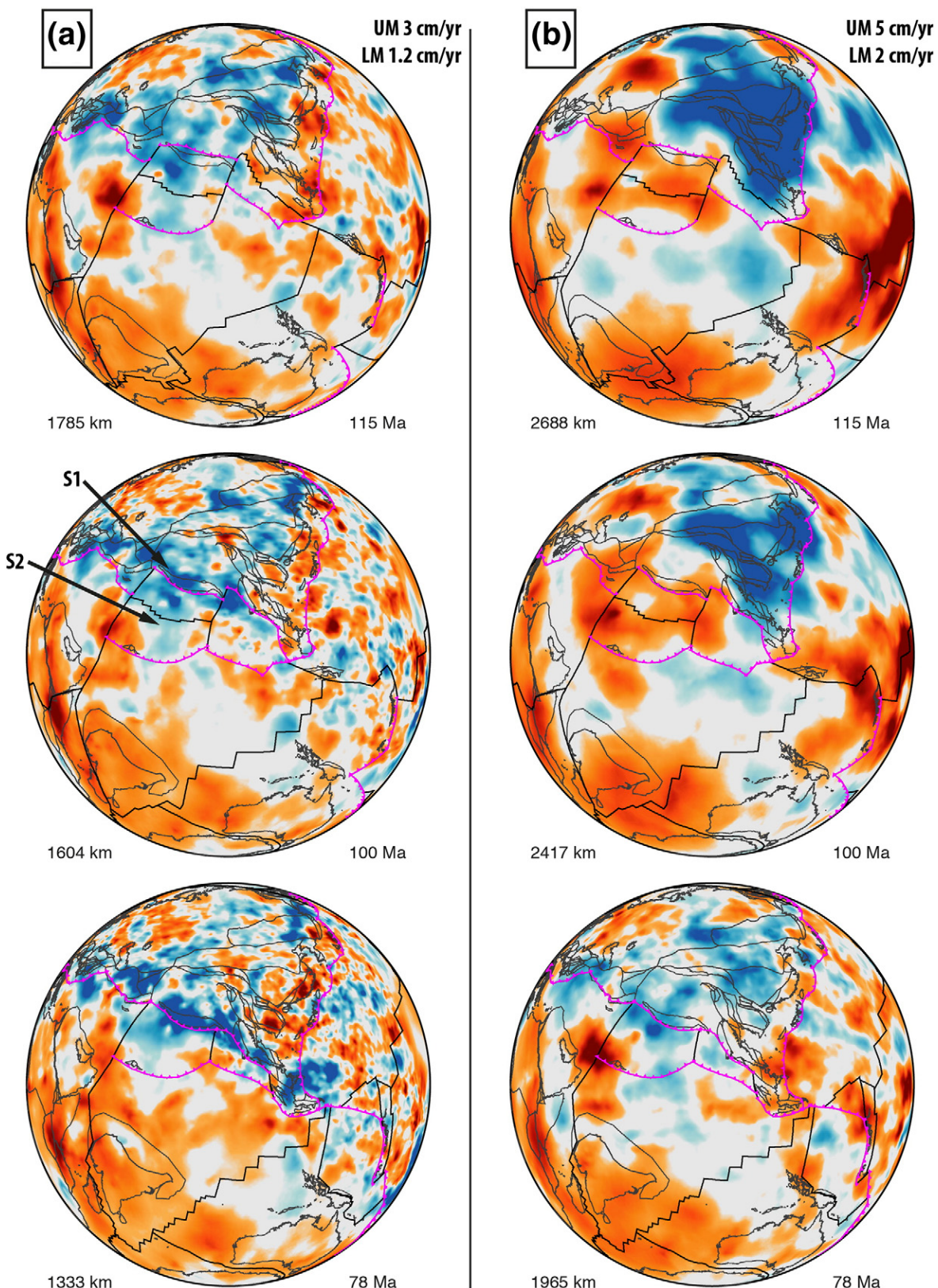


Fig. 9. Plate reconstructions superimposed on age-coded depth slices from P-wave seismic tomography (Li et al., 2008) using first-order assumptions of near-vertical slab sinking, with a) 3.0 and 1.2 cm/yr constant sinking rates in the upper and lower mantle, respectively, following Zahirovic et al. (2012), and b) 5.0 and 2.0 cm/yr upper and lower mantle sinking rates, respectively, following Replumaz et al. (2004). Both end-member sinking rates indicate bands of slab material (blue, S1–S2) offset southward from the Andean-style subduction zone along southern Lhasa, consistent with the interpretations of Tethyan subducted slabs by Hafkenscheid et al. (2006). However, although the P-wave tomography provides higher resolution than S-wave tomography, the amplitude of the velocity perturbation is significantly lower in oceanic regions (e.g., S2) and the southern hemisphere due to continental sampling biases. Orthographic projection centred on 0°N, 90°E.

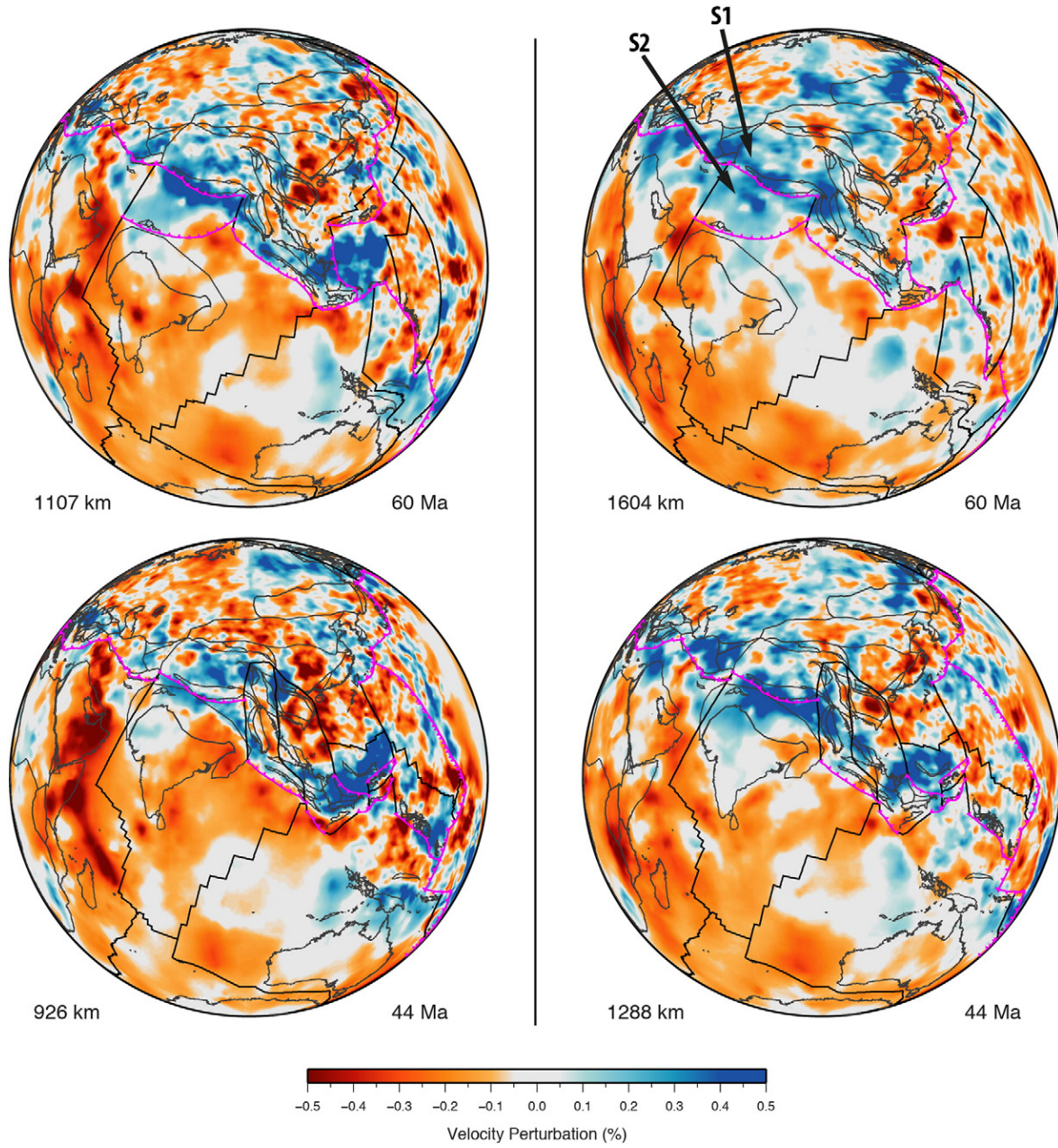


Fig. 9 (continued).

depths, is compatible with intra-oceanic subduction in the NeoTethys and a two-stage India–Eurasia collision. However, the remaining controversy revolves around the paleo-latitudinal motion of the intra-oceanic subduction zone, as well as the eastward extent into the YTSZ. Addressing these issues will require progress in tomographic techniques to image the mantle beneath oceanic regions with improved resolution, in addition to more geological data collection and geodynamic modelling to test a wider range of possible convergence scenarios.

5. Conclusions

A new, regional tectonic model, incorporating a revision of potential field data in all the abyssal plains off West Australia and Antarctica (Fig. 1) was used to constrain the motion of the continental blocks that formed the NeoTethys, helping recreate the morphology of this ocean basin including features such as fracture zones and submerged

plateaus (Fig. 1), in a self-consistent way (Gibbons et al., 2012, 2013). Dredged and dated Jurassic gabbro offshore NW Australia (Fig. 1) led to redefining the northern limits of Greater India to include a narrow indenter (Gascoyne Block) which was originally juxtaposed to the Exmouth Plateau (Fig. 1), off NW Australia, and an extended continental sliver (Argoland), originally located adjacent to the northern margins of both Greater India and Australia. Constrained by the geological and geophysical data described in this paper, these geometries have implications for the timing of collision between Argoland, Greater India, the Eurasian (Figs. 2, 3 and 4) and SE Asian margins (Fig. 5), and any associated oceanic arcs, of which there are outcrops in the southern/youngest suture zones surrounding India's northern margin. Our model (Fig. 6) also reconciles magmatic gaps along southern Tibet between ~150–100 Ma (rollback of the intra-oceanic arc) and ~80–65 Ma (approach of the intra-oceanic arc mid-oceanic ridge).

We argue that the lack of direct evidence for collision between Eurasia and Argoland is because Argoland first collided with a Tethyan

intra-oceanic arc, which originated from the Eurasia margin (Lhasa and Karakoram) from Late Jurassic time. In our model, the intra-oceanic arc includes the KLA and YTSZ supra-subduction zone ophiolites. Paleomagnetic studies indicate that the intra-oceanic arc reached equatorial latitudes in the mid-Early Cretaceous where we model that the western portion of Argoland first began to collide obliquely from ~100 Ma, roughly 20 Myr earlier than the collision between eastern Argoland and the Southeast Asian intra-oceanic arc (Woyla). Further south, Greater India and the Gascoyne Block (northeast Greater India), having separated from Gondwana from ~136 Ma, migrated northwest until a spreading reorganisation in the Albian caused India's separation from Madagascar and northward motion. India collided with the intra-oceanic arc at ~54 Ma, likely destroying evidence of Argoland. The Gascoyne Block either reached the intra-oceanic arc or West Burma at ~50 Ma. Greater India, bearing the intra-oceanic arc (including the KLA), accreted to the Eurasian margin from ~44 Ma, possibly diachronously from west to east, and continued to deform/subduct beneath Eurasia.

We present this self-consistent, plate kinematic model as a best-fit scenario to a large number of (sometimes contradictory) Eurasian, Southeast Asian, Tethyan, and Indian Ocean constraints (Fig. 8, Tables 1 and 2), in the hope that it may be utilised and improved by future studies.

Acknowledgements

We gratefully acknowledge the funding support received from the Department of Innovation, Industry, Science and Research (DIISR), Govt. of Australia (ST0050084) and the Department of Science and Technology (DST), Govt. of India (DST/INT/AUS/P-41/2011), under an Australia–India Strategic Research Fund (AISRF). The project was also supported by ARC grant FL0992245 and JW by DE140100376. We also thank Statoil (Norway), the Petroleum Exploration Society of Australia (PESA), and the School of Geosciences at the University of Sydney for support. Yatheesh is grateful to the Director, CSIR-National Institute of Oceanography (CSIR-NIO, Goa) for permission to publish this paper. This is NIO contribution 5709. Sabin Zahirovic was supported by an Australian Postgraduate Award (APA) and University of Sydney Vice-Chancellor's Research Scholarship (VCRS). All figures were made using GMT (Wessel and Smith, 1998), with reconstruction geometries extracted from GPlates (Boyden et al., 2011), except for Fig. 8, which used TimeScale Creator (www.tscreator.org) to produce the framework.

The plate model and animations can be downloaded from here (~130 Mb).

ftp://ftp.earthbyte.org/papers/Gibbons_et.al_IndiaEurasia/Gibbons_et.al_IndiaEurasia_Supplement.zip.

Alternatively, you can browse for the individual files by going here:

ftp://ftp.earthbyte.org/papers/Gibbons_et.al_IndiaEurasia/Gibbons_et.al_IndiaEurasia_Supplement/.

Appendix A. Supplementary data

Supplementary data to this article can be found online at <http://dx.doi.org/10.1016/j.gr.2015.01.001>.

References

- Abrajevitch, A.V., Ali, J.R., Aitchison, J.C., Badengzhu, Davis, A.M., Liu, J.B., Zabrev, S.V., 2005. Neotethys and the India–Asia collision: insights from a palaeomagnetic study of the Dazhuqu ophiolite, southern Tibet. *Earth and Planetary Science Letters* 233, 87–102.
- Achache, J., Courtillot, V., Zhou, Y.X., 1984. Paleogeographic and tectonic evolution of southern Tibet since Middle Cretaceous time – new paleomagnetic data and synthesis. *Journal of Geophysical Research* 89, 311–339.
- Acharyya, S., 1998. Break-up of the greater Indo-Australian continent and accretion of blocks framing south and east Asia. *Journal of Geodynamics* 26, 149–170.
- Acton, G.D., 1999. Apparent polar wander of India since the Cretaceous with implications for regional tectonics and true polar wander. *Memoirs of the Geological Society of India* 44, 129–175.
- Ahmad, M.N., Yoshida, M., Fujiwara, Y., 2000. Paleomagnetic study of Utro Volcanic Formation: remagnetizations and postfolding rotations in Utro area, Kohistan arc, northern Pakistan. *Earth, Planets and Space* 52, 425–436.
- Ahmad, M.N., Fujiwara, Y., Paudel, L.P., 2001. Remagnetization of igneous rocks in Gupis area of Kohistan arc, northern Pakistan. *Earth, Planets and Space* 53, 373–384.
- Ahmad, T., Tanaka, T., Sachan, H.K., Asahara, Y., Islam, R., Khanna, P.P., 2008. Geochemical and isotopic constraints on the age and origin of the Nidar Ophiolitic Complex, Ladakh, India: implications for the Neo-Tethyan subduction along the Indus suture zone. *Tectonophysics* 451, 206–224.
- Aikman, A.B., Harrison, T.M., Lin, D., 2008. Evidence for early (>44 Ma) Himalayan crustal thickening, Tethyan Himalaya, southeastern Tibet. *Earth and Planetary Science Letters* 274, 14–23.
- Aitchison, J.C., Badengzhu, Davis, A.M., Liu, J.B., Luo, H., Malpas, J.G., McDermid, I.R.C., Wu, H.Y., Ziabrev, S.V., Zhou, M.F., 2000. Remnants of a Cretaceous intra-oceanic subduction system within the Yarlung-Zangbo suture (southern Tibet). *Earth and Planetary Science Letters* 183, 231–244.
- Aitchison, J.C., Abrajevitch, A., Ali, J.R., Badengzhu, Davis, A.M., Luo, H., Liu, J.B., McDermid, I.R.C., Ziabrev, S., 2002a. New insights into the evolution of the Yarlung Tsangpo suture zone, Xizang (Tibet), China. *Episodes* 25, 90–94.
- Aitchison, J.C., Davis, A.M., Badengzhu, B., Luo, H., 2002b. New constraints on the India–Asia collision: the Lower Miocene Gangrinboche conglomerates, Yarlung Tsangpo suture zone, SE Tibet. *Journal of Asian Earth Sciences* 21, 251–263.
- Aitchison, J.C., Davis, A.M., Abrajevitch Jr., A.V., Liu, J.B., Luo, H., McDermid, I.R.C., Ziabrev, S.V., 2003. Stratigraphic and sedimentological constraints on the age and tectonic evolution of the Neotethyan ophiolites along the Yarlung Tsangpo suture zone, Tibet. *Ophiolites in Earth History* 218, 147–164.
- Aitchison, J.C., Ali, J.R., Davis, A.M., 2007. When and where did India and Asia collide? *Journal of Geophysical Research – Solid Earth* 112.
- Aitchison, J.C., Ali, J.R., Chan, A., Davis, A.M., Lo, C.H., 2009. Tectonic implications of felsic tuffs within the Lower Miocene Gangrinboche conglomerates, southern Tibet. *Journal of Asian Earth Sciences* 34, 287–297.
- Aitchison, J.C., Xia, X.P., Baxter, A.T., Ali, J.R., 2011. Detrital zircon U-Pb ages along the Yarlung-Tsangpo suture zone, Tibet: implications for oblique convergence and collision between India and Asia. *Gondwana Research* 20, 691–709.
- Alam, M., Alam, M.M., Curran, J.R., Chowdhury, M., Gani, M.R., 2003. An overview of the sedimentary geology of the Bengal Basin in relation to the regional tectonic framework and basin-fill history. *Sedimentary Geology* 155, 179–208.
- Ali, J.R., Aitchison, J.C., 2005. Greater India. *Earth-Science Reviews* 72, 169–188.
- Allegré, C.J., Courtillot, V., Tapponnier, P., Hirn, A., Mattauer, M., Coulon, C., Jaeger, J.J., Achache, J., Schärer, U., Marcoux, J., Burg, J.P., Girardeau, J., Armijo, R., Gariepy, C., Gopel, C., Li, T.D., Xiao, X.C., Chang, C.F., Li, G.Q., Lin, B.Y., Teng, J.W., Wang, N.W., Chen, G.M., Han, T.L., Wang, X.B., Den, W.M., Sheng, H.B., Cao, Y.G., Zhou, J., Qiu, H.R., Bao, P.S., Wang, S.C., Wang, B.X., Zhou, Y.X., Ronghua, X., 1984. Structure and evolution of the Himalaya–Tibet orogenic belt. *Nature* 307, 17–22.
- Amante, C., Eakins, B., Boulder, C., 2009. ETOP01 1 arc-minute global relief model: procedures, data sources and analysis. *NOAA Technical Memorandum*.
- Anczkiewicz, R., Burg, J.P., Villa, I.M., Meier, M., 2000. Late Cretaceous blueschist metamorphism in the Indus Suture Zone, Shangla region, Pakistan Himalaya. *Tectonophysics* 324, 111–134.
- Audley-Charles, M.G., Ballantyne, P.D., Hall, R., 1988. Mesozoic–Cenozoic rift-drift sequence of Asian fragments from Gondwanaland. *Tectonophysics* 155, 317–330.
- Bajolet, F., Replumaz, A., Lainé, R., 2013. Orocline and syntaxes formation during subduction and collision. *Tectonics* 32, 1–18.
- Bao, P., Su, L., Wang, J., Zhai, Q., 2013. Study on the tectonic setting for the ophiolites in Xigaze, Tibet. *Acta Geologica Sinica-English Edition* 87, 395–425.
- Barber, A.J., 2000. The origin of the Woyla terranes in Sumatra and the Late Mesozoic evolution of the Sundaland margin. *Journal of Asian Earth Sciences* 18, 713–738.
- Barber, A.J., Crow, M.J., 2009. Structure of Sumatra and its implications for the tectonic assembly of Southeast Asia and the destruction of Paleotethys. *Island Arc* 18, 3–20.
- Bard, J.P., 1983. Metamorphism of an obducted island-arc – example of the Kohistan sequence (Pakistan) in the Himalayan colliding range. *Earth and Planetary Science Letters* 65, 133–144.
- Bastia, R., Das, S., Radhakrishna, M., 2010. Pre- and post-collisional depositional history in the upper and middle Bengal fan and evaluation of deepwater reservoir potential along the northeast Continental Margin of India. *Marine and Petroleum Geology* 27, 2051–2061.
- Baxter, A.T., Aitchison, J.C., Ziabrev, S.V., 2009. Radiolarian age constraints on Mesotethyan ocean evolution, and their implications for development of the Bangong–Nujiang suture, Tibet. *Journal of the Geological Society* 166, 689–694.
- Baxter, A.T., Aitchison, J.C., Ali, J.R., Ziabrev, S.V., 2010. Early Cretaceous radiolarians from the Spongtag massif, Ladakh, NW India: implications for Neo-Tethyan evolution. *Journal of the Geological Society* 167, 511–517.
- Baxter, A.T., Aitchison, J.C., Ziabrev, S.V., Ali, J.R., 2011. Upper Jurassic radiolarians from the Naga Ophiolite, Nagaland, northeast India. *Gondwana Research* 20, 638–644.
- Bedard, E., Hebert, R., Guillette, C., Lesage, G., Wang, C.S., Dostal, J., 2009. Petrology and geochemistry of the Saga and Sangsang ophiolitic massifs, Yarlung Zangbo Suture Zone, Southern Tibet: evidence for an arc-back-arc origin. *Lithos* 113, 48–67.
- Bennett, J.D., Bridge, D.M., Cameron, N.R., Djunuddin, A., Ghazali, S.A., Jeffrey, D.H., Kartawa, W., Keats, W., Rock, N.M.S., Thompson, S.J., Whandoyo, R., 1981. The Geology of the Calang Quadrangle, Sumatra (1:250,000). *Geological Research and Development Centre, Bandung*.
- Bernard, A., Munschy, M., 2000. Were the Mascarene and Laxmi basins (western Indian Ocean) formed at the same spreading centre? *Comptes Rendus de l'Academie des*

- Sciences Series IIA Earth and Planetary Science 330 (11), 777–783. [http://dx.doi.org/10.1016/S1251-8050\(00\)00221-4](http://dx.doi.org/10.1016/S1251-8050(00)00221-4).
- Bertrand, G., Rangin, C., Maluski, H., Han, T.A., Thein, M., Myint, O., Maw, W., Lwin, S., 1999. Cenozoic metamorphism along the Shan Scarp (Myanmar): evidences for ductile shear along the Sagaing Fault or the northward migration of the Eastern Himalayan Syntaxis? *Geophysical Research Letters* 26, 915–918.
- Besse, J., Courtillot, V., Pozzi, J.P., Westphal, M., Zhou, Y.X., 1984. Paleomagnetic estimates of crustal shortening in the Himalayan thrusts and Zangbo suture. *Nature* 311, 621–626.
- Bhutani, R., Pande, K., Venkatesan, T.R., 2009. (40)Ar–(39)Ar dating of volcanic rocks of the Shyok suture zone in north-west trans-Himalaya: implications for the post-collision evolution of the Shyok suture zone. *Journal of Asian Earth Sciences* 34, 168–177.
- Bijwaard, H., Spakman, W., Engdahl, E., 1998. Closing the gap between regional and global travel time tomography. *Journal of Geophysical Research* 103, 30055.
- Bird, P., 2003. An updated digital model of plate boundaries. *Geochemistry, Geophysics, Geosystems* 4, 1027.
- Bouilhol, P., Burg, J.P., Bodinier, J.L., Schmidt, M.W., Dawood, H., Hussain, S., 2009. Magma and fluid percolation in arc to forearc mantle: evidence from Sapat (Kohistan, North-east Pakistan). *Lithos* 107, 17–37.
- Bouilhol, P., Schaltegger, U., Chiaradia, M., Ovtcharova, M., Stracke, A., Burg, J.P., Dawood, H., 2011. Timing of juvenile arc crust formation and evolution in the Sapat Complex (Kohistan–Pakistan). *Chemical Geology* 280, 243–256.
- Bouilhol, P., Jagoutz, O., Hanchar, J.M., Dudas, F.O., 2013. Dating the India–Eurasia collision through arc magmatic records. *Earth and Planetary Science Letters* 366, 163–175.
- Boyden, J.A., Müller, R.D., Gurnis, M., Torsvik, T.H., Clark, J.A., Turner, M., Ivey-Law, H., Watson, R.J., Cannon, J.S., 2011. Next-generation plate-tectonic reconstructions using GPlates. In: Keller, G.R., Baru, C. (Eds.), *Geoinformatics: Cyberinfrastructure for the Solid Earth Sciences*. Cambridge University Press.
- Brookfield, M.E., Reynolds, P.H., 1981. Late Cretaceous emplacement of the Indus Suture Zone ophiolitic melanges and an Eocene–Oligocene magmatic arc on the northern edge of the Indian plate. *Earth and Planetary Science Letters* 55, 157–162.
- Burg, J.P., 2011. The Asia–Kohistan–India collision: review and discussion. In: Brown, D., Ryan, P.D. (Eds.), *Arc–Continent Collision. Frontiers in Earth Sciences*. Springer-Verlag, Berlin Heidelberg, pp. 279–308 (Chapter 10).
- Burg, J.P., Chen, G.M., 1984. Tectonics and structural zonation of southern Tibet, China. *Nature* 311, 219–223.
- Burg, J.P., Bodinier, J.L., Chaudhry, S., Hussain, S., Dawood, H., 1998. Infra-arc mantle–crust transition and intra-arc mantle diapirs in the Kohistan Complex (Pakistani Himalaya): petro-structural evidence. *Terra Nova* 10, 74–80.
- Burg, J.P., Jagoutz, O., Dawood, H., Hussain, S.S., 2006. Precollision tilt of crustal blocks in rifted island arcs: structural evidence from the Kohistan Arc. *Tectonics* 25.
- Cameron, N.R., Clarke, M.C.G., Aldiss, D.T., Aspden, J.A., Djunuddin, A., 1980. The geological evolution of North Sumatra. *Proceedings of the Indonesian Petroleum Association, Annual Convention* 9, pp. 149–187.
- Cande, S.C., Kent, D.V., 1995. Revised calibration of the geomagnetic polarity timescale for the Late Cretaceous and Cenozoic. *Journal of Geophysical Research* 100, 6093–6095.
- Cande, S.C., Stegman, D.R., 2011. Indian and African plate motions driven by the push force of the Reunion plume head. *Nature* 475, 47–52.
- Cande, S.C., Patriat, P., Dyment, J., 2010. Motion between the Indian, Antarctic and African plates in the early Cenozoic. *Geophysical Journal International* 183, 127–149.
- Capitanio, F.A., Replumaz, A., 2013. Subduction and slab breakoff controls on Asian Indentation tectonics and Himalayan Western Syntaxis formation. *Geochemistry, Geophysics, Geosystems* 14, 3515–3531.
- Capitanio, F., Morra, G., Goes, S., Weinberg, R., Moresi, L., 2010. India–Asia convergence driven by the subduction of the Greater Indian continent. *Nature Geoscience* 3, 136–139.
- Chan, G.H.N., Crowley, O., Searle, M., Aitchison, J.C., Horstwood, M., 2007a. U–Pb zircon ages of the Yarlung Zangbo suture zone ophiolites, south Tibet. Abstract Volume 22th Himalaya–Karakoram–Tibet Workshop, Hong Kong, China, p. 12.
- Chan, G.H.N., Searle, M., Aitchison, J., Ma, G.S.K., 2007b. Geochemistry and tectonic significance of peridotites from the Kigolar ophiolite, SW Tibet. *Geochimica et Cosmochimica Acta* 71 Supplement 159.
- Chan, G.H., Aitchison, J.C., Crowley, Q.G., Horstwood, M.S., Searle, M.P., Parrish, R.R., Chan, J.S.-L., 2013. U–Pb zircon ages for Yarlung Tsango suture zone ophiolites, southwestern Tibet and their tectonic implications. *Gondwana Research* 719–732.
- Chang, C., Chen, N., Coward, M.P., Deng, W., Dewey, J.F., Ganster, A., Harris, N.B.W., Jin, C., Kidd, W.S.F., Leeder, M.R., Li, H., Lin, J., Liu, C., Mei, H., Molnar, P., Pan, Y., Pan, Y., Pearce, J.A., Shackleton, R.M., Smith, A.B., Sun, Y., Ward, M., Watts, D.R., Xu, J., Xu, R., Yin, J., Zhang, Y., 1986. Preliminary conclusions of the Royal Society and Academia Sinica 1985 geotraverse of Tibet. *Nature (London)* 323, 501–507.
- Charlton, T.R., Barber, A.J., McGowan, A.J., Nicoll, R.S., Roniewicz, E., Cook, S.E., Barkham, S.T., Bird, P.R., 2009. The Triassic of Timor: lithostratigraphy, chronostratigraphy and palaeogeography. *Journal of Asian Earth Sciences* 36, 341–363.
- Chatterjee, S., Scotese, C., 2010. The wandering Indian plate and its changing biogeography during the Late Cretaceous–Early Tertiary period. *New Aspects of Mesozoic Biodiversity*. Springer, pp. 105–126.
- Chatterjee, S., Goswami, A., Scotese, C.R., 2013. The longest voyage: tectonic, magmatic, and paleoclimatic evolution of the Indian plate during its northward flight from Gondwana to Asia. *Gondwana Research* 23, 238–267.
- Chaubey, A., Dyment, J., Bhattacharya, G.C., Royer, J.-Y., Srinivas, K., Yatheesh, V., 2002. Paleogene magnetic isochrons and palaeo-propagators in the Arabian and Eastern Somali basins, NW Indian Ocean. *Geological Society, London, Special Publications* 195, 71–85.
- Chen, J.S., Huang, B.C., Sun, L.S., 2010. New constraints to the onset of the India–Asia collision: paleomagnetic reconnaissance on the Linzizong Group in the Lhasa Block, China. *Tectonophysics* 489, 189–209.
- Chen, W., Yang, T., Zhang, S., Yang, Z., Li, H., Wu, H., Zhang, J., Ma, Y., Cai, F., 2012. Paleomagnetic results from the Early Cretaceous Zenong Group volcanic rocks, Cuoqin, Tibet, and their paleogeographic implications. *Gondwana Research* 22, 461–469.
- Chiu, H.Y., Chung, S.L., Wu, F.Y., Liu, D.Y., Liang, Y.H., Lin, I.J., Iizuka, Y., Xie, L.W., Wang, Y.B., Chu, M.F., 2009. Zircon U–Pb and Hf isotopic constraints from eastern Transhimalayan batholiths on the precollisional magmatic and tectonic evolution in southern Tibet. *Tectonophysics* 477, 3–19.
- Chu, M.F., Chung, S.L., Song, B.A., Liu, D.Y., O'Reilly, S.Y., Pearson, N.J., Ji, J.Q., Wen, D.J., 2006. Zircon U–Pb and Hf isotope constraints on the Mesozoic tectonics and crustal evolution of southern Tibet. *Geology* 34, 745–748.
- Chu, M.F., Chung, S.L., O'Reilly, S.Y., Pearson, N.J., Wu, F.Y., Li, X.H., Liu, D.Y., Ji, J.Q., Chu, C.H., Lee, H.Y., 2011. India's hidden inputs to Tibetan orogeny revealed by Hf isotopes of Transhimalayan zircons and host rocks. *Earth and Planetary Science Letters* 307, 479–486.
- Chung, S., Chu, M., Zhang, Y., Xie, Y., Lo, C., Lee, T., Lan, C., Li, X., Zhang, Q., Wang, Y., 2005. Tibetan tectonic evolution inferred from spatial and temporal variations in post-collisional magmatism. *Earth-Science Reviews* 68, 173–196.
- Clements, B., Hall, R., 2011. A record of continental collision and regional sediment flux for the Cretaceous and Palaeogene core of SE Asia: implications for early Cenozoic palaeogeography. *Journal of the Geological Society* 168, 1187–1200.
- Clift, P.D., Degnan, P.J., Hannigan, R., Blusztajn, J., 2000. Sedimentary and geochemical evolution of the Dras forearc basin, Indus suture, Ladakh Himalaya, India. *Geology Society of America Bulletin* 112, 450–466.
- Clift, P.D., Carter, A., Krol, M., Kirby, E., 2002a. Constraints on India–Eurasia collision in the Arabian Sea region taken from the Indus Group, Ladakh Himalaya, India. *Geological Society Special Publication* 195, 97–116.
- Clift, P.D., Hannigan, R., Blusztajn, J., Draut, A.E., 2002b. Geochemical evolution of the Dras–Kohistan Arc during collision with Eurasia: evidence from the Ladakh Himalaya, India. *Island Arc* 11, 255–273.
- Corfield, R.I., Searle, M.P., 2000. Crustal shortening estimates across the north Indian continental margin, Ladakh, NW India. *Tectonics of the Nanga Parbat Syntaxis and the Western Himalaya* 170, pp. 395–410.
- Corfield, R.I., Searle, M.P., Green, O.R., 1999. Photang thrust sheet: an accretionary complex structurally below the Spontang ophiolite constraining timing and tectonic environment of ophiolite obduction, Ladakh Himalaya, NW India. *Journal of the Geological Society of London* 156, 1031–1044.
- Coulon, C., Maluski, H., Bollinger, C., Wang, S., 1986. Mesozoic and Cenozoic volcanic-rocks from central and southern Tibet – Ar-39–Ar-40 dating, petrological characteristics and geodynamical significance. *Earth and Planetary Science Letters* 79, 281–302.
- Coward, M.P., Rex, D.C., Asif Khan, M., Windley, B.F., Broughton, R.D., Luff, I.W., Pettersson, M.G., Pudsey, C.J., 1986. Collision tectonics in the NW Himalayas. *Geological Society, London, Special Publications* 19, 203–219. <http://dx.doi.org/10.1144/GSL.SP.1986.019.01.11>.
- Coward, M.P., Butler, R.W.H., Asif Khan, M., Knipe, R.J., 1987. The tectonic history of Kohistan and its implications for Himalayan structure. *Journal of the Geological Society of London* 144, 377–391.
- Dai, J.G., Wang, C.S., Hebert, R., Li, Y.L., Zhong, H.T., Guillaume, R., Bezard, R., Wei, Y.S.A., 2011a. Late Devonian OIB alkaline gabbro in the Yarlung Zangbo Suture Zone: remnants of the Paleo-Tethys? *Gondwana Research* 19, 232–243.
- Dai, J.G., Wang, C.S., Hebert, R., Santosh, M., Li, Y.L., Xu, J.Y., 2011b. Petrology and geochemistry of peridotites in the Zhongba ophiolite, Yarlung Zangbo Suture Zone: implications for the Early Cretaceous intra-oceanic subduction zone within the Neo-Tethys. *Chemical Geology* 288, 133–148.
- Dai, J., Wang, C., Li, Y., 2012. Relicts of the Early Cretaceous seamounts in the central-western Yarlung Zangbo Suture Zone, southern Tibet. *Journal of Asian Earth Sciences* 53, 25–37.
- Dai, J., Wang, C., Polat, A., Santosh, M., Li, Y., Ge, Y., 2013. Rapid forearc spreading between 130–120 Ma: evidence from geochronology and geochemistry of the Xigaze ophiolite, southern Tibet. *Lithos* 172–173, 1–16.
- Davie, T., Luyendyk, B., Rodolfo, K., Kempe, D., McKelvey, B., Leidy, R., Horvath, G., Hyndman, R., Thierstein, H., Boltovskoy, E., Doyle, P., 1974. Site 256. Deep Sea Drilling Project Reports and Publications 26, p. 31.
- Davis, A.M., Aitchison, J.C., Badengzhu, L.H., Malpas, J., S., Z., 1999. Eocene oblique-slip basin development, Tibet: terrane tracks on the roof of the world. In: Evenchick, C.A., Woodsworth, G.J., Jongens, R. (Eds.), *Terrane Paths 99, Circum Pacific Terrane Conference Abstracts and Program* (1999), p. 28.
- Davis, A.M., Aitchison, J.C., Badengzhu, L.H., Zyabrev, S., 2002. Paleogene island arc collision-related conglomerates, Yarlung-Tsangpo suture zone, Tibet. *Sedimentary Geology* 150, 247–273.
- Debon, F., Le Fort, P., Dauteil, D., Sonet, J., Zimmermann, J.L., 1987. Granites of western Karakorum and northern Kohistan (Pakistan): a composite mid-Cretaceous to upper Cenozoic magmatism. *Lithos* 20, 19–40.
- DeCelles, P.G., Robinson, D.M., Zandt, G., 2002. Implications of shortening in the Himalayan fold-thrust belt for uplift of the Tibetan Plateau. *Tectonics* 21, 1062.
- DeConto, R.M., Pollard, D., 2003. Rapid Cenozoic glaciation of Antarctica induced by declining atmospheric CO₂. *Nature* 421, 245–249.
- Deschamps, A., Lallemand, S., 2003. Geodynamic setting of Izu–Bonin–Mariana boninites. *Geological Society of London, Special Publication* 219, 163–185.
- Dewey, J.F., Shackleton, R.M., Chang, C.F., Sun, Y.Y., 1988. The tectonic evolution of the Tibetan plateau. *Philosophical Transactions of the Royal Society of London Series A - Mathematical Physical and Engineering Sciences* 327, 379–413.
- Dhuime, B., Bosch, D., Bodinier, J.L., Garrido, C.J., Bruguier, O., Hussain, S.S., Dawood, H., 2007. Multistage evolution of the Jijal ultramafic–mafic complex (Kohistan, N Pakistan): implications for building the roots of island arcs. *Earth and Planetary Science Letters* 261, 179–200.
- Dhuime, B., Bosch, D., Garrido, C.J., Bodinier, J.L., Bruguier, O., Hussain, S.S., Dawood, H., 2009. Geochemical architecture of the lower- to middle-crustal section of a

- paleo-island arc (Kohistan Complex, Jijal/Kamila Area, Northern Pakistan): implications for the evolution of an oceanic subduction zone. *Journal of Petrology* 50, 531–569.
- Dobrzhinetskaya, L.F., Wirth, R., Yang, J., Hutcheon, I.D., Weber, P.K., Green, H.W., 2009. High-pressure highly reduced nitrides and oxides from chromitite of a Tibetan ophiolite. *Proceedings of the National Academy of Sciences* 106, 19233–19238.
- Dobson, P.F., Blank, J.G., Maruyama, S., Liou, J.G., 2006. Petrology and geochemistry of boninitic-series volcanic rocks, Chichi-Jima, Bonin Islands, Japan. *International Geology Review* 48, 669–701.
- Dong, Y.H., Xu, J.F., Zeng, Q.G., Wang, Q., Mao, G.Z., Li, J., 2006. Is there a Neo-Tethys' subduction record earlier than arc volcanic rocks in the Sangri Group? *Acta Petrologica Sinica* 22, 661–668.
- Dunlap, W.J., Wysocki, R., 2002. Thermal evidence for early Cretaceous metamorphism in the Shyok suture zone and age of the Khardung volcanic rocks, Ladakh, India. *Journal of Asian Earth Sciences* 20, 481–490.
- Dupont-Nivet, G., Krijgsman, W., Langereis, C.G., Abels, H.A., Dai, S., Fang, X., 2007. Tibetan plateau aridification linked to global cooling at the Eocene–Oligocene transition. *Nature* 445, 635–638.
- Dupont-Nivet, G., Hoorn, C., Konert, M., 2008. Tibetan uplift prior to the Eocene–Oligocene climate transition: evidence from pollen analysis of the Xining Basin. *Geology* 36, 987–990.
- Dupont-Nivet, G., Lippert, P.C., van Hinsbergen, D.J.J., Meijers, M.J.M., Kapp, P., 2010. Palaeolatitude and age of the Indo-Asia collision: palaeomagnetic constraints. *Geophysics Journal International* 182, 1189–1198.
- Dupuis, C., Hebert, R., Dubois-Cote, V., Guilmette, C., Wang, C.S., Li, Y.L., Li, Z.J., 2005a. The Yarlung Zangbo Suture Zone ophiolitic melange (southern Tibet): new insights from geochemistry of ultramafic rocks. *Journal of Asian Earth Sciences* 25, 937–960.
- Dupuis, C., Hebert, R., Dubois-Cote, V., Wang, C.S., Li, Y.L., Li, Z.J., 2005b. Petrology and geochemistry of mafic rocks from melange and flysch units adjacent to the Yarlung Zangbo Suture Zone, southern Tibet. *Chemical Geology* 214, 287–308.
- Durr, S.B., 1996. Provenance of Xigaze fore-arc basin clastic rocks (Cretaceous, south Tibet). *Geological Society of America Bulletin* 108, 669–684.
- Dyment, J., 1991. Structure et évolution de la lithosphère océanique dans l'océan Indien: apport des anomalies magnétiques. Ph.D. Thesis. Univ. Louis Pasteur, Strasbourg, France, p. 374.
- Eagles, G., Wibisono, A.D., 2013. Ridge push, mantle plumes and the speed of the Indian plate. *Geophysical Journal International* 194 (2), 670–677. <http://dx.doi.org/10.1093/gji/ggt162> (First published online: May 27, 2013).
- Einsele, G., Liu, B., Durr, S., Frisch, W., Liu, G., Luterbacher, H.P., Ratschbacher, L., Ricken, W., Wendt, J., Wetzel, A., Yu, G., Zheng, H., 1994. The Xigaze fore-arc basin – evolution and facies architecture (Cretaceous, Tibet). *Sedimentary Geology* 90, 1–32.
- Falloon, T.J., Danyushevsky, L.V., Crawford, A.J., Meffre, S., Woodhead, J.D., Bloomer, S.H., 2008. Boninites and adakites from the northern termination of the Tonga trench: implications for adakite petrogenesis. *Journal of Petrology* 49, 697–715.
- Fan, P., Ko, K., 1994. Accreted terranes and mineral deposits of Myanmar. *Journal of Southeast Asian Earth Sciences* 10, 95–100.
- Fraser, J.E., Searle, M.P., Parrish, R.R., Noble, S.R., 2001. Chronology of deformation, metamorphism, and magmatism in the southern Karakoram Mountains. *Geological Society of America Bulletin* 113, 1443–1455.
- Fuchs, G., 1981. Outline of the geology of the Himalaya. *Mitteilungen. Österreichische Geologische Gesellschaft* 74 (75), 101–127.
- Fuchs, G., 1982. The geology of western Zanskar. *Jahrbuch der Geologischen Bundesanstalt* 125, 1–50.
- Fullerton, L.G., Sager, W.W., Handschumacher, D.W., 1989. Late Jurassic–Early Cretaceous evolution of the eastern Indian Ocean adjacent to northwest Australia. *Journal of Geophysical Research* 94, 2937–2953.
- Garrido, C.J., Bodinier, J.L., Burg, J.P., Zeilinger, G., Hussain, S.S., Dawood, H., Chaudhry, M.N., Gervilla, F., 2006. Petrogenesis of mafic garnet granulite in the lower crust of the Kohistan paleo-arc complex (Northern Pakistan): implications for intra-crustal differentiation of island arcs and generation of continental crust. *Journal of Petrology* 47, 1873–1914.
- Garzanti, E., 2008. Comment on "When and where did India and Asia collide?" by Jonathan C. Aitchison, Jason R. Ali, and Aileen M. Davis. *Journal of Geophysical Research: Solid Earth* (1978–2012) 113.
- Garzanti, E., Baud, A., Mascle, G., 1987. Sedimentary record of the northward flight of India and its collision with Eurasia (Ladakh Himalaya, India). *Geodinamica Acta* 1, 297–312.
- Gehrels, G., Kapp, P., DeCelles, P., Pullen, A., Blakey, R., Weislogel, A., Ding, L., Guynn, J., Martin, A., McQuarrie, N., Yin, A., 2011. Detrital zircon geochronology of pre-Tertiary strata in the Tibetan–Himalayan orogen. *Tectonics* 30.
- Geng, Q.R., Pan, G.T., Zheng, LL., Chen, Z.L., Fisher, R.D., Sun, Z.M., Ou, C.S., Han, D., Wang, X.W., Sheng, L., Lou, X.Y., Fu, H., 2006. The Eastern Himalaya syntaxis: major tectonic domains, ophiolitic mélanges and geologic evolution. *Journal of Asian Earth Sciences* 27, 265–285.
- Gibbons, A.D., Barckhausen, U., van den Bogaard, P., Hoernle, K., Werner, R., Whittaker, J.M., Muller, R.D., 2012. Constraining the Jurassic extent of Greater India: tectonic evolution of the West Australian margin. *Geochemistry, Geophysics, Geosystems* 13.
- Gibbons, A.D., Whittaker, J.M., Dietmar Müller, R., 2013. The breakup of East Gondwana: assimilating constraints from Cretaceous ocean basins around India into a best-fit tectonic model. *Journal of Geophysical Research, Solid Earth* 118 (3), 808–822.
- Girardeau, J., Marcoux, J., Allegre, C.J., Bassoulet, J.P., Tang, Y.K., Xiao, X.C., Zao, Y.G., Wang, X.B., 1984a. Tectonic environment and geodynamic significance of the Neo-Cimmerian Donqiao ophiolite, Bangong–Nujiang Suture Zone, Tibet. *Nature* 307, 27–31.
- Girardeau, J., Marcoux, J., Yougong, Z., 1984b. Lithologic and tectonic environment of the Xigaze Ophiolite (Yarlung Zangbo Suture Zone, Southern Tibet, China), and kinematics of its emplacement. *Eclogae Geologicae Helvetiae* 77, 153–170.
- Girardeau, J., Marcoux, J., Fourcade, E., Bassoulet, J.P., Tang, Y.K., 1985a. Xainxa ultramafic rocks, Central Tibet, China – tectonic environment and geodynamic significance. *Geology* 13, 330–333.
- Girardeau, J., Mercier, J.C.C., Yougong, Z., 1985b. Origin of the Xigaze ophiolite, Yarlung Zangbo Suture Zone, Southern Tibet. *Tectonophysics* 119, 407–433.
- Gradstein, F.M., 1992. Leg 122–123, northwestern Australian margin; a stratigraphic and paleogeographic summary. *Proceedings of the Ocean Drilling Program Scientific Results* 123, 801–816.
- Gradstein, F., Ludden, J., 1992. Radiometric age determinations for basement from Sites 765 and 766, Argo Abyssal Plain and northwestern Australian margin. *Proceedings of the Ocean Drilling Program, Scientific Results* 557–559.
- Gradstein, F.M., Agterberg, F.P., Ogg, J.G., Hardenbol, J., van Veen, P., Thierry, J., Huang, Z., 1994. A Mesozoic time scale. *Journal of Geophysical Research* 99, 24,051–24,074.
- Green, O.R., Searle, M.P., Corfield, R.I., Corfield, R.M., 2008. Cretaceous–tertiary carbonate platform evolution and the age of the India–Asia collision along the Ladakh Himalaya (northwest India). *Journal of Geology* 116, 331–353.
- Guan, Q., Zhu, D.C., Zhao, Z.D., Zhang, L.L., Liu, M., Li, X.W., Yu, F., Mo, X.X., 2010. Late Cretaceous adakites in the eastern segment of the Gangdese Belt, southern Tibet: products of Neo-Tethyan ridge subduction? *Acta Petrologica Sinica* 26, 2165–2179.
- Guillot, S., Garzanti, E., Baratoux, D., Marquer, D., Mahéo, G., De Sigoyer, J., 2003. Reconstructing the total shortening history of the NW Himalaya. *Geochemistry, Geophysics, Geosystems* 4.
- Guilmette, C., 2005. Petrology, geochemistry and geochronology of highly foliated amphibolites from the ophiolitic melange beneath the Yarlung Zangbo ophiolites, Xigaze area, Tibet. (MSc Thesis). Quebec University.
- Guilmette, C., Hebert, R., Wang, C.S., Villeneuve, M., 2009. Geochemistry and geochronology of the metamorphic sole underlying the Xigaze Ophiolite, Yarlung Zangbo Suture Zone, South Tibet. *Lithos* 112, 149–162.
- Guilmette, C., Hébert, R., Dostal, J., Indares, A., Ullrich, T., Bédard, E., Wang, C., 2012. Discovery of a dismembered metamorphic sole in the Saga ophiolitic mélange, South Tibet: assessing an Early Cretaceous disruption of the Neo-Tethyan suprasubduction zone and consequences on basin closing. *Gondwana Research* 22 (2), 398–414.
- Guo, L., Zhang, H.F., Harris, N., Pan, F.B., Xu, W.C., 2011. Origin and evolution of multi-stage felsic melts in eastern Gangdese belt: constraints from U–Pb zircon dating and Hf isotopic composition. *Lithos* 127, 54–67.
- Guo, L., Zhang, H.-F., Harris, N., Pan, F.-B., Xu, W.-C., 2013. Late Cretaceous (~81 Ma) high-temperature metamorphism in the southeastern Lhasa terrane: implication for the Neo-Tethys ocean ridge subduction. *Tectonophysics* 608, 112–126.
- Gurnis, M., Turner, M., Zahirovic, S., DiCaprio, L., Spasovic, S., Müller, R., Boyden, J., Seton, M., Manea, V., Bower, D., 2012. Plate tectonic reconstructions with continuously closing plates. *Computers & Geosciences* 38, 35–42.
- Guynn, J.H., Kapp, P., Pullen, A., Heizer, M., Gehrels, G., Ding, L., 2006. Tibetan basement rocks near Amdo reveal "missing" Mesozoic tectonism along the Bangong suture, central Tibet. *Geology* 34, 505–508.
- Hafkenscheid, E., Wortel, M., Spakman, W., 2006. Subduction history of the Tethyan region derived from seismic tomography and tectonic reconstructions. *Journal of Geophysical Research – Solid Earth* 111, B08401.
- Hall, R., 2002. Cenozoic geological and plate tectonic evolution of SE Asia and the SW Pacific: computer-based reconstructions, model and animations. *Journal of Asian Earth Sciences* 20, 353–431.
- Hall, R., 2011. Australia–SE Asia collision: plate tectonics and crustal flow. *Geological Society, London, Special Publications* 355, 75–109.
- Hall, R., 2012. Late Jurassic–Cenozoic reconstructions of the Indonesian region and the Indian Ocean. *Tectonophysics* 570, 1–41.
- He, S., Leier, A.L., Kapp, P., 2003. Upper crustal deformation in southern Tibet before and during the Indo-Asian collision. 2003 Seattle Annual Meeting (November 2–5, 2003). *Geological Society of America Abstracts with Programs* vol. 35, No. 6, p. 30 (September 2003).
- He, S.D., Kapp, P., DeCelles, P.G., Gehrels, G.E., Heizler, M., 2007. Cretaceous–Tertiary geology of the Gangdese Arc in the Linzhou area, southern Tibet. *Tectonophysics* 433, 15–37.
- Hearn, P., Hare, T., Schruben, P., Sherrill, D., LaMar, C., Tushimura, P., 2003. Global GIS, Global Coverage DVD (USGS). American Geological Institute, Alexandria, Virginia, USA.
- Hébert, R., Huot, F., Wang, C.S., Liu, Z.F., 2003. Yarlung Zangbo ophiolites (Southern Tibet) revisited: geodynamic implications from the mineral record. *Ophiolites in Earth History* 218, 165–190.
- Hébert, R., Bezard, R., Guilmette, C., Dostal, J., Wang, C., Liu, Z., 2012. The Indus–Yarlung Zangbo ophiolites from Nanga Parbat to Namche Barwa syntaxes, southern Tibet: first synthesis of petrology, geochemistry, and geochronology with incidences on geodynamic reconstructions of Neo-Tethys. *Gondwana Research* 22, 377–397.
- Heine, C., Müller, R., 2005. Late Jurassic rifting along the Australian North West Shelf: margin geometry and spreading ridge configuration. *Australian Journal of Earth Sciences* 52, 27–39.
- Henderson, A.L., Foster, G.L., Najman, Y., 2010a. Testing the application of in situ Sm–Nd isotopic analysis on detrital apatites: a provenance tool for constraining the timing of India–Eurasia collision. *Earth and Planetary Science Letters* 297, 42–49.
- Henderson, A.L., Najman, Y., Parrish, R., BouDagher-Fadel, M., Barford, D., Garzanti, E., Ando, S., 2010b. Geology of the Cenozoic Indus Basin sedimentary rocks: paleoenvironmental interpretation of sedimentation from the western Himalaya during the early phases of India–Eurasia collision. *Tectonics* 29.

- Henderson, A.L., Najman, Y., Parrish, R., Mark, D.F., Foster, G.L., 2011. Constraints to the timing of India–Eurasia collision: a re-evaluation of evidence from the Indus Basin sedimentary rocks of the Indus-Tsangpo Suture Zone, Ladakh, India. *Earth-Science Reviews* 106, 265–292.
- Hennig, A., 1915. Zur Petrographie und Geo-logie von Siidwest Tibet, Southern Tibet. 5. *Lithographic Institute of the General Staff of the Swedish Army*, p. 220.
- Hetzel, R., Dunkl, I., Haider, V., Strobl, M., von Eynatten, H., Ding, L., Frei, D., 2011. Peneplain formation in southern Tibet predates the India–Asia collision and plateau uplift. *Geology* 39, 983–986.
- Heuberger, S., 2004. The Karakoram-Kohistan suture zone in NW Pakistan – Hindu Kush mountain range. (Ph.D. Thesis), The Kinematics of the Karakoram-Kohistan Suture, Chitral, NW Pakistan. Geological Institute, Zurich (supervisor: Prof. J. P. Burg).
- Heuberger, S., Schaltegger, U., Burg, J.P., Villa, I.M., Frank, M., Dawood, H., Hussain, S., Zanchi, A., 2007. Age and isotopic constraints on magmatism along the Karakoram-Kohistan Suture Zone, NW Pakistan: evidence for subduction and continued convergence after India–Asia collision. *Swiss Journal of Geosciences* 100, 85–107.
- Hickey, R.L., Frey, F.A., 1982. Geochemical characteristics of boninite series volcanics: implications for their source. *Geochimica et Cosmochimica Acta* 46, 2099–2115.
- Honegger, K., Dietrich, V., Frank, W., Gansser, A., Thoni, M., Trommsdorff, V., 1982. Magmatism and metamorphism in the Ladakh Himalayas (the Indus-Tsangpo Suture Zone). *Earth and Planetary Science Letters* 60, 253–292.
- Honegger, K., Lefort, P., Mascle, G., Zimmermann, J.L., 1989. The blueschists along the Indus Suture Zone in Ladakh, NW Himalaya. *Journal of Metamorphic Geology* 7, 57–72.
- Hu, X.M., Sinclair, H.D., Wang, J.G., Jiang, H.H., Wu, F.Y., 2012. Late Cretaceous-Palaeogene stratigraphic and basin evolution in the Zhepure Mountain of southern Tibet: implications for the timing of India–Asia initial collision. *Basin Research* 24, 520–543.
- Huang, W., Dupont-Nivet, G., Lippert, P.C., van Hinsbergen, D.J., Hallot, E., 2013. Inclination shallowing in Eocene Linzizong sedimentary rocks from Southern Tibet: correction, possible causes and implications for reconstructing the India–Asia collision. *Geophysical Journal International* 188, 1–22.
- Huang, W., Dupont-Nivet, G., van Hinsbergen, D.J., Lippert, P.C., Dekkers, M.J., Guo, Z., Waldrip, R., Li, X., Zhang, X., Liu, D., 2015. Can a primary remanence be retrieved from partially remagnetized Eocene volcanic rocks in the Nanmulun Basin (southern Tibet) to date the India–Asia collision? *Journal of Geophysical Research, Solid Earth* <http://dx.doi.org/10.1002/2014JB011599>.
- Hutchison, C.S., 1975. Ophiolite in Southeast Asia. *Geological Society of America Bulletin* 86, 797–806.
- Ivany, L.C., Patterson, W.P., Lohmann, K.C., 2000. Cooler winters as a possible cause of mass extinctions at the Eocene/Oligocene boundary. *Nature* 407, 887–890.
- Jacob, J., Dymnt, J., Yatheesh, V., 2014. Revisiting the structure, age, and evolution of the Wharton Basin to better understand subduction under Indonesia. *Journal of Geophysical Research, Solid Earth* 119, 169–190.
- Jagoutz, O., Muntener, O., Burg, J.P., Ulmer, P., Jagoutz, E., 2006. Lower continental crust formation through focused flow in km-scale melt conduits: the zoned ultramafic bodies of the Chilas complex in the Kohistan island arc (NW Pakistan). *Earth and Planetary Science Letters* 242, 320–342.
- Jagoutz, O.E., Burg, J.P., Hussain, S., Dawood, H., Pettke, T., Iizuka, T., Maruyama, S., 2009. Construction of the granitoid crust of an island arc part I: geochronological and geochemical constraints from the plutonic Kohistan (NW Pakistan). *Contributions to Mineralogy and Petrology* 158, 739–755.
- Jan, M.Q., Howie, R.A., 1981. The mineralogy and geochemistry of the metamorphosed basic and ultrabasic rocks of the Jijal Complex, Kohistan, NW Pakistan. *Journal of Petrology* 22, 85–126.
- Jan, M.Q., Khan, M.A., Qazi, M.S., 1993. The Sapat mafic-ultramafic complex, Kohistan Arc, North Pakistan. *Geological Society Special Publication* 74, 113–121.
- Ji, W.Q., Wu, F.Y., Chung, S.L., Li, J.X., Liu, C.Z., 2009a. Zircon U–Pb geochronology and Hf isotopic constraints on petrogenesis of the Gangdese batholith, southern Tibet. *Chemical Geology* 262, 229–245.
- Ji, W.Q., Wu, F.Y., Liu, C.Z., Chung, S.L., 2009b. Geochronology and petrogenesis of granitic rocks in Gangdese batholith, southern Tibet. *Science in China Series D* 52, 1240–1261.
- Ji, W.Q., Wu, F.Y., Liu, C.Z., Chung, S.L., 2012. Early Eocene crustal thickening in southern Tibet: new age and geochemical constraints from the Gangdese batholith. *Journal of Asian Earth Sciences* 53, 82–95.
- Jin, X.C., 2002. Permo-Carboniferous sequences of Gondwana affinity in southwest China and their paleogeographic implications. *Journal of Asian Earth Sciences* 20, 633–646.
- Kanao, N.e.a., 1971. Summary Report on the Survey of Sumatra, Block 5, Japanese Overseas Mineral Development Company Limited. unpublished manuscript.
- Kapp, P., Murphy, M.A., Yin, A., Harrison, T.M., Ding, L., Guo, J.H., 2003. Mesozoic and Cenozoic tectonic evolution of the Shiquanhe area of western Tibet. *Tectonics* 22.
- Kapp, P., Yin, A., Harrison, T.M., Ding, L., 2005. Cretaceous–Tertiary shortening, basin development, and volcanism in central Tibet. *Geological Society of America Bulletin* 117, 865–878.
- Kellett, D.A., Cottle, J.M., Smit, M., 2014. Eocene deep crust at Ama Drime, Tibet: early evolution of the Himalayan orogen. *Lithosphere* L350, 351.
- Khan, T., Khan, M.A., Jan, M.Q., Naseem, M., 1996. Back-arc basin assemblages in Kohistan, northern Pakistan. *Geodinamica Acta* 9, 30–40.
- Khan, A., Murata, M., Ozawa, H., Kausar, A.B., 2004. Origin of dunite of the Sapat Complex, Himalaya, North Pakistan. Extended Abstracts: 19th Himalaya-Karakoram-Tibet Workshop, 2004, Niseko, Japan.
- Khan, T., Murata, M., Karim, T., Zafar, M., Ozawa, H., Hafeez-ur-Rehman, 2007. A Cretaceous dike swarm provides evidence of a spreading axis in the back-arc basin of the Kohistan paleo-island arc, northwestern Himalaya, Pakistan. *Journal of Asian Earth Sciences* 29, 350–360.
- Khan, S., Walker, D., Hall, S., Burke, K., Shah, M., Stockli, L., 2009. Did the Kohistan–Ladakh island arc collide first with India? *Geological Society of America Bulletin* 121, 366–384.
- Kidd, W.S.F., Pan, Y.S., Chang, C.F., Coward, M.P., Dewey, J.F., Gansser, A., Molnar, P., Shackleton, R.M., Sun, Y.Y., 1988. Geological mapping of the 1985 Chinese–British Tibetan (Xizang-Qinghai) plateau geotraverse route. *Philosophical Transactions of the Royal Society of London Series A – Mathematical Physical and Engineering Sciences* 327, 287–305.
- Kojima, S., Ahmad, T., Tanaka, T., Bagati, T.N., Mishra, M., Kumar, R., Islam, R., Khanna, P.P., 2001. Early Cretaceous radiolarians from the Indus suture zone, Ladakh, northern India. *News of Osaka Micropaleontologists (NOM)* 12, pp. 257–270.
- Krishna, K., Rao, D.G., Ramana, M., Subrahmanyam, V., Sarma, K., Pilipenko, A., Scherbakov, V., Murthy IV, R., 1995. Tectonic model for the evolution of oceanic crust in the northeastern Indian Ocean from the Late Cretaceous to the early Tertiary. *Journal of Geophysical Research: Solid Earth* (1978–2012) 100, 20011A–20024.
- Krishna, K.S., Abraham, H., Sager, W.W., Pringle, M.S., Frey, F., Gopala Rao, D., Levchenko, O.V., 2012. Tectonics of the Ninetyeast Ridge derived from spreading records in adjacent oceanic basins and age constraints of the ridge. *Journal of Geophysical Research: Solid Earth* (1978–2012) 117.
- Lacassin, R., Valli, F., Arnaud, N., Leloup, P.H., Paquette, J.L., Haibing, L., Tappognier, P., Chevalier, M.-L., Guillot, S., Maheo, G., 2004. Large-scale geometry, offset and kinematic evolution of the Karakorum fault, Tibet. *Earth and Planetary Science Letters* 219, 255–269.
- Lee, T.-Y., Lawver, L.A., 1995. Cenozoic plate reconstruction of Southeast Asia. *Tectonophysics* 251, 85–138.
- Lee, H.Y., Chung, S.L., Lo, C.H., Ji, J.Q., Lee, T.Y., Qian, Q., Zhang, Q., 2009. Eocene Neotethyan slab breakoff in southern Tibet inferred from the Linzizong volcanic record. *Tectonophysics* 477, 20–35.
- Lee, H.Y., Chung, S.L., Ji, J., Qian, Q., Gallet, S., Lo, C.H., Lee, T.Y., Zhang, Q., 2012. Geochemical and Sr–Nd isotopic constraints on the genesis of the Cenozoic Linzizong volcanic successions, southern Tibet. *Journal of Asian Earth Sciences* 53, 96–114.
- Leech, M.L., Singh, S., Jain, A.K., Klemperer, S.L., Manickavasagam, R.M., 2005. The onset of India–Asia continental collision: early, steep subduction required by the timing of UHP metamorphism in the western Himalaya. *Earth and Planetary Science Letters* 234, 83–97.
- Leier, A.L., 2005. The Cretaceous Evolution of the Lhasa Terrane, Southern Tibet. (PhD Thesis). Department of Geosciences, The University of Arizona.
- Leier, A.L., DeCelles, P.G., Kapp, P., Ding, L., 2007a. The Takena Formation of the Lhasa terrane, southern Tibet: the record of a Late Cretaceous retroarc foreland basin. *Geology Society of America Bulletin* 119, 31–48.
- Leier, A.L., Kapp, P., Gehrels, G.E., DeCelles, P.G., 2007b. Detrital zircon geochronology of carboniferous–cretaceous strata in the Lhasa terrane, Southern Tibet. *Basin Research* 19, 361–378.
- Leloup, P.H., Arnaud, N., Lacassin, R., Kienast, J., Harrison, T., Trong, T.T.P., Replumaz, A., Tappognier, P., 2001. New constraints on the structure, thermochronology, and timing of the Ailao Shan-Red River shear zone, SE Asia. *Journal of Geophysical Research* 106, 6683–6732.
- Leloup, P.H., Tappognier, P., Lacassin, R., 2007. Discussion on the role of the Red River shear zone, Yunnan and Vietnam, in the continental extrusion of SE Asia. *Journal of the Geological Society* 164, 1253–1260.
- Leloup, P.H., Maheo, G., Arnaud, N., Kali, E., Boutonnet, E., Liu, D.Y., Liu, X.H., Li, H.B., 2010. The South Tibet detachment shear zone in the Dinggye area time constraints on extrusion models of the Himalayas. *Earth and Planetary Science Letters* 292, 1–16.
- Leloup, P.H., Boutonnet, E., Davis, W.J., Hattori, K., 2011. Long-lasting intracontinental strike-slip faulting: new evidence from the Karakorum shear zone in the Himalayas. *Terra Nova* 23, 92–99.
- Li, C., van der Hilst, R., Engdahl, E., Burdick, S., 2008. A new global model for P wave speed variations in Earth's mantle. *Geochemistry, Geophysics, Geosystems* 9, 21.
- Liebke, U., Appel, E., Ding, L., Neumann, U., Antolin, B., Xu, Q.A., 2010. Position of the Lhasa terrane prior to India–Asia collision derived from palaeomagnetic inclinations of 53 Ma old dykes of the Linzhou Basin: constraints on the age of collision and post-collisional shortening within the Tibetan Plateau. *Geophysical Journal International* 182, 1199–1215.
- Lin, I.J., Chung, S.L., Chu, C.H., Lee, H.Y., Gallet, S., Wu, G.Y., Ji, J.Q., Zhang, Y.Q., 2012. Geochemical and Sr–Nd isotopic characteristics of Cretaceous to Paleocene granitoids and volcanic rocks, SE Tibet: petrogenesis and tectonic implications. *Journal of Asian Earth Sciences* 53, 131–150.
- Lippert, P.C., Zhao, X.X., Coe, R.S., Lo, C.H., 2011. Palaeomagnetism and Ar-40/Ar-39 geochronology of upper Palaeogene volcanic rocks from Central Tibet: implications for the Central Asia inclination anomaly, the palaeolatitude of Tibet and post-50 Ma shortening within Asia. *Geophysical Journal International* 184, 131–161.
- Lippert, P.C., van Hinsbergen, D.J.J., Dupont-Nivet, G., 2014. A paleomagnetic synthesis with implications for Cenozoic tectonics, paleogeography and climate of Asia. In: Nie, J.S., Hoke, G.D., Horton, B.K. (Eds.), Towards an Improved Understanding of Uplift Mechanisms and the Elevation History of the Tibetan Plateau. Geological Society of America Special Paper.
- Liu, J.B., Aitchison, J.C., 2002. Upper Paleocene radiolarians from the Yamdrok melange, south Xizang (Tibet), China. *Micropaleontology* 48, 145–154.
- Liu, G., Einsele, G., 1994. Sedimentary history of the Tethyan basin in the Tibetan Himalayas. *Geologische Rundschau* 83, 32–61.
- Liu, C.-S., Curraj, J.R., McDonald, J., 1983. New constraints on the tectonic evolution of the eastern Indian Ocean. *Earth and Planetary Science Letters* 65, 331–342.
- Lu, Z.W., Gao, R., Li, Q.S., He, R.Z., Kuang, C.Y., Hou, H.S., Xiong, X.S., Guan, Y., Wang, H.Y., Klemperer, S.L., 2009. Test of deep seismic reflection profiling across central uplift of Qiangtang terrane in Tibetan plateau. *Journal of Earth Science* 20, 438–447.

- Maheo, G., Bertrand, H., Guillot, S., Villa, I.M., Keller, F., Capiez, P., 2004. The South Ladakh ophiolites (NW Himalaya, India): an intra-oceanic tholeiitic arc origin with implications for the closure of the Neo-Tethys. *Chemical Geology* 203, 273–303.
- Maheo, G., Fayoux, X., Guillot, S., Garzanti, E., Capiez, P., Mascle, G., 2006. Relicts of an intra-oceanic arc in the Sapi-Shergol melange zone (Ladakh, NW Himalaya, India): implications for the closure of the Neo-Tethys Ocean. *Journal of Asian Earth Sciences* 26, 695–707.
- Malpas, J., 1979. Dynamothermal aureole of the Bay of Islands ophiolite suite. *Canadian Journal of Earth Sciences* 16, 2086–2101.
- Malpas, J., Zhou, M.F., Robinson, P.T., Reynolds, P.H., 2003. Geochemical and geochronological constraints on the origin and emplacement of the Yarlung Zangbo ophiolites, Southern Tibet. *Ophiolites in Earth History* 218, 191–206.
- Maluski, H., Matte, P., 1984. Ages of alpine tectonometamorphic events in the north-western Himalaya (Northern Pakistan) by Ar-39/Ar-40 method. *Tectonics* 3, 1–18.
- Maluski, H., Proust, F., Xiao, X.C., 1982. Ar-39/Ar-40 dating of the trans-Himalayan calc-alkaline magmatism of southern Tibet. *Nature* 298, 152–154.
- Matsuoka, A., Yang, Q., Kobayashi, K., Takei, M., Nagahashi, T., Zeng, Q.G., Wang, Y.J., 2002. Jurassic–Cretaceous radiolarian biostratigraphy and sedimentary environments of the Ceno-Tethys: records from the Xialu Chert in the Yarlung-Zangbo Suture Zone, southern Tibet. *Journal of Asian Earth Sciences* 20, 277–287.
- Matte, P., Tapponnier, P., Arnaud, N., Bourjot, L., Avouac, J.P., Vidal, P., Qing, L., Pan, Y.S., Yi, W., 1996. Tectonics of Western Tibet, between the Tarim and the Indus. *Earth and Planetary Science Letters* 142, 311–330.
- Matthews, K.J., Müller, R.D., Wessel, P., Whittaker, J.M., 2011. The tectonic fabric of the ocean basins. *Journal of Geophysical Research* 116, 1–28.
- Matthews, K.J., Seton, M., Müller, R.D., 2012. A global-scale plate reorganization event at 105–100 Ma. *Earth and Planetary Science Letters* 355, 283–298.
- Maurin, T., Masson, F., Rangin, C., Min, U.T., Collard, P., 2010. First global positioning system results in northern Myanmar: constant and localized slip rate along the Sagaing fault. *Geology* 38, 591–594.
- McDermid, I.R.C., Aitchison, J.C., Davis, A.M., Harrison, T.M., Grove, M., 2002. The Zedong terrane: a Late Jurassic intra-oceanic magmatic arc within the Yarlung-Tsangpo suture zone, southeastern Tibet. *Chemical Geology* 187, 267–277.
- Metcalfe, I., 1988. Origin and assembly of southeast Asian continental terranes. In: Audley-Charles, M.G., Hallam, A. (Eds.), *Gondwana and Tethys*. Geological Society of London, London, pp. 101–117.
- Metcalfe, I., 1996. Gondwanaland dispersion, Asian accretion and evolution of eastern Tethys. *Australian Journal of Earth Sciences* 43, 605–623.
- Metcalfe, I., 2006. Paleozoic and Mesozoic tectonic evolution and palaeogeography of East Asian crustal fragments: the Korean Peninsula in context. *Gondwana Research* 9, 24–46.
- Metcalfe, I., 2011a. Palaeozoic–Mesozoic history of SE Asia. Geological Society, London, Special Publications 355, 7–35.
- Metcalfe, I., 2011b. Tectonic framework and Phanerozoic evolution of Sundaland. *Gondwana Research* 19, 3–21.
- Miller, C., Thoni, M., Frank, W., Schuster, R., Melcher, F., Meisel, T., Zanetti, A., 2003. Geochemistry and tectonomagmatic affinity of the Yungbwa ophiolite, SW Tibet. *Lithos* 66, 155–172.
- Mitchell, A.H.G., 1981. Phanerozoic plate boundaries in mainland SE Asia, the Himalayas and Tibet. *Journal of the Geological Society, London* 138, 109–122.
- Mitchell, A.H.G., 1993. Cretaceous–Cenozoic tectonic events in the Western Myanmar (Burma) Assam Region. *Journal of the Geological Society, London* 150, 1089–1102.
- Mo, X., Zhao, Z., Zhou, S., Huang, G., 2008. Complexity in ages and tectonic settings of Yarlung Zangbo Ophiolite Belt. International Geological Congress, Oslo, 6–14 August 2008.
- Molnar, P., Stock, J.M., 2009. Slowing of India's convergence with Eurasia since 20 Ma and its implications for Tibetan mantle dynamics – art. no. TC3001. *Tectonics* 28, C3001.
- Molnar, P., Tapponnier, P., 1975. Cenozoic tectonics of Asia: effects of a continental collision. *Science* 189, 419–426.
- Molnar, P., Boos, W.R., Battisti, D.S., 2010. Orographic controls on climate and paleoclimate of Asia: thermal and mechanical roles for the Tibetan Plateau. *Annual Review of Earth and Planetary Sciences* 38, 77.
- Müller, R.D., Mihut, D., Baldwin, S., 1998. A new kinematic model for the formation and evolution of the west and northwest Australian margin. *The Sedimentary Basins of Western Australia*. 2, pp. 55–72.
- Müller, R.D., Gaina, C., Roest, W., Hansen, D.L., 2002. A recipe for microcontinent formation. *Geology* 29, 203–206.
- Müller, R.D., Goncharov, A., Kritski, A., 2005. Geophysical evaluation of the enigmatic Bedout basement high, offshore northwestern Australia. *Earth and Planetary Science Letters* 237, 264–284.
- Müller, R.D., Sdrolias, M., Gaina, C., Roest, W., 2008. Age, spreading rates, and spreading asymmetry of the world's ocean crust. *Geochemistry, Geophysics, Geosystems* 9, 19.
- Murphy, M.A., Yin, A., Kapp, P., Harrison, T.M., Lin, D., Guo, J.H., 2000. Southward propagation of the Karakoram fault system, southwest Tibet: timing and magnitude of slip. *Geology* 28, 451–454.
- Mutter, J.C.A., Hegarty, K., Cande, S.C., Weissel, J.K., 1985. Breakup between Australia and Antarctica: a brief review in the light of new data. *Tectonophysics* 114, 255–279.
- Norin, E., 1946. Geological Explorations in Western Tibet: Reports From the Scientific Expedition to the Northwestern Provinces of China Under the Leadership of Dr. Sven Hedin. *Geology* 7. Tryckeri Aktiebolaget, Thule, Stockholm, p. 205 (Publication 29 (III)).
- Pan, Y., Kidd, W.S.F., 1999. Shortening in the southern Lhasa block during India–Asia collision. 14th Himalaya-Karakorum-Tibet Workshop, Abstracts. *Terra Nostra* 99, 111–112.
- Pan, G.T., Wang, L.Q., Li, R.S., Yuan, S.H., Ji, W.H., Yin, F.G., Zhang, W.P., Wang, B.D., 2012. Tectonic evolution of the Qinghai-Tibet Plateau. *Journal of Asian Earth Sciences* 53, 3–14.
- Patriat, P., Achache, J., 1984. India–Eurasia collision chronology has implications for crustal shortening and driving mechanism of plates. *Nature* 311, 615–621.
- Patzelt, A., Li, H.M., Wang, J.D., Appel, E., 1996. Palaeomagnetism of Cretaceous to Tertiary sediments from southern Tibet: evidence for the extent of the northern margin of India prior to the collision with Eurasia. *Tectonophysics* 259, 259–284.
- Pearce, J.A., Deng, W., 1988. The ophiolites of the 1985 Tibet Geotraverse – Lhasa to Golmud (1985) and Lhasa to Kathmandu (1986). *Philosophical Transactions of the Royal Society of London Series A - Mathematical Physical and Engineering Sciences* 327, 215–238.
- Pedersen, R.B., Seale, M.P., Corfield, R.I., 2001. U–Pb zircon ages from the Spontang Ophiolite, Ladakh Himalaya. *Journal of the Geological Society* 158, 513–520.
- Pedersen, R., Seale, M., Carter, A., Bandopadhyay, P., 2010. U–Pb zircon age of the Andaman ophiolite: implications for the beginning of subduction beneath the Andaman–Sumatra arc. *Journal of the Geological Society* 167, 1105–1112.
- Peltzer, G., Tapponnier, P., 1988. Formation and evolution of strike-slip faults, rifts, and basins during India–Asia collision: an experimental approach. *Journal of Geophysical Research* 93, 15,085–15,117.
- Petterson, M.G., 1985, unpublished Ph.D. Thesis. The structure, petrology and geochemistry of the Kohistan batholith, Gilgit, Karhmir, N. Pakistan. Ph.D. Thesis, Leicester.
- Petterson, M.G., 2010. A Review of the geology and tectonics of the Kohistan island arc, north Pakistan. *The Geological Society of London* 338, 287–327.
- Petterson, M.G., Windley, B.F., 1985. Rb–Sr dating of the Kohistan Arc-batholith in the trans-Himalaya of North-Pakistan, and tectonic implications. *Earth and Planetary Science Letters* 74, 45–57.
- Petterson, M.G., Windley, B.F., 1992. Field relations, geochemistry and petrogenesis of the Cretaceous basaltic Jatal Dykes, Kohistan, Northern Pakistan. *Journal of the Geological Society of London* 149, 107–114.
- Pozzi, J.P., Westphal, M., Girardeau, J., Besse, J., Zhou, Y.X., Chen, X.Y., Xing, L.S., 1984. Palaeomagnetism of the Xigaze Ophiolite and Flysch (Yarlung Zangbo Suture Zone, Southern Tibet) – latitude and direction of spreading. *Earth and Planetary Science Letters* 70, 383–394.
- Pudsey, C.J., 1986. The northern suture, Pakistan – margin of a Cretaceous island-arc. *Geological Magazine* 123, 405–423.
- Pullen, A., Kapp, P., Gehrels, G.E., Vervoort, J.D., Ding, L., 2008. Triassic continental subduction in central Tibet and Mediterranean-style closure of the Paleo-Tethys Ocean. *Geology* 36, 351–354.
- Rai, H., 1982. Geological Evidence Against the Shyok Palaeo-suture, Ladakh Himalaya.
- Rai, H., Pandey, K., 1978. Geology of the Kargil igneous complex Ladakh, Jammu and Kashmir, India. *Recent Research in Geology* 5, 219–228.
- Rao, D.R., Rai, H., 2009. Geochemical studies of granitoids from Shyok tectonic zone of Khardung-Panamik section, Ladakh, India. *Journal of the Geological Society of India* 73, 553–566.
- Ravikant, V., Pal, T., Das, D., 2004. Chromites from the Nidar ophiolite and Karzok complex, Transhimalaya, eastern Ladakh: their magmatic evolution. *Journal of Asian Earth Sciences* 24, 177–184.
- Raymo, M., Ruddiman, W.F., 1992. Tectonic forcing of late Cenozoic climate. *Nature* 359, 117–122.
- Replumaz, A., Tapponnier, P., 2003. Reconstruction of the deformed collision zone between India and Asia by backward motion of lithospheric blocks. *Journal of Geophysical Research: Solid Earth* (1978–2012) 108, 1–24.
- Replumaz, A., Kárasón, H., van der Hilst, R.D., Besse, J., Tapponnier, P., 2004. 4-D evolution of SE Asia's mantle from geological reconstructions and seismic tomography. *Earth and Planetary Science Letters* 221, 103–115.
- Replumaz, A., Negredo, A.M., Villasenor, A., Guillot, S., 2010. Indian continental subduction and slab break-off during Tertiary collision. *Terra Nova* 22, 290–296.
- Replumaz, Anne, Capitanio, Fabio A., Guillot, Stéphane, Negredo, Ana M., Villasenor, Antonio, 2014. The coupling of Indian subduction and Asian continental tectonics. *Gondwana Research* 608–626.
- Reuber, I., 1986. Geometry of accretion and oceanic thrusting of the Spongtag Ophiolite, Ladakh-Himalaya. *Nature* 321, 592–596.
- Reuber, I., 1989. The Dras Arc – two successive volcanic events on eroded oceanic crust. *Tectonophysics* 161, 93–106.
- Rex, A.J., Searle, M.P., Tirrul, R., Crawford, M.B., Prior, D.J., Rex, D.C., Barnicoat, A., 1988. The geochemical and tectonic evolution of the Central Karakoram, North Pakistan. *Philosophical Transactions of the Royal Society of London Series A - Mathematical Physical and Engineering Sciences* 326, 229–255.
- Reynolds, P.H., Brookfield, M.E., McNutt, R.H., 1983. The age and nature of Mesozoic–Tertiary magmatism across the Indus Suture Zone in Kashmir and Ladakh (NW India and Pakistan). *Geologische Rundschau* 72, 981–1003.
- Richards, S., Lister, G., Kennett, B., 2007. A slab in depth: three-dimensional geometry and evolution of the Indo-Australian plate. *Geochemistry, Geophysics, Geosystems* 8, Q12003.
- Ricou, L., Mercier de Lepinay, B., Marcoux, J., 1986. Evolution of the Tethyan seaways and implications for the oceanic circulation around the Eocene–Oligocene boundary. *Developments in Palaeontology and Stratigraphy* 9, 387–394.
- Robertson, A.H.F., 2000. Formation of melanges in the Indus Suture Zone, Ladakh Himalaya by successive subduction-related, collisional and post-collisional processes during Late Mesozoic–Late Tertiary time. *Geological Society Special Publication* 170, 333–374.
- Robertson, A.H.F., Collins, A.S., 2002. Shyok Suture Zone, N Pakistan: late Mesozoic–Tertiary evolution of a critical suture separating the oceanic Ladakh Arc from the Asian continental margin. *Journal of Asian Earth Sciences* 20, 309–351.
- Robertson, A.H.F., Degnan, P.J., 1993. Sedimentology and tectonic implications of the Lamayuru Complex – deep-water facies of the Indian Passive Margin, Indus Suture Zone, Ladakh Himalaya. *Geological Society Special Publication* 74, 299–321.

- Robertson, A., Degnan, P., 1994. The Dras Arc Complex – lithofacies and reconstruction of a Late Cretaceous oceanic volcanic arc in the Indus Suture Zone, Ladakh-Himalaya. *Sedimentary Geology* 92, 117–145.
- Robinson, A.C., 2009. Geologic offsets across the northern Karakorum fault: implications for its role and terrane correlations in the western Himalayan-Tibetan orogen. *Earth and Planetary Science Letters* 279, 123–130.
- Robinson, P., Bai, W.J., Malpas, J., Yang, J.S., Zhou, M.F., Fang, Q.S., Hu, X.F., Cameron, S., Staudigel, H., 2004. Ultra-high pressure minerals in the Luobusa Ophiolite, Tibet, and their tectonic implications. *The Geological Society of London* 226, 247–271.
- Rohrmann, A., Kapp, P., Carrapa, B., Reiners, P.W., Guynn, J., Ding, L., Heizler, M., 2012. Thermochronologic evidence for plateau formation in central Tibet by 45 Ma. *Geological Society of America* 40, 187–190.
- Rolland, Y., 2002. From intra-oceanic convergence to post-collisional evolution: example of the India-Asia convergence in NW Himalaya, from Cretaceous to present. *Journal of the Virtual Explorer* 8, 193–216.
- Rolland, Y., Pecher, A., Picard, C., 2000. Middle Cretaceous back-arc formation and arc evolution along the Asian margin: the Shyok Suture Zone in northern Ladakh (NW Himalaya). *Tectonophysics* 325, 145–173.
- Rolland, Y., Picard, C., Pecher, A., Lapierre, H., Bosch, D., Keller, F., 2002. The cretaceous Ladakh arc of NW Himalaya – slab melting and melt-mantle interaction during fast northward drift of Indian Plate. *Chemical Geology* 182, 139–178.
- Rowley, D.B., 1998. Minimum age of initiation of collision between India and Asia north of Everest based on the subsidence history of the Zhepure Mountain section. *The Journal of Geology* 106, 220–235.
- Royer, J.-Y., Chang, T., 1991. Evidence for relative motions between the Indian and Australian Plates during the last 20 m.y. from plate tectonic reconstructions: implications for the deformation of the Indo-Australian Plate. *Journal of Geophysical Research, Solid Earth* 96, 11779–11802.
- Sandwell, D., Smith, W., 2009. Global marine gravity from retracked Geosat and ERS-1 altimetry: ridge segmentation versus spreading rate. *Journal of Geophysical Research, Solid Earth* 114.
- Schaltegger, U., Zeilinger, G., Frank, M., Burg, J.P., 2002. Multiple mantle sources during island arc magmatism: U-Pb and Hf isotopic evidence from the Kohistan arc complex, Pakistan. *Terra Nova* 14, 461–468.
- Schaltegger, U., Frank, M., Burg, J.P., 2003. A 120 million years record of magmatism and crustal melting in the Kohistan Batholith. EGS-AGU-EUG Joint Assembly, Abstracts From the Meeting Held in Nice, France, 6–11 April 2003 (abstract #6816).
- Scharer, U., 1984. The effect of initial Th-230 disequilibrium on young U-Pb Ages – the Makalu Case, Himalaya. *Earth and Planetary Science Letters* 67, 191–204.
- Schneider, W., Mattern, F., Wang, P.J., Li, C., 2003. Tectonic and sedimentary basin evolution of the eastern Bangong-Nujiang zone (Tibet): a Reading cycle. *International Journal of Earth Sciences* 92, 228–254.
- Sciunnach, D., Garzanti, E., 2012. Subsidence history of the Tethys Himalaya. *Earth Science Reviews* 111, 179–198.
- Searle, M.P., 2011. Geological evolution of the Karakoram Ranges. *Italian Journal of Geosciences* 130, 147–159.
- Searle, M.P., Treloar, P.J., 2010. Was Late Cretaceous-Paleocene obduction of ophiolite complexes the primary cause of crustal thickening and regional metamorphism in the Pakistan Himalaya? *Geological Society, London, Special Publications* 338, 345–359.
- Searle, M.P., Windley, B.F., Coward, M.P., Cooper, D.J.W., Rex, A.J., Rex, D., Li, T.D., Xiao, X.C., Jan, M.Q., Thakur, V.C., Kumar, S., 1987. The closing of Tethys and the tectonics of the Himalaya. *Geological Society of America Bulletin* 98, 678–701.
- Searle, M.P., Parrish, R.R., Tirul, R., Rex, D.C., 1990a. Age of crystallization and cooling of the K2 gneiss in the Baltoro Karakoram. *Journal of the Geological Society of London* 147, 603–606.
- Searle, M.P., Pickering, K.T., Cooper, D.J.W., 1990b. Restoration and evolution of the intermontane Indus Molasse Basin, Ladakh Himalaya, India. *Tectonophysics* 174, 301–314.
- Searle, M.P., Weinberg, R.F., Dunlap, W.J., 1998. Transpressional tectonics along the Karakoram fault zone, northern Ladakh: constraints on Tibetan extrusion. *Geological Society, London, Special Publications* 135, 307–326.
- Searle, M.P., Khan, M.A., Fraser, J.E., Gough, S.J., Jan, M.Q., 1999. The tectonic evolution of the Kohistan-Karakoram collision belt along the Karakoram Highway transect, north Pakistan. *Tectonics* 18, 929–949.
- Sengor, A.M.C., 1987. Tectonics of the Tethysides: orogenic collage development in a collisional setting. *Annual Review of Earth and Planetary Sciences* 15, 213–244.
- Sengör, A., Altiner, D., Cin, A., Ustaömer, T., Hsü, K., 1988. Origin and assembly of the Tethyside orogenic collage at the expense of Gondwana Land. *Geological Society, London, Special Publications* 37, 119–181.
- Seton, M., Müller, R., Zahirovic, S., Gaina, C., Torsvik, T., Shephard, G., Talsma, A., Gurnis, M., Turner, M., Maus, S., Chandler, M., 2012. Global continental and ocean basin reconstructions since 200 Ma. *Earth-Science Reviews* 113, 212–270.
- Seton, M., Whittaker, J.M., Wessel, P., Müller, R.D., DeMets, C., Merkouriev, S., Cande, S., Gaina, C., Eagles, C., Granot, R., 2014. Community infrastructure and repository for marine magnetic identifications. *Geochemistry, Geophysics, Geosystems* 15, 1629–1641.
- Sharma, K.K., 1987. Crustal growth and two-stage India-Eurasia collision in Ladakh. *Tectonophysics* 134, 17–28.
- Sharma, K.K., Gupta, K.R., Sah, S.C.D., 1980. Discovery of upper Gondwana plants, north of Indus Suture Zone, Ladakh, India. *Current Science India* 49, 470–472.
- Shellnutt, J.G., Bhat, G.M., Brookfield, M.E., Jahn, B.M., 2011. No link between the Panjal Traps and the Late Permian mass extinctions. *Geophysical Research Letters* 38, L19308.
- Shellnutt, J.G., Bhat, G.M., Wang, K.L., Brookfield, M.E., Dostal, J., Jahn, B.M., 2014a. Petrogenesis of the flood basalts from the Early Permian Panjal Traps, Kashmir, India: geochemical evidence for shallow melting of the mantle. *Lithos* 204, 159–171.
- Shellnutt, J.G., Lee, T.-Y., Brookfield, M.E., Chung, S.-L., 2014b. Correlation between magmatism and convergence rates during the Indo-Eurasia collision. *Gondwana Research* 26, 1051–1059.
- Singh, S., Kumar, R., Barley, M.E., Jain, A.K., 2007. SHRIMP U-Pb ages and depth of emplacement of Ladakh Batholith, Eastern Ladakh, India. *Journal of Asian Earth Sciences* 30, 490–503.
- Smewing, J., Abbotts, I., Dunne, L., Rex, D., 1991. Formation and emplacement ages of the Masirah ophiolite, Sultanate of Oman. *Geology* 19, 453–456.
- Smit, M.A., Hacker, B.R., Lee, J., 2014. Tibetan garnet records early Eocene initiation of thickening in the Himalaya. *Geology* G35524, 35521.
- Smyth, H.R., Hamilton, P.J., Hall, R., Kinny, P.D., 2007. The deep crust beneath island arcs: inherited zircons reveal a Gondwana continental fragment beneath East Java, Indonesia. *Earth and Planetary Science Letters* 258, 269–282.
- Soler-Gijón, R., López-Martínez, N., 1998. Sharks and rays (chondrichthytes) from the Upper Cretaceous red beds of the south-central Pyrenees (Lleida, Spain): indices of an India-Eurasia connection. *Paleogeography, Palaeoclimatology, Palaeoecology* 141, 1–12.
- Sone, M., Metcalfe, I., Chaodumrong, P., 2012. The Chanthaburi terrane of southeastern Thailand: stratigraphic confirmation as a disrupted segment of the Sukhothai Arc. *Journal of Asian Earth Sciences* 61, 16–32.
- Srivastava, A.K., Agnihotri, D., 2010. Dilemma of late Palaeozoic mixed floras in Gondwana. *Paleogeography, Palaeoclimatology, Palaeoecology* 298, 54–69.
- Stern, R.J., 2010. The anatomy and ontogeny of modern intra-oceanic arc systems. *Geological Society, London, Special Publications* 338, 7–34.
- Stocklin, J., 1980. Geology of Nepal and its regional frame. *Journal of the Geological Society of London* 137, 1–34.
- St-Onge, M.R., Rayner, N., Searle, M.P., 2010. Zircon age determinations for the Ladakh batholith at Chumathang (Northwest India): implications for the age of the India-Asia collision in the Ladakh Himalaya. *Tectonophysics* 495, 171–183.
- Styron, R., Taylor, M., Okoronkwo, K., 2010. Database of active structures from the Indo-Asian collision. *EOS, Transactions of the American Geophysical Union* 91, 20.
- Su, W., Zhang, M., Liu, X.H., Lin, J.F., Ye, K., Liu, X., 2012. Exact timing of granulite metamorphism in the Namche-Barwa, eastern Himalayan syntaxis: new constraints from SIMS U-Pb zircon age. *International Journal of Earth Sciences* 101, 239–252.
- Sun, D.L., 1993. On the Permian biogeographic boundary between Gondwana and Eurasia in Tibet, China as the Eastern Section of the Tethys. *Paleogeography, Palaeoclimatology, Palaeoecology* 100, 59–77.
- Sun, Z.M., Jiang, W., Li, H.B., Pei, J.L., Zhu, Z.M., 2010. New paleomagnetic results of Paleocene volcanic rocks from the Lhasa block: tectonic implications for the collision of India and Asia. *Tectonophysics* 490, 257–266.
- Tan, X.D., Gilder, S., Kodama, K.P., Jiang, W., Han, Y.L., Zhang, H., Xu, H.H., Zhou, D., 2010. New paleomagnetic results from the Lhasa block: revised estimation of latitudinal shortening across Tibet and implications for dating the India-Asia collision. *Earth and Planetary Science Letters* 293, 396–404.
- Tapponnier, P., Mercier, J.L., Proust, F., Andrieux, J., Armijo, R., Bassoulet, J.P., Brunel, M., Burg, J.P., Colchen, M., Dupre, B., Girardeau, J., Marcoux, J., Mascle, G., Matte, P., Nicolas, A., Li, T.D., Xiao, X.C., Chang, C.F., Lin, P.Y., Li, G.C., Wang, N.W., Chen, G.M., Han, T.L., Wang, X.B., Den, W.M., Zhen, H.X., Sheng, H.B., Cao, Y.G., Zhou, J., Qiu, H.S., 1981. The Tibetan side of the India-Eurasia collision. *Nature* 294, 405–410.
- Tapponnier, P., Lacassin, R., Leloup, P.H., Scharer, U., Dalai, Z., Haiwei, W., Xiaohan, L., Shaocheng, J., Lianshang, Z., Jiayou, Z., 1990. The Ailao Shan/Red River metamorphic belt: tertiary left-lateral shear between Indochina and South China. *Nature* 343, 431–437.
- Thakur, V.C., 1990. Indus Tsangpo Suture Zone in Ladakh—its tectonostratigraphy and tectonics. *Proceedings of the Indian Academy of Science (Earth and Planetary Sciences)* 99, 169–185.
- Thakur, V.C., Misra, D.K., 1984. Tectonic framework of the Indus and Shyok suture zones in eastern Ladakh, northwest Himalaya. *Tectonophysics* 101, 207–220.
- Thanh, N.X., Itaya, T., Ahmad, T., Kojima, S., Ohtani, T., Ehiro, M., 2010. Mineral chemistry and K-Ar ages of plutons across the Karakoram fault in the Shyok-Nubra confluence of northern Ladakh Himalaya, India. *Gondwana Research* 17, 180–188.
- Thanh, N.X., Rajesh, V.J., Itaya, T., Windley, B., Kwon, S., Park, C.S., 2012. A Cretaceous forearc ophiolite in the Shyok suture zone, Ladakh, NW India: implications for the tectonic evolution of the Northwest Himalaya. *Lithos* 155, 81–93.
- Totterdell, J., Blevin, J., Struckmeyer, H., Bradshaw, B., Colwell, J., Kennard, J., 2000. Petroleum frontiers, systems and plays—a new sequence framework for the Great Australian Bight: starting with a clean slate. *APPEA Journal-Australian Petroleum Production and Exploration Association* 40, 95–120.
- Treloar, P.J., Rex, D.C., Guise, P.G., Coward, M.P., Searle, M.P., Windley, B.F., Petterson, M.G., Jan, M.Q., Luff, I.W., 1989. K-Ar and Ar-Ar geochronology of the Himalayan collision in NW Pakistan – constraints on the timing of suturing, deformation, metamorphism and uplift. *Tectonics* 8, 881–909.
- Treloar, P.J., Potts, G.J., Wheeler, J., Rex, D.C., 1991. Structural evolution and asymmetric uplift of the Nanga Parbat Syntaxis, Pakistan Himalaya. *Geologische Rundschau* 80, 411–428.
- Treloar, P.J., Petterson, M.G., Jan, M.Q., Sullivan, M.A., 1996. A re-evaluation of the stratigraphy and evolution of the Kohistan arc sequence, Pakistan Himalaya: implications for magmatic and tectonic arc-building processes. *Journal of the Geological Society of London* 153, 681–693.
- Treloar, P.J., Rex, D.C., Guise, P.G., Wheeler, J., Hurford, A.J., Carter, A., 2000. Geochronological constraints on the evolution of the Nanga Parbat Syntaxis, Pakistan Himalaya. *Tectonics of the Nanga Parbat Syntaxis and the Western Himalaya* 170, pp. 137–162.
- Van der Voo, R., Spakman, W., Bijwaard, H., 1999. Tethyan subducted slabs under India. *Earth and Planetary Science Letters* 171, 7–20.

- van Hinsbergen, D.J.J., Kapp, P., Dupont-Nivet, G., Lippert, P.C., Decelles, P.G., Torsvik, T., 2011a. Restoration of Cenozoic deformation in Asia and the size of Greater India. *Tectonics* 30, 1–31.
- van Hinsbergen, D.J.J., Steinberger, B., doubrrovine, P.V., Gassmoller, R., 2011b. Acceleration and deceleration of India–Asia convergence since the Cretaceous: roles of mantle plumes and continental collision. *Journal of Geophysical Research* 116.
- van Hinsbergen, D.J.J., Lippert, P.C., Dupont-Nivet, G., McQuarrie, N., Doubrrovine, P.V., Spakman, W., Torsvik, T.H., 2012. Greater India Basin hypothesis and a two-stage Cenozoic collision between India and Asia. *Proceedings of the National Academy of Sciences* 109, 7659–7664.
- Veevers, J., 2000. Change of tectono-stratigraphic regime in the Australian plate during the 99 Ma (mid-Cretaceous) and 43 Ma (mid-Eocene) swerves of the Pacific. *Geology* 28, 47–50.
- Veevers, J.J., et al., 1974. Initial Reports of the Deep Sea Drilling Project vol. 27. U.S. Government Print Office, Washington, D.C.
- Veevers, J.J., Powell, C.M., Roots, S.R., 1991. Review of seafloor spreading around Australia. I. Synthesis of the patterns of spreading. *Australian Journal of Earth Sciences* 38, 373–389.
- Virdi, N.S., 1987. Northern margin of the Indian Plate – some litho-tectonic constraints. *Tectonophysics* 134, 29–38.
- von Rad, U., Exon, N.F., Haq, B.U., 1992. Rift-to-drift history of the Wombat Plateau, Northwest Australia; Triassic to Tertiary Leg 122 results. In: von Rad, U., Haq Bilal, U., Suzanne, O.C., Bent, B., Blome, D., Charles, Borella, E., Peter, Boyd, R., Bralower, J., Timothy, Brenner, W., Wolfram, De Carlo, H., Eric, Dumont, T., Exon, F., Neville, Galbrun, B., Golovchenko, X., Gorur, N., Ito, M., Lorenzo, M., Juan, Myers, A., Philip, Moxon, I., K.O.B.D., Oda, M., Sarti, M., Siesser, G., William, Snowdon, R., Lloyd, Tang, C., Wilkens, H., Roy, Williamson, E., Paul, Wonders, A.H., Antonius, Dearmont, H., Lona, Mazzullo, K., Elsa (Eds.), *Proceedings of the Ocean Drilling Program, Exmouth Plateau; Covering Leg 122 of the Cruises of the Drilling Vessel JOIDES Resolution*, Singapore, Rep. of Sing., Sites 759–764, 28 June 1988–28 August 1988. Texas A & M University, Ocean Drilling Program, College Station, TX, United States, pp. 765–800.
- Wakabayashi, J., Dilek, Y., 2003. What constitutes ‘emplacement’ of an ophiolite?: mechanisms and relationship to subduction initiation and formation of metamorphic soles. *Ophiolites in Earth History* 218, 427–447.
- Wakita, K., 2000. Cretaceous accretionary–collision complexes in central Indonesia. *Journal of Asian Earth Sciences* 18, 739–749.
- Wan, X.Q., Jansa, L.F., Sarti, M., 2002. Cretaceous and Paleogene boundary strata in southern Tibet and their implication for the India–Eurasia collision. *Lethaia* 35, 131–146.
- Wang, C.S., Li, X.H., Hu, X.M., Jansa, L.F., 2002. Latest marine horizon north of Qomolangma (Mt Everest): implications for closure of Tethys seaway and collision tectonics. *Terra Nova* 14, 114–120.
- Wang, J.G., Hu, X.M., Wu, F.Y., Jansa, L., 2010. Provenance of the Liuqu Conglomerate in southern Tibet A Paleogene erosional record of the Himalayan–Tibetan orogen. *Sedimentary Geology* 231, 74–84.
- Wang, C.S., Li, X.H., Liu, Z.F., Li, Y.L., Jansa, L., Dai, J.G., Wei, Y.S., 2012. Revision of the Cretaceous–Paleogene stratigraphic framework, facies architecture and provenance of the Xigaze forearc basin along the Yarlung Zangbo suture zone. *Gondwana Research* 22, 415–433.
- Wei, Z.Q., Xia, B., Zhang, Y.Q., Wang, R., 2006. SHRIMP zircon dating of diabase in the Xiugugabu ophiolite in Tibet and its geological implications. *Geotectonica et Metallogenio* 30, 93–97.
- Wei, L.J., Liu, X.H., Yan, F.H., Mai, X.S., Li, G.W., Liu, X.B., Zhou, X.J., 2011. Palynological evidence sheds new light on the age of the Liuqu Conglomerates in Tibet and its geological significance. *Science China Earth Sciences* 54, 901–911.
- Weinberg, R.F., Dunlap, W.J., 2000. Growth and deformation of the Ladakh batholith, northwest Himalayas: implications for timing of continental collision and origin of calc-alkaline batholiths. *Journal of Geology* 108, 303–320.
- Weinberg, R.F., Dunlap, W.J., Whitehouse, M., 2000. New field, structural and geochronological data from the Shyok and Nubra valleys, northern Ladakh: linking Kohistan to Tibet. *Tectonics of the Nanga Parbat Syntaxis and the Western Himalaya* 170, pp. 253–275.
- Wen, D.R., Liu, D.Y., Chung, S.I., Chu, M.F., Ji, J.Q., Zhang, Q., Song, B., Lee, T.Y., Yeh, M.W., Lo, C.H., 2008. Zircon SHRIMP U–Pb ages of the Gangdese Batholith and implications for Neotethyan subduction in southern Tibet. *Chemical Geology* 252, 191–201.
- Wessel, P., Smith, W.H.F., 1998. New, improved version of Generic Mapping Tools released. *EOS Transactions of the American Geophysical Union* 79.
- White, L.T., Ahmad, T., Ireland, T.R., Lister, G.S., Forster, M.A., 2011. Deconvolving episodic age spectra from zircons of the Ladakh Batholith, northwest Indian Himalaya. *Chemical Geology* 289, 179–196.
- Whittaker, J., Müller, R., Leitchenkov, G., Stagg, H., Sdrolias, M., Gaina, C., Goncharov, A., 2007. Major Australian–Antarctic plate reorganization at Hawaiian–Emperor bend time. *Science* 318, 83–86.
- Whittaker, J.M., Williams, S.E., Müller, R.D., 2013. Revised tectonic evolution of the Eastern Indian Ocean. *Geochemistry, Geophysics, Geosystems* 14, 1891–1909.
- Willems, H., Zhou, Z., Zhang, B., Grafe, K.-U., 1996. Stratigraphy of the Upper Cretaceous and Lower Tertiary strata in the Tethyan Himalayas of Tibet (Tingri area, China). *Geologische Rundschau* 85, 723–754.
- Windley, B.F., 1988. Tectonic framework of the Himalaya, Karakoram and Tibet, and problems of their evolution. *Philosophical Transactions of the Royal Society A* 326, 3–16.
- Wu, F.Y., Clift, P.D., Yang, J.H., 2007. Zircon Hf isotopic constraints on the sources of the Indus Molasse, Ladakh Himalaya, India. *Tectonics* 26.
- Wu, F.Y., Ji, W.Q., Liu, C.Z., Chung, S.L., 2010. Detrital zircon U–Pb and Hf isotopic data from the Xigaze fore-arc basin: constraints on Transhimalayan magmatic evolution in southern Tibet. *Chemical Geology* 271, 13–25.
- Xia, B., Li, J., Xu, L., Wang, R., Yang, Z., 2011. Sensitive high resolution ion micro-probe U–Pb zircon geochronology and geochemistry of mafic rocks from the Pulan–Xiangquanhe ophiolite, Tibet: constraints on the evolution of the neo-Tethys. *Acta Geologica Sinica–English Edition* 85, 840–853.
- Xingxue, L., Xiuyuan, X., 1994. The Cathaysian and Gondwana floras: their contribution to determining the boundary between eastern Gondwana and Laurasia. *Journal of Southeast Asian Earth Sciences* 9, 309–317.
- Xu, R.H., Schärer, U., Allegre, C.J., 1985. Magmatism and metamorphism in the Lhasa Block (Tibet) – a geochronological study. *Journal of Geology* 93, 41–57.
- Yamamoto, H., Nakamura, E., 2000. Timing of magmatic and metamorphic events in the Jijal complex of the Kohistan are deduced from Sm–Nd dating of mafic granulites. *Tectonics of the Nanga Parbat Syntaxis and the Western Himalaya* 170, pp. 313–319.
- Yamamoto, H., Kobayashi, K., Nakamura, E., Kaneko, Y., Kausar, A.B., 2005. U–Pb zircon dating of regional deformation in the lower crust of the Kohistan arc. *International Geology Review* 47, 1035–1047.
- Yang, J.S., Dobrzhinetskaya, L., Bai, W.J., Fang, Q.S., Robinson, P.T., Zhang, J., Green, H.W., 2007. Diamond- and coesite-bearing chromitites from the Luobusa ophiolite, Tibet. *Geology* 35, 875–878.
- Yang, J.S., Xu, Z.Q., Li, Z.L., Xua, X.Z., Li, T.F., Ren, Y.F., Li, H.Q., Chen, S.Y., Robinson, P.T., 2009. Discovery of an eclogite belt in the Lhasa block, Tibet: a new border for Paleo-Tethys? *Journal of Asian Earth Sciences* 34, 76–89.
- Yatheesh, V., Bhattacharya, G.C., Mahender, K., 2006. The terrace like feature in the mid-continent slope region off Trivandrum and a plausible model for India–Madagascar juxtaposition in immediate pre-drift scenario. *Gondwana Research* 10, 179–185.
- Yi, Z.Y., Huang, B.C., Chen, J.S., Chen, L.W., Wang, H.L., 2011. Paleomagnetism of early Paleogene marine sediments in southern Tibet, China: implications to onset of the India–Asia collision and size of Greater India. *Earth and Planetary Science Letters* 309, 153–165.
- Yin, J., Grant-Mackie, J.A., 2005. Late Triassic–Jurassic bivalves from volcanic sediments of the Lhasa block, Tibet. *New Zealand Journal of Geology and Geophysics* 48, 555–577.
- Yin, A., Harrison, T.M., 2000. Geologic evolution of the Himalayan–Tibetan orogen. *Annual Review of Earth and Planetary Sciences* 28, 211–280.
- Yin, A., Kapp, P., Manning, C.E., Harrison, T.M., Din, L., Deng, X., 1998. Extensive exposure of Mesozoic melange in Qiangtang and its role in the Cenozoic development of the Tibetan plateau. *Eos* 79, 816.
- Yin, A., Harrison, T.M., Murphy, M.A., Grove, M., Nie, S., Ryerson, F.J., Feng, W.X., Le, C.Z., 1999. Tertiary deformation history of southeastern and southwestern Tibet during the Indo-Asian collision. *Geological Society of America Bulletin* 111, 1644–1664.
- Zachos, J.C., Kump, L.R., 2005. Carbon cycle feedbacks and the initiation of Antarctic glaciation in the earliest Oligocene. *Global and Planetary Change* 47, 51–66.
- Zahirovic, S., Müller, R.D., Seton, M., Flament, N., Gurnis, M., Whittaker, J., 2012. Insights on the kinematics of the India–Eurasia collision from global geodynamic models. *Geochemistry, Geophysics, Geosystems* 13.
- Zahirovic, S., Seton, M., Müller, R.D., 2014. The Cretaceous and Cenozoic tectonic evolution of Southeast Asia. *Solid Earth Discussions* 5, 227–273.
- Zaman, H., Torii, M., 1999. Palaeomagnetic study of Cretaceous red beds from the eastern Hindukush ranges, northern Pakistan: palaeoreconstruction of the Kohistan–Karakoram composite unit before the India–Asia collision. *Geophysical Journal International* 136, 719–738.
- Zhai, Q.G., Zhang, R.Y., Jahn, B.M., Li, C., Song, S.G., Wang, J., 2011. Triassic eclogites from central Qiangtang, northern Tibet, China: petrology, geochronology and metamorphic P–T path. *Lithos* 125, 173–189.
- Zhang, K.J., 2004. Secular geochemical variations of the Lower Cretaceous siliciclastic rocks from central Tibet (China) indicate a tectonic transition from continental collision to back-arc rifting. *Earth and Planetary Science Letters* 229, 73–89.
- Zhang, Z.J., Klempener, S.L., 2005. West–east variation in crustal thickness in northern Lhasa block, central Tibet, from deep seismic sounding data. *Journal of Geophysical Research – Solid Earth* 110.
- Zhang, K.J., Tang, X.C., 2009. Eclogites in the interior of the Tibetan Plateau and their geodynamic implications. *Chinese Scientific Bulletin* 54, 2556–2567.
- Zhang, Z.M., Zhao, G.C., Santosh, M., Wang, J.L., Dong, X., Liou, J.G., 2010a. Two stages of granulite facies metamorphism in the eastern Himalayan syntaxis, south Tibet: petrology, zircon geochronology and implications for the subduction of Neo-Tethys and the Indian continent beneath Asia. *Journal of Metamorphic Geology* 28, 719–733.
- Zhang, Z.M., Zhao, G.C., Santosh, M., Wang, J.L., Dong, X., Shen, K., 2010b. Late Cretaceous charnockite with adakitic affinities from the Gangdese batholith, southeastern Tibet: evidence for Neo-Tethyan mid-ocean ridge subduction? *Gondwana Research* 17, 615–631.
- Zhang, K.-J., Zhang, Y.-X., Tang, X.-C., Xia, B., 2012a. Late Mesozoic tectonic evolution and growth of the Tibetan plateau prior to the Indo-Asian collision. *Earth-Science Reviews* 114, 236–249.
- Zhang, Z.-M., Dong, X., Liu, F., Lin, Y.-H., Yan, R., Santosh, M., 2012b. Tectonic evolution of the Amdo Terrane, Central Tibet: petrochemistry and zircon U–Pb geochronology. *The Journal of Geology* 120, 431–451.
- Zhang, Z.M., Dong, X., Santosh, M., Liu, F., Wang, W., Yiu, F., He, Z.Y., Shen, K., 2012c. Petrology and geochronology of the Namche Barwa Complex in the eastern Himalayan syntaxis, Tibet: constraints on the origin and evolution of the north-eastern margin of the Indian Craton. *Gondwana Research* 21, 123–137.
- Zhao, T.P., Zhou, M.F., Zhao, J.H., Zhang, K.J., Chen, W., 2008. Geochronology and geochemistry of the c. 80 Ma Rutog granitic pluton, northwestern Tibet: implications for the tectonic evolution of the Lhasa Terrane. *Geology Magazine* 145, 845–857.
- Zhou, M.F., Robinson, P.T., Malpas, J., Li, Z.J., 1996. Podiform chromitites in the Luobusa ophiolite (southern Tibet): implications for melt–rock interaction and chromite segregation in the upper mantle. *Journal of Petrology* 37, 3–21.

- Zhou, M.F., Malpas, J., Robinson, P.T., Reynolds, P.H., 1997. The dynamothermal aureole of the Dongqiao ophiolite (northern Tibet). *Canadian Journal of Earth Sciences* 34, 59–65.
- Zhou, S., Fang, N., Dong, G., Zhao, Z.-d., Liu, X.-m., 2001. Argon dating on the volcanic rocks of the Linzizong group, Tibet. *Bulletin of Mineralogy, Petrology and Geochemistry* 20, 317–319.
- Zhou, S., Mo, X.X., Dong, G.C., Zhao, Z.D., Qiu, R.Z., Guo, T.Y., Wang, L.L., 2004. Ar-40–Ar-39 geochronology of Cenozoic Linzizong volcanic rocks from Linzhou Basin, Tibet, China, and their geological implications. *Chinese Scientific Bulletin* 49, 1970–1979.
- Zhou, S., Mo, X., Niu, Y., Qiu, R., Zhao, Z., Xie, G., Sun, K., 2010a. The distribution of the Linzizong sequences along the Indo-Asian collision belt. *American Geophysical Union, Fall Meeting 2010* (abstract #T43B-2186).
- Zhou, S., Mo, X.X., Qiu, R.Z., Zhao, Z.D., Zhang, S.Q., Guo, T.Y., Qiu, L., 2010b. Sm–Nd dating of whole rock and mineral separates from Dangqiong Gabbro, Yarlung-Tsangpo Suture. *Geochimica et Cosmochimica Acta* 74 Supplement 1228.
- Zhu, D.C., Mo, X.X., Zhao, Z.D., Xu, J.F., Zhou, C.Y., Sun, C.G., Wang, L.Q., Chen, H.H., Dong, G.C., Zhou, S., 2008a. Zircon U–Pb geochronology of Zenong Group volcanic rocks in Coqen area of the Gangdese, Tibet and tectonic significance. *Acta Petrolei Sinica* 24, 401–412.
- Zhu, D.C., Pan, G.T., Chung, S.L., Liao, Z.L., Wang, L.Q., Li, G.M., 2008b. SHRIMP zircon age and geochemical constraints on the origin of lower Jurassic volcanic rocks from the Yeba formation, Southern Gangdese, south Tibet. *International Geology Reviews* 50, 442–471.
- Zhu, D.C., Mo, X.X., Niu, Y.L., Zhao, Z.D., Wang, L.Q., Liu, Y.S., Wu, F.Y., 2009a. Geochemical investigation of Early Cretaceous igneous rocks along an east–west traverse throughout the central Lhasa Terrane, Tibet. *Chemical Geology* 268, 298–312.
- Zhu, D.C., Zhao, Z.D., Pan, G.T., Lee, H.Y., Kang, Z.Q., Liao, Z.L., Wang, L.Q., Li, G.M., Dong, G.C., Liu, B., 2009b. Early cretaceous subduction-related adakite-like rocks of the Gangdese Belt, southern Tibet: products of slab melting and subsequent melt–peridotite interaction? *Journal of Asian Earth Sciences* 34, 298–309.
- Zhu, D.C., Zhao, Z.D., Niu, Y.L., Mo, X.X., Chung, S.L., Hou, Z.Q., Wang, L.Q., Wu, F.Y., 2011. The Lhasa Terrane: record of a microcontinent and its histories of drift and growth. *Earth and Planetary Science Letters* 301, 241–255.
- Zhu, D.-C., Zhao, Z.-D., Niu, Y., Dilek, Y., Hou, Z.-Q., Mo, X.-X., 2013. The origin and pre-Cenozoic evolution of the Tibetan Plateau. *Gondwana Research* 23, 1429–1454.
- Zibarev, S.V., Aitchison, J.C., Abrajevitch, A.V., Badengzhu, Davis, A.M., Luo, H., 2003. Precise radiolarian age constraints on the timing of ophiolite generation and sedimentation in the Dazhuqu terrane, Yarlung-Tsangpo suture zone, Tibet. *Journal of the Geological Society of London* 160, 591–599.
- Zibarev, S.V., Aitchison, J.C., Abrajevitch, A.V., Badengzhu, Davis, A.M., Luo, H., 2004. Bainang Terrane, Yarlung-Tsangpo suture, southern Tibet (Xizang, China): a record of intra-Neotethyan subduction–accretion processes preserved on the roof of the world. *Journal of the Geological Society of London* 161, 523–538.
- Zyabrev, S.V., Kojima, S., Ahmad, T., 2008. Radiolarian biostratigraphic constraints on the generation of the Nidar ophiolite and the onset of Dras are volcanism: tracing the evolution of the closing Tethys along the Indus – Yarlung-Tsangpo suture. *Stratigraphy* 5, 99–112.



Ana Gibbons attained a B.Sc. in Marine Biology and Coastal Management from the University of Newcastle Upon Tyne (UK), and a PhD in Marine Geophysics from the University of Sydney in 2012, investigating the tectonic evolution of the Indian Ocean. During this time she was invited as Visiting Scientist to work with several internationally renowned marine geophysicists at Institut de Physique du Globe de Paris (IPGP), France, and the National Institute for Oceanography (NIO), India. Ana then remained at the University of Sydney for a further year as a post-doc fellow for Australian-Indian Science Research Fund (AISRF) initiative, in order to combine her PhD work with plate reconstructions for the Eurasian collision zone. Presently she is a senior researcher at Statoil ASA, where she continues to focus on regional-scale plate tectonics and geodynamics.



Sabin Zahirovic graduated from the University of Sydney in 2011 with a Bachelor of Science and Technology (Hons.), majoring in geography, geology and geophysics. Sabin's previous research includes the first numerical models coupling detailed plate reconstructions with global mantle convection simulations to test end-member scenarios of India–Eurasia convergence. He is currently completing his Ph.D. candidature within the EarthByte group (Sydney), with a focus on plate kinematics and geodynamics, in particular the post-Jurassic tectonic evolution of Southeast Asia.



Dietmar Müller received his Ph.D. in Earth Science from the Scripps Institution of Oceanography in La Jolla/California in 1993. After joining the University of Sydney in the same year he started building the EarthByte e-research group (www.earthbyte.org). The EarthByters are pursuing open innovation, involving the collaborative development of open-source software as well as global digital data sets made available under a creative commons licence. One of the fundamental aims of the EarthByte Group is geodata synthesis through space and time, assimilating the wealth of disparate geological and geophysical data into a four-dimensional Earth model. Currently his research is focussed on building a prototype for a Virtual Geological Observatory built around the GPlates open innovation platform (www.gplates.org).



Jo Whittaker currently works for the Institute for Marine and Antarctic Science (IMAS) at the University of Tasmania. Her research interests are predominantly in plate tectonics, marine geophysics and geodynamics. Jo completed a combine science/commerce undergraduate degree with Honours in Geophysics from the University of Sydney in 2003, followed by a Masters in Geophysics from Victoria University, Wellington, New Zealand. She received her Ph.D., on the tectonic consequences of mid-ocean ridge formation, evolution and subduction, from the University of Sydney in 2008. Following graduation she worked both for industry (GETECH in the UK) and academia (University of Sydney).



Yatheesh Vadakkeyath is a Scientist from CSIR-National Institute of Oceanography, Goa, India. He obtained his Masters in Marine Geophysics from Cochin University of Science and Technology, India. Subsequently, he received his PhD Degree in Earth Science from Goa University, India and then worked as Post-Doc at Institut de Physique du Globe de Paris (IPGP), France. He was invited as Visiting Scientist to work with several internationally renowned marine Geophysicists at IPGP, France and the University of Sydney, Australia. His research focuses on understanding crustal architecture of the continental margins of India and the adjoining deep-sea basins; and deciphering plate tectonic evolution of the Indian Ocean in high-resolution. He is also associated with the multi-disciplinary investigations carried out over the mid-oceanic ridges in the Indian Ocean and the Andaman subduction